The utilisation of the ash disposal system as a salt sink:

Enhancement and optimisation of chemical interactions

by

Jacobus A. van den Berg

Thesis submitted in partial fulfilment of the requirements

for the Degree

Master of Science in Engineering

(Chemical Engineering)

in the Department of Process Engineering

University of Stellenbosch

Supervised by

Prof L. Lorenzen and B. Schutte

Stellenbosch

December 2004

Declaration

I, the undersigned, hereby declare that the work presented in this thesis is my own original work except where acknowledged in the text. Furthermore, neither this entire thesis, nor part thereof, has been submitted previously for a degree at any university.

Jacobus A. van den Berg

Date

Abstract

The fine ash produced at the Sasol Secunda Petrochemical Plant is disposed of through a wet ash disposal system. Other process waste streams with high salt concentrations are co-disposed of in the Sasol Secunda ash disposal system. This has led to a steady rise in the salt concentrations of the recycled clear ash effluent (CAE) over the past 17 years. To combat this increase in salt concentrations, the capability of the Sasol Secunda ash disposal system to act as a salt sink, needs to be enhanced.

This investigation focussed on ways to enhance the salt removal/retention capabilities of the Sasol Secunda ash disposal system and consisted of the following:

- A literature survey of relevant information.
- The mixing of different combinations of fine ash, brine and CAE.
- Adding CO_2 to the fine ash and CAE mixtures.
- Investigation to enhance salt precipitation in the CAE and Evaporation dams.
- Salt balances and a residence time calculation over the CAE and Evaporation dams.

From these investigations it were concluded that the Sasol Secunda ash disposal system could be used as a salt sink for SO_4 ions. Up to 43% of the SO_4 is removed from the brines after the initial ash/water contact. It was also found that the tubular reverse osmosis (TRO) brine could be used as a carrier medium for the ash. The large amounts of Ca that is leached into the ash water during the mixing of the CAE and fine ash can be prevented by the addition of CO_2 to the mixing point. There is usually an increase of 240% in the Ca concentration and this is reduced to only an 8% increase with the CO_2 addition.

The most feasible precipitation enhancement for the CAE and Evaporation dams is an increase in evaporation. This enhances $CaCO_3$ precipitation, which is the main mechanism for salt removal in the CAE and Evaporation dams.

Ca, Na and Cl are retained in the evaporation and CAE dams. SO_4 is leached from solid phases in the dams. There is however an overall decrease in the total dissolved solids (TDS) of the ash water. The salt removal of the CAE and Evaporation dams is approximately 57 tons per day.

The capability of the Sasol Secunda ash disposal system to act as a salt sink can be enhanced by the addition of CO_2 at the mixing point and by increasing the evaporation rate in the CAE and Evaporation dams. Using the TRO brine as carrier medium may also increase the SO_4 precipitation capabilities of the Sasol Secunda ash disposal system.

Opsomming

Die fynas wat by die Sasol Secunda Petrochemiese Aanleg geproduseer word, word verwyder deur ‘n geslote nat asstelsel. Ander afvalstrome wat hoë konsentrasies soute bevat word ook in die Sasol Secunda asstelsel gestort. Dit het tot gevolg dat daar oor die afgelope 17 jaar ‘n volgehoue styging in die sout konsentrasies van die hergebruikte aswater (genoem CAE – “clear ash effluent”) was. ‘n Manier om hierdie styging in die sout konsentrasies teen te werk, is om die sout verwyderingsvermoë van die Sasol Secunda asstelsel te verbeter.

Hierdie ondersoek het gefokus op maniere om die sout verwyderings-/terughoudingsvermoë van die Sasol Secunda asstelsel te verbeter en het die volgende ingesluit:

- ‘n Literatuur oorsig van toepaslike inligting.
- Die meng van verskillende kombinasies van fynas, soutstrome en CAE.
- Toediening van CO_2 by die fynas en CAE mengsels.
- ‘n Ondersoek na metodes om die soutverwydering in die CAE en Verdampingsdamme te verbeter.
- Soutbalanse en ‘n residensie tyd berekening vir die CAE en Verdampingsdamme.

Na hierdie ondersoeke kon die gevolgtrekking gemaak word dat die Sasol Secunda asstelsel ‘n sout sink vir SO_4 ione is. Tot 43% van die SO_4 word verwyder na die aanvanklike as/water kontak. Daar is ook gevind dat die TRO (“tubular reverse osmosis”) soutstroom gebruik kan word as ‘n draer vir die fynas. Die groot hoeveelhede Ca wat in die aswater in loog, kan voorkom word deur die toediening van CO_2 by die mengpunt van die fynas en aswater. Daar is normaalweg ‘n verhoging van 240% in die Ca konsentrasie van die aswater en dit word verminder na ‘n skrale 8% met die toediening van CO_2.

Die mees praktiese metode om die soutverwydering in die CAE en Verdampingsdamme te verbeter, is met die verhoging van die verdamping. Dit sal die neerslag van $CaCO_3$, wat die meeste soutverwydering tot gevolg het, verhoog.

Ca, Na en Cl word teruggehou in die Verdampings en CAE damme. SO_4 loog uit soliede fases in die damme. Daar is wel ‘n afname in die algehele opgeloste spesies (“TDS”) van die aswater. Die soutverwydering van die Verdampings en CAE damme is ongeveer 57 ton per dag.

Die vermoë van die Sasol Secunda asstelsel om as ‘n sout sink gebruik te word, kan verbeter word deur CO_2 by die mengpunt by te voeg en die verdampingstempo in die Verdampings en CAE damme te verhoog. Die gebruik van die TRO pekelstroom as draer van die as kan die SO_4 neerslag in die Sasol Secunda asstelsel ook verhoog.

Acknowledgements

I would like to express my most sincere gratitude to the following people and institutions for their assistance during the course of my studies:

SASOL, for their financial backing, interest and support throughout the duration of this project. In particular I would like to extend my most sincere appreciation to all those people at the Water Research Division of SASTECH R&D in Secunda, for their constant support and guidance.

My supervisors, Professor L. Lorenzen and Mr B. Schutte, for their valuable guidance, discussion, advice, and support during the course of this project. I would also like to thank Mr B. Schutte for his assistance during the site visits.

The staff at the Department of Process Engineering (University of Stellenbosch) for their invaluable assistance with different aspects of this project: The workshop personnel for the construction of the laboratory set-up, Mrs J.E. Botha for her assistance with the operation of the AA and Dionex machines and also the analyses she did.

The staff at the Department of Geology (University of Stellenbosch) for their invaluable advice and assistance pertaining to the analyses of my ash samples: Ms E. Spicer for her assistance with the XRF analyses.

The people at Outside Ash at the Sasol Secunda plant for their help with the installation of the weirs for the flow measurements. Thanks also for the help with gathering and providing data.

Finally I would like to thank Dr. Remy Bucher of iThemba Labs that helped with the XRD analyses.

Table of Contents

List of Tables

List of Figures

Nomenclature

AA	Atomic Absorption Spectrophotometer	-
b	width of weir	[m]
B	base width of weir	[m]
CAE	Clear Ash Effluent	-
C_e	discharge coefficient	-
CSTR	Continuous-Stirred Tank Reactor	-
EC	Electrical Conductivity	[mS/m]
EDR	Electrodialysis Reversal	-
FAD	Fine Ash Dam	-
FCD	Fine Coal Dam	-
g	gravitational acceleration	[m/s^2]
h	head of water over weir	[m]
LOI	Loss on ignition	%
L:S	Liquids to Solids ratio	-
P	height of weir from ground	[m]
pH	measured pH of the water	-
Q	flow rate	[m^3/s]
TDS	Total Dissolved Solids	mg/L
TRO	Tubular Reverse Osmosis	-
XRD	X-Ray Diffraction	-
XRF	X-Ray Fluorescence	-

Chapter 1
Introduction

The production processes of Sasol Secunda are responsible for the production of huge amounts of ash. Low grade coal is gasified together with steam and oxygen to produce gas that is turned into liquid fuel and other value-added chemicals. The ash is a by-product of this process.

The coarse ash that is produced (753 ton/h), is transported to ash heaps next to the plant by means of conveyers. The fine ash (444 ton/h), which is a mixture of the fly ash from the gasifiers and the fine ash from the power plants, is disposed of through a closed loop wet ash disposal system with ash water as the carrier medium. After solids separation on the ash dam, the ash water is stored in the Evaporation dams and called the clear ash effluent (CAE).

The CAE is mixed with the hot ash at the steam plant and a thickened mixture (ash/water slurry) is then pumped to the fine ash dams (FAD) on the outskirts of the plant. The ash settles and the CAE is recycled back to the plant through the CAE and Evaporation dams. To decrease the amount of raw water used by the Sasol Secunda Petrochemical Plant, some of the CAE is purified by the tubular reverse osmosis (TRO) plant and mine water is purified by the electrodialysis reversal (EDR) plant. The TRO brine produced, are dumped in the Sasol Secunda ash disposal system.

These and other process streams containing high salt concentrations (brines) are also disposed of in the ash disposal system (See Appendix A, Figures A1 and A2). To prevent the build up of salts in the system it would be advantages if most of the salts can be removed by the ash dams. As the amount of salty process streams increase, the removal of salts by the ash

disposal system is not sufficient. Other methods to remove salt within the system must be investigated.

The salt removal capabilities (using the system as a salt sink and minimising the salt intake) of the Sasol Secunda ash disposal system can be enhanced by increasing the amount of ash water (salt in the ash water) retained in the ash dams and also by immobilising the salts in the ash dams. The immobilising of the salts is a more permanent way of removing the salts.

Koch (2002) focussed thoroughly on the disposal system and the potential of the fine ash dams as salt sinks. The dominance of the $CaCO_3$ chemistry in the ash disposal system was established in the study conducted by Koch (2002). She concentrated on the following elements:

- Identifying the salts of primary concern to the operation of the Sasol Secunda ash disposal system
- Evaluating the efficiency of the disposal system under field conditions.
- Investigating the chemical changes, which occur from the time the ash, is mixed with the effluent, to the time it is recycled back to the Sasol Secunda Petrochemical Plant.

This study was a continuation of the work started by Koch (2002) and focussed on the enhanced removal of salts during the initial mixing of the ash and effluent (by forming salt complexes) and in the CAE and Evaporation dams (principally precipitation of $CaCO_3$) of the Sasol Secunda ash disposal system. This study also forms part of a much larger investigation at the Sasol Secunda ash disposal system to find solutions for the salt problem at the plant. The objectives of this investigation were:

- To evaluate the addition of different brine streams to the fine ash at the initial mixing point in Phase 1 (Simulating hot ash and CAE contact in the Steam Plant).
- To investigate the influence of CO_2 addition at the mixing point.

- To evaluate different methods to increase $CaCO_3$ precipitation in the clear ash effluent (CAE) dams.
- To obtain flow data at the Sasol Secunda ash disposal system to produce an actual mass balance to enable the measurement of the retention time and salt removal capability throughout the Evaporation and CAE dams.

All these objectives constituted the main aim of the project and that was to increase the salt precipitation of the system and in doing so minimising the build-up of salts in the ash water of the Sasol Secunda ash disposal system.

Chapter 2
Literature review and relevant information

Wet ash disposal systems are very complex and it is important to have a good overview of the specific system and of ash disposal systems in general. Complex chemical interactions take place in the ash disposal system. This chapter evaluates ash disposal systems in general as well as previous investigations that were performed on the Sasol Secunda ash disposal system.

The possible chemical interactions that take place in the Sasol Secunda ash disposal system are also discussed in this chapter. Important information about the experimental design and statistics performed on the data is also discussed.

2.1 Wet ash disposal systems

Wet ash disposal systems are widespread across the northeastern parts of South Africa. This is where most of the coal-powered power stations are situated and where the Sasol Secunda Petrochemical Plant is also situated (Figure 2.1). Different studies have been done on ash disposal systems in South Africa and the most important ones pertaining to this study will be reviewed here. The focus will be on wet ash disposal systems.

Most of the studies concentrated on disposal systems where only ash and the ash water were mixed. It was found that the dominant cations and anions in the water were Ca, Na, K, Mg and SO_4 (Villaume et al., 1987). Lee and Hahn (1997) confirmed that the ash water contained high concentrations of Ca, Na

and SO_4. The ash water usually also have a high total dissolved solids (TDS) concentration and a pH of around 12.

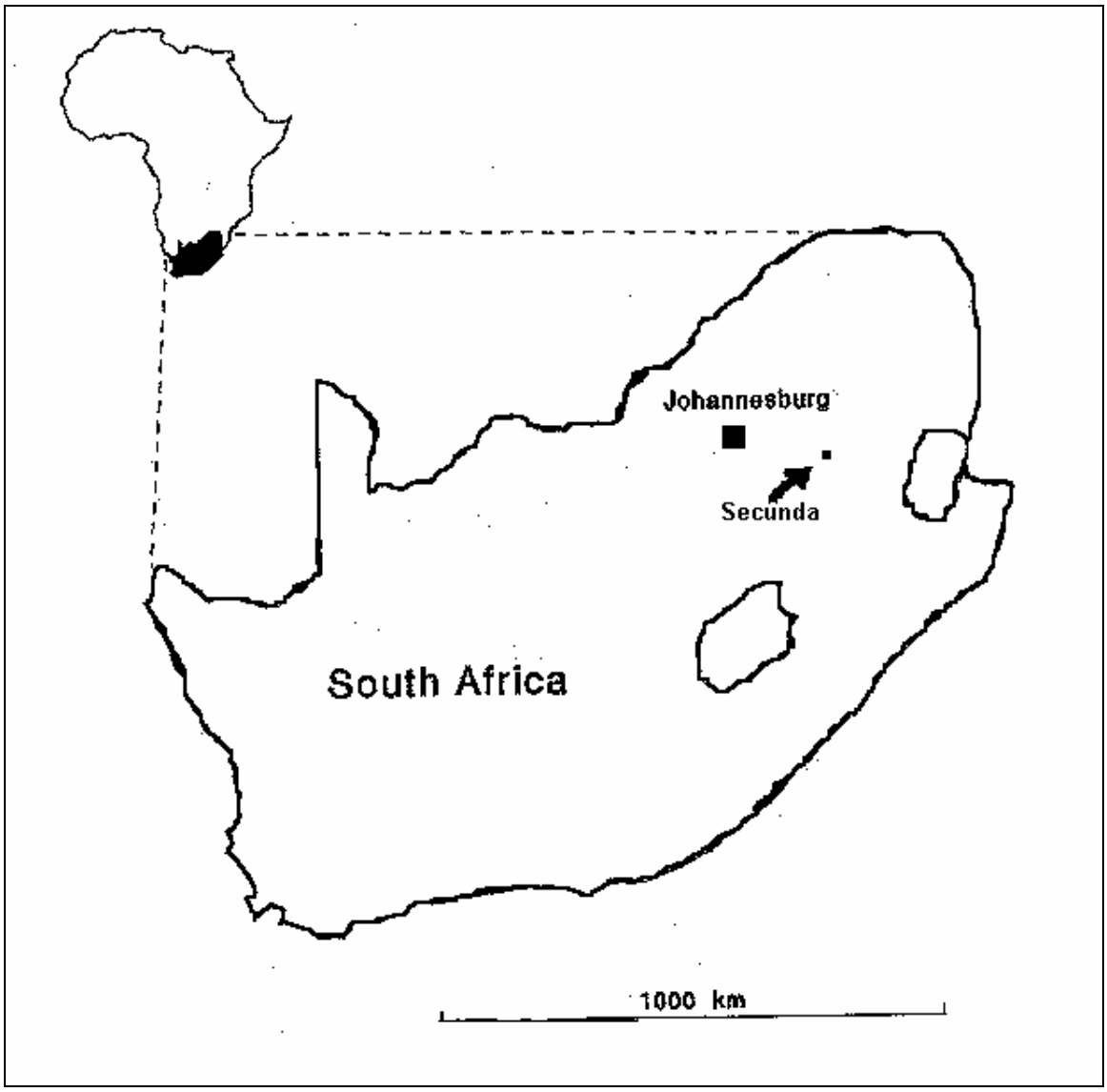

Figure 2.1: Map of South Africa showing relative location of Secunda

Bezuidenhout (1995) did an in depth study of the ash system at the Kriel power station in South Africa. He also found that the ash water had high Ca, Na, K and SO_4 concentrations, a pH of above 12 and high alkalinity values, as expected.

Table 2.1: Ash water composition for most recent studies

Composition of ash water for different studies			
Component	**Bezuidenhout (1995)**	**Koch (2002)**	**Van den Berg (2004)**
	Kriel Power Station	**Sasol Secunda**	**Sasol Secunda**
Ca (mg/l)	877	443	645
Na (mg/l)	266	826	1962
Cl (mg/l)	25	721	1250
SO_4 (mg/l)	1134	2623	3768
Cond (mS/m)	768	669	1075
pH	12.8	10.2	11.7
TDS (mg/l)	Not analysed	5184	7110

Table 2.1 indicates the composition of the ash water for this study and the study done by Koch (2002) on the Sasol Secunda ash disposal system. The composition of the ash water from Bezuidenhout's (1995) study at the Kriel Power Station is also shown. It can be seen that the water at the Sasol Secunda ash disposal system contains the same main components but the concentrations are much higher and also increased over the last couple of years, because of the continuous disposal of highly saline brines in the ash disposal system. This Sasol Secunda ash disposal system will be discussed in more detail in the next section.

2.2 Sasol Secunda ash disposal system

The wet ash disposal system at the Sasol Secunda Petrochemical Plant is a closed loop system. No water is disposed of to an outside source except through natural evaporation losses. The ash water, also known as clear ash effluent (CAE), is recycled back to the Petrochemical Plant to be mixed with new fine ash and then the ash slurry is transported via a pumping system to the fine ash dams (FAD) on the outskirts of the plant. The coarse ash is transported with conveyers to ash heaps on the outside of the plant. Diagrams of the Sasol Secunda ash disposal system (East and West) can be found in Appendix A (Figures A1 and A2).

Under its current operation the ash system serves as a salt sink, which buffers the salt variations of the inlet streams. These inlet streams are, amongst others, salty brines that are disposed of in the system. The Sasol Secunda ash disposal system can be divided into three different phases, which are discussed in a later section. The experiments done on the Sasol Secunda ash disposal system have also been performed separately on the different phases.

2.2.1 Description of the Sasol Secunda ash disposal system

Coarse and fine ash are produced at the Sasol Secunda Petrochemical Plant by the power station (steam plant) and the gasification of coal (to produce liquid fuels and chemicals). Figure 2.2 is a diagram of the entire Sasol Secunda ash disposal system. This system is divided into different phases that are discussed in a later section.

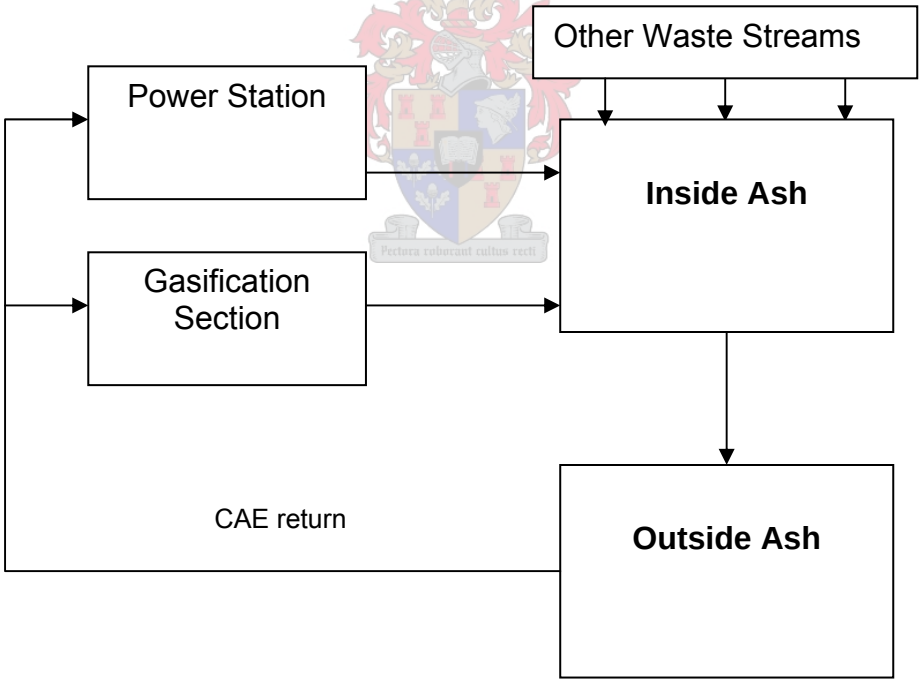

Figure 2.2: Diagram of Sasol Secunda ash disposal system (Koch, 2002).

The ash is then cooled by the ash water and transported to Inside Ash (Figure 2.2 and Figure 2.3). At Inside Ash the coarse and fine ash are dewatered and separated and the coarse ash is taken by conveyers to the coarse ash heaps.

After the separation of the fine and coarse ash the fine ash is transported to thickeners. The underflow of the thickeners goes to a slurry sump from where it is pumped as a slurry to the fine ash dams (Koch, 2002). At the slurry sump some waste streams enter the ash system. These streams are described in Tables 2.2, 2.3 and Figure 2.6. The overflow of the thickeners is used as carrier medium and shortages made up from CAE.

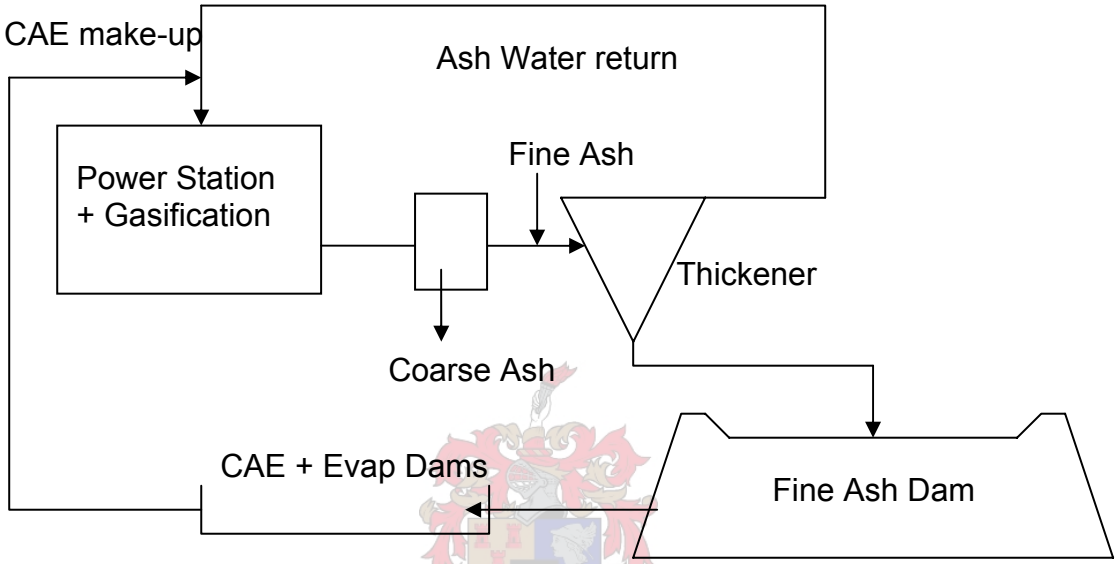

Figure 2.3: Diagram of the fine ash loop at Inside Ash at Sasol Secunda

The slurry is pumped onto the fine ash dams where the ash settles. Most of the water then flows out through a penstock overflow. This water flows into Evaporation dams. From the Evaporation dams it flows to the CAE dams where it stays until it is needed for re-use inside the plant. Some of the clear ash effluent is used as feed for the desalination and evaporation plants to produce boiler feed water. This decreases the amount of raw water that needs to be processed as boiler feed water.

Figure 2.4 shows the slurry from Inside Ash being pumped onto the ash dam on the outside of the Sasol Secunda Petrochemical Plant. The dams seen in Figure 2.5 are the Evaporation and CAE dams which provide the CAE for re-use.

Figure 2.4: Slurry pumped onto ash dam

Figure 2.5: Evaporation dams

As mentioned earlier, there are some waste streams entering the ash disposal system at the slurry sump. This happens just before the fine ash slurry is pumped to the ash dams on the outside of the plant. These streams come from different units of the Sasol Secunda Petrochemical Plant. A description of each of these units can be found in Table 2.2.

Table 2.2: Description of waste and salts-contributing units at Sasol Secunda Petrochemical Plant

Description of units	
Unit No.	**Description**
U01/201	Wet screening plants
U20/220	Synthol plant (spent catalyst)
U44/244	Hot lime treatment process units, demineralisation plant - cation regeneration waste
U45/245	Process cooling water system
U55/255	Flocculation unit
U66	Salty water system
U67/U69	TRO plant

Table 2.3 and Figure 2.6 give a description of each of the process waste streams entering the Sasol Secunda ash disposal system:

Table 2.3: Process waste streams entering the ash disposal system (Koch, 2002)

Stream	Description
1	Wastewater from the TRO (tubular reverse osmosis desalination) plant
2	Water from the sump at U66 (salty water system)
3	Blow-down from U45 (process cooling water)
4	Spent catalyst from Synthol
5	Saline water from hot lime treatment process units, demineralisation plant – cation regeneration waste
6	Sludge from the flocculation units
7	Wash-water overflow from gasification
8	Overflow effluent from the wet screening plants

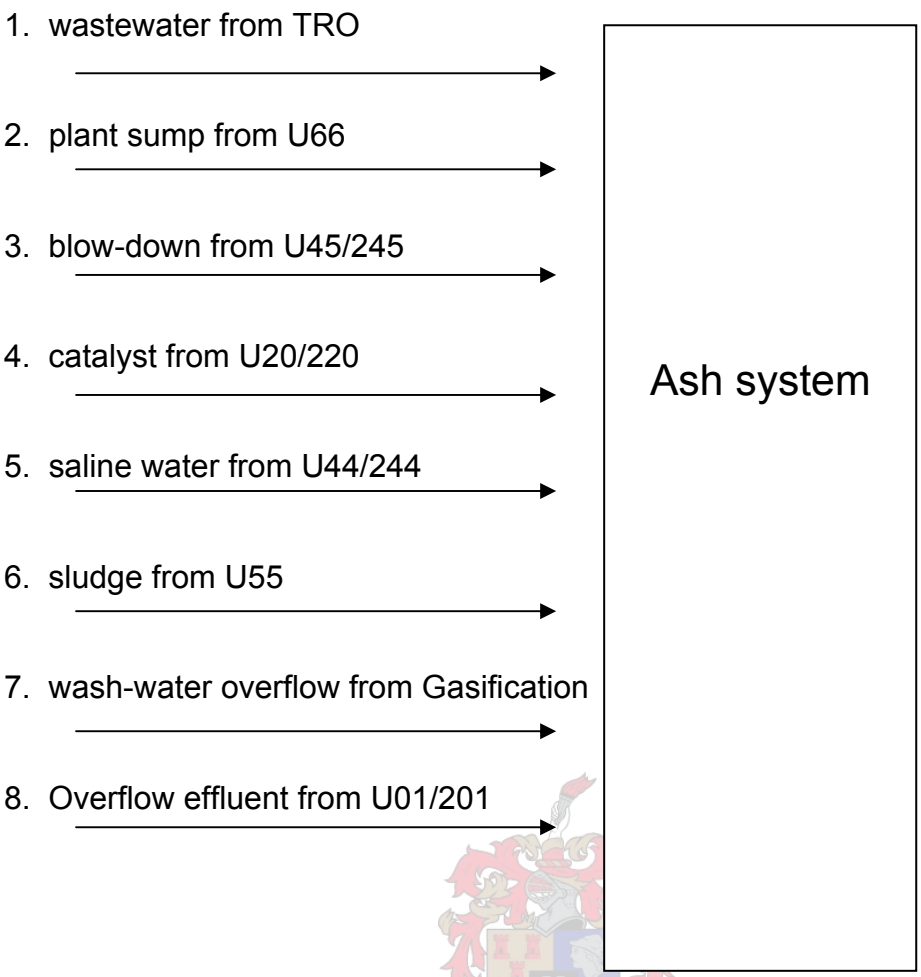

Figure 2.6: Foreign process streams entering ash system (Koch, 2002)

2.2.2 Description of Phases in the Sasol Secunda ash disposal system

To describe the different reactions that may occur in the ash system better it was divided into phases. Koch (2002) described the different phases as follows:

Phase 1: The initial contact of the ash with the ash water at Power Station.

Phase 2: The time the ash spends in contact with the water (i.e. from the point where the slurry is pumped from Inside Ash, to the penstock over-flow from the ash dams).

Phase 3: The period of time the ash water spends in the evaporation and CAE dams before being recycled to the factories for re-use in the ash water system.

The three different phases can be seen in Figure 2.7.

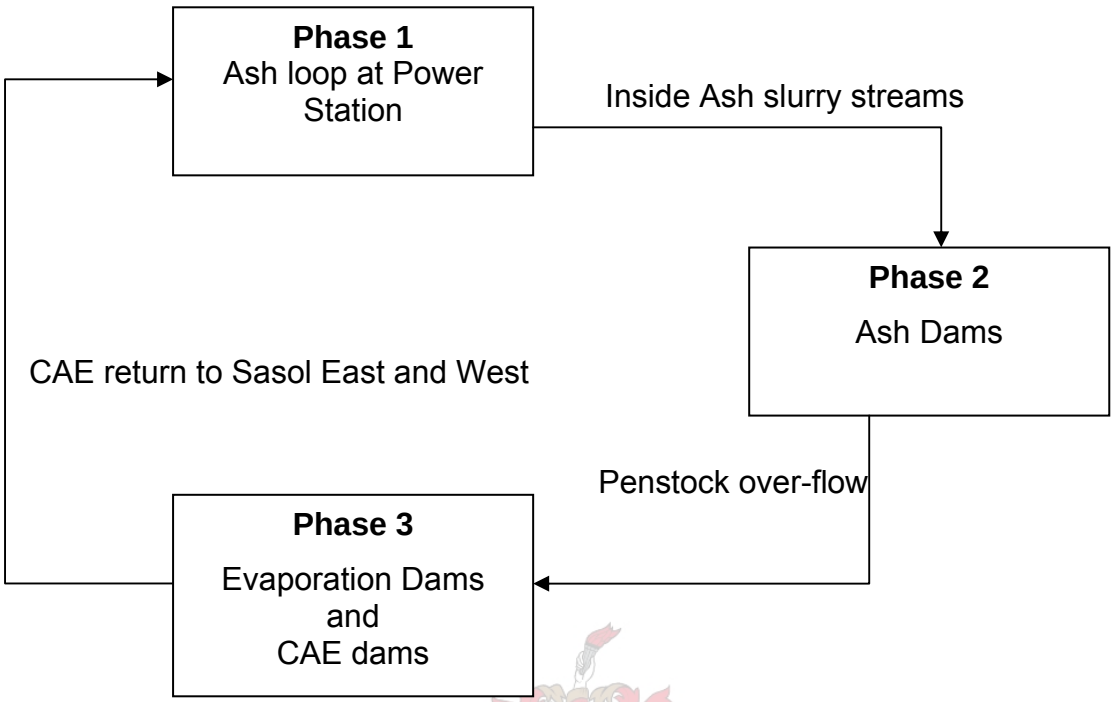

Figure 2.7: Phase identification diagram

2.2.3 Composition of fine ash

The ash composition depends on the composition of the coal from which the ash is produced. Koch (2002) found that the fine ash that is found in the Sasol Secunda Ash disposal system is a combination of the following types of ash:

62% fly ash
26% fine ash from gasification
12% bottom ash

The chemical composition found by Koch (2002) is displayed in the Figure 2.8 below.

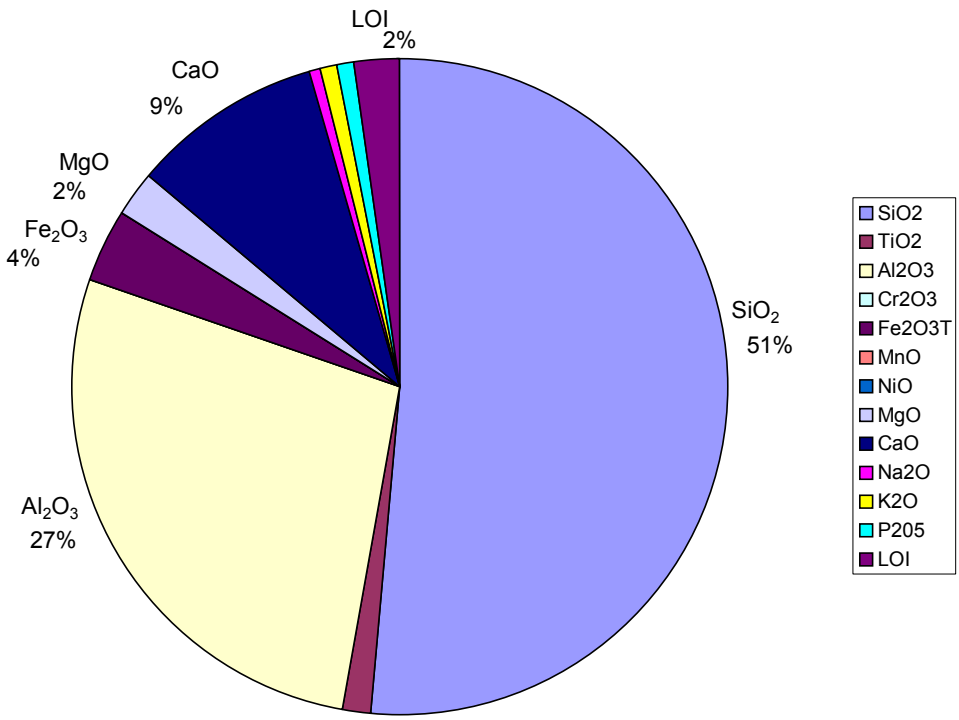

Figure 2.8: Fine ash composition (Koch, 2002)

2.3 Chemical elements

The most important chemical elements in the Sasol Secunda Ash disposal system are Ca, Na, Cl and SO_4. Most of the chemical interactions occur with the Ca and SO_4 and therefore, they are discussed here.

2.3.1 Calcium

Calcium is not a volatile component and the amount of calcium found in the ash and the parent coal is quite similar. The oxidation state of the calcium is +2 in the solid and aqueous phase (Koch, 2002). Dhanpat et al. (1986) found that most of the calcium present in coal is in the inorganic phase and that only a small amount is found in the organic phase.

Before the calcium chemistry can be analysed, the origin of Ca in ash must be investigated. The following was found:

- CaO and $CaSO_4$ occur as small particles with a higher density as the aluminosilicate spheres or are attached to the larger glassy spheres in the fresh ash (Jones, 1995).
- Dhanpat et al. (1986) found that CaO is formed by the decarbonisation of $CaCO_3$ in the coal.

Chemical reactions

There are four main compounds, which are of importance in the calcium chemistry. They are CaO, $CaCO_3$, $CaSO_4.2H_2O$ and $Ca(OH)_2$. Of these compounds CaO is the most soluble. In an alkaline environment $CaCO_3$ is the least soluble and will precipitate quickly. It was found that $CaCO_3$ controls the Ca concentration in an alkaline environment and that $CaSO_4.2H_2O$ controls the Ca concentration in an acidic environment (Dhanpat et al., 1986). CO_2 also plays an important part in the chemistry as will be shown by the following reactions:

$$CaO_{(s)} + H_2O \rightarrow Ca(OH)_2 \qquad [2.1]$$

$$CO_2 + H_2O \rightarrow H_2CO_3 \qquad [2.2]$$

$$Ca(OH)_2 + H_2CO_3 \rightarrow CaCO_3 \qquad [2.3]$$

This $CaCO_3$ chemistry is widely supported by the literature. The most important ones reported by Koch (2002) are given here:

- The solubility of Ca is pH dependant because the solubility of $CaCO_3$ is dependant on the pH. $CaCO_3$ therefore controls the concentration of the calcium (Hassett et al., 1984).
- Formation of a $CaCO_3$ solid phase may be controlled by the availability of CO_2 (Villaume et al., 1987).

- Dhanpat et al. (1986) reported that calcite and $CaSO_4.H_2O$ are present in both weathered and unweathered ash.

Stability and solubility

Fytianos et. al. (1998) found that calcium is the metal that has the highest leachability. The experiments were done on fly ash from coal combustion, which were taken from four different locations in Greece. The fly ashes produced a strong alkaline environment that is similar to that of the Sasol Secunda ash disposal system.

Calcium is one of the most important elements in the Sasol Secunda ash disposal system. This makes it important to know what type of reactions Ca can undergo in the presence of water. The information found in Table 2.5 and Figures 2.9 and 2.10 provides a better understanding of the stability of Ca in a water environment. Ca is unstable in the presence of water and has a great affinity to react with water. The anhydrous oxide CaO is also unstable in water and tends to become hydrated.

Pourbaix (1966) gave the following information pertaining to Ca reaction equations in a water environment:

Table 2.4: Different forms of Calcium

Calcium			
Occurrence	**Oxidation number**	**Species**	**Name**
Solid Substances	-2	CaH_2	calcium hydride
	0	Ca	calcium
	2	CaO hydr.	hydroxide
	2	CaO anh.	anhydrous calcium oxide
Dissolved Substances	4	CaO_2	calcium peroxide
	2	Ca^{2+}	Divalent calcium ion

Two Solid Substances:

$$CaH_2 \leftrightarrow Ca + 2H^+ + 2e^- \quad [2.4]$$

$$CaH_2 + H_2O \leftrightarrow CaO + 4H^+ + 4e^- \quad [2.5]$$

$$Ca + H_2O \leftrightarrow CaO + 2H^+ + 2e^- \quad [2.6]$$

$$CaO + H_2O \leftrightarrow CaO_2 + 2H^+ + 2e^- \quad [2.7]$$

One Solid Substance and One Dissolved Substance:

$$Ca^{2+} + H_2O \leftrightarrow CaO + 2H^+ \quad [2.8]$$

$$CaH_2 \leftrightarrow Ca^{2+} + 2H^+ + 4e^- \quad [2.9]$$

$$Ca \leftrightarrow Ca^{2+} + 2e^- \quad [2.10]$$

$$Ca^{2+} + 2H_2O \leftrightarrow CaO_2 + 4H^+ + 2e^- \quad [2.11]$$

Figure 2.9 is a potential-pH diagram for a calcium-water system. Figure 2.10 indicates the effect that the pH has on the solubility of Ca confirming the dominance of $CaCO_3$ species at a high pH. Table 2.5 indicates the reactions which lead to the formation of the substances on Figure 2.9.

Table 2.5: Numbers in Figures 2.9 and 2.10, and corresponding reaction

Number in figures 2.9 and 2.10	Corresponding reaction
1	[2.4]
2	[2.5]
3	[2.6]
4	[2.7]
5	[2.8]
6	[2.9]
7	[2.10]
8	[2.11]

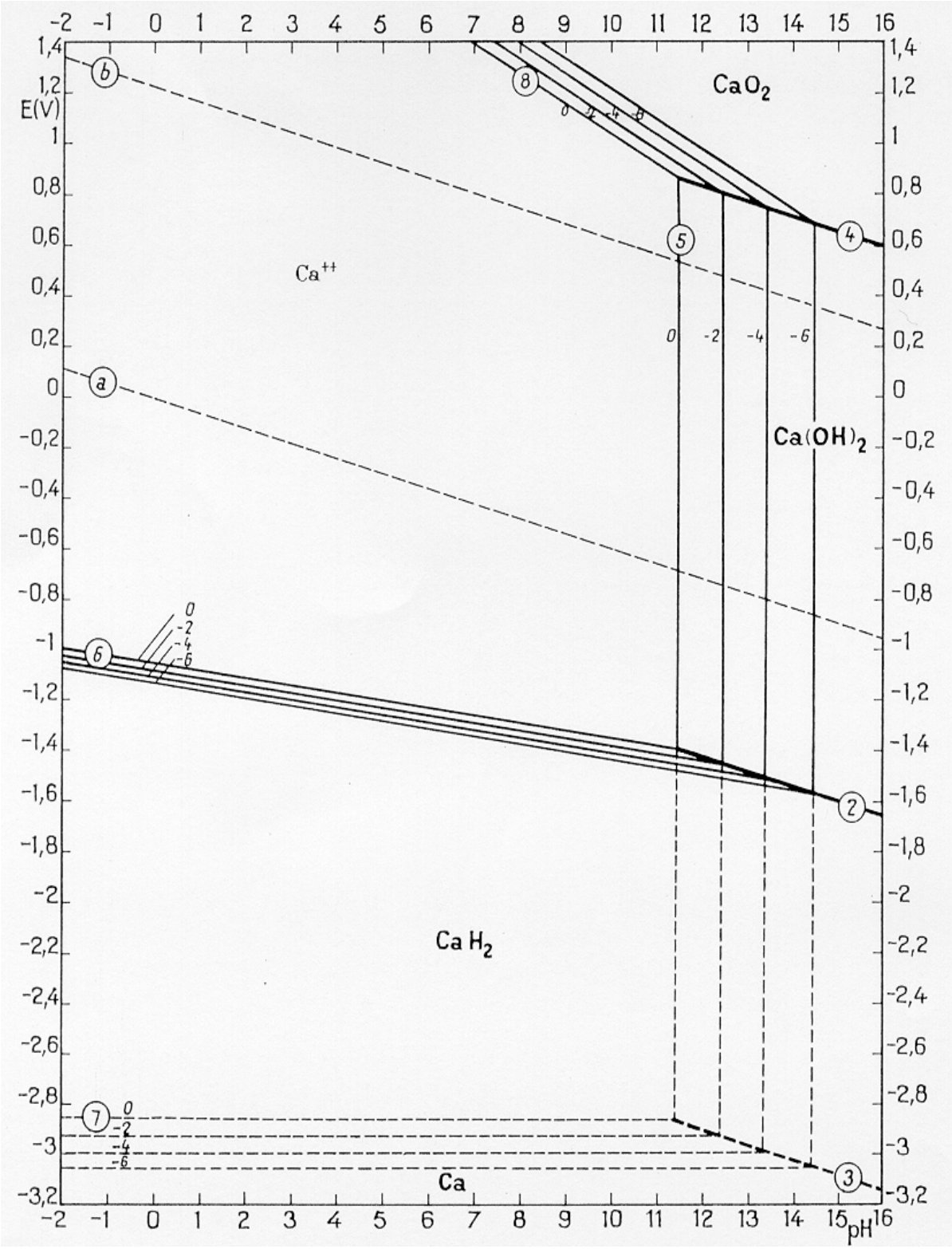

Figure 2.9: Potential-pH equilibrium diagram for the calcium-water system, at 25°C (Pourbaix, 1966)

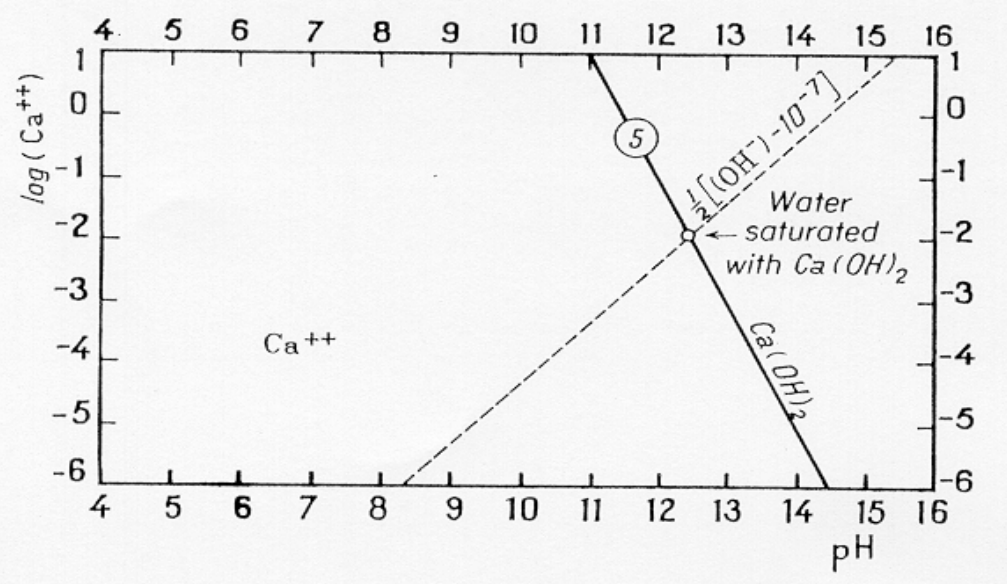

Figure 2.10: Influence of pH on the solubility of $Ca(OH)_2$ at 25°C (Pourbaix, 1966)

If the potential and pH of the solution is known this point can be found on the potential-pH diagram. All the reactions below this point can only take place in the oxidation direction. The reactions above the point can only take place in the reduction direction (Koch 2002).

Mineral phases

In fly ash there are a lot of minerals that contain calcium. Table 2.6 found in Dhanpat et al. (1986) gives an overview of the different minerals.

The unpredictability of the Sasol Secunda ash disposal system makes it impossible to predict all the mineral phases that may be found in the ash. Calcite, anhydrite, gypsum and ettringite are the most important minerals studied in this project.

Table 2.6: Possible mineral phases containing calcium

Unweathered Ash		Weathered Ash		
Predicted	**Observed**	**Predicted**	**Observed**	**Mineral name**
$CaCO_3$	$CaCO_3$	$CaCO_3$	$CaCO_3$	Calcite
$CaSO_4$	$CaSO_4$	$CaSO_4$		Anhydrite
CaO	CaO			Lime
	$CaSO_4.2H_2O$		$CaSO_4.2H_2O$	Gypsum
	$Ca(OH)_2$	$Ca(OH)_2$	$Ca(OH)_2$	Portlandite
	Ca-Ferrite			
	Ca_2SiO_4			Bredigite
	Ca_3SiO_5			
	$Ca_3Al_2O_6$			
	$CaSiO_3$			Wollastonite
	$CaMgSi_2O_6$			Diopside
	$Ca_2MgSi_2O_7$			Melilite
	$Ca_3Mg(SiO_4)_2$			Merwinite
	Ca_3SiO_5			Alite
	$Ca_6Al_4Fe_2O_{15}$			Brownmillerite
	$CaMg(CO_3)_2$	$CaMg(CO_3)_2$		Dolomite
		$CaAl_2Si_4O_{12}.4H_2O$		Laumontite
		$Ca_6Al_2(SO_4)_3(OH)_{12}.26H_2O$	$Ca_6Al_2(SO_4)_3(OH)_{12}.26H_2O$	Ettringite
			Ca-silicate	
			Ca-aluminate	

2.3.2 Sulphur

In general, sulphate is the main component in fly ash that contains sulphur (Hassett et al., 1985.) They also found that reasonable amounts of sulphate could be extracted from the ash. This primary extraction subsided within a few days and it is suggested that the sulphate concentration was controlled by a secondary solid phase. No decrease in the sulphate concentration was found in the leachate.

A MINTEQA2 speciation done by Bezuidenhout (1995) indicated that the liquid phase was under-saturated with respect to gypsum. This was strange because he found a decrease in the SO_4 concentration. A possible explanation suggested by him was the formation of a less soluble SO_4

containing a mineral such as ettringite. The formation of ettringite was confirmed by borehole analysis done by Koch (2002) on the fine ash dams at the Sasol Secunda ash disposal system.

Mineral phases

Table 2.7 indicates mineral phases containing SO_4 that may be found in fly ash (Adapted from Dhanpat et.al., 1986).

Table 2.7: Sulphate containing minerals in fly ash

Mineral	Formula
Anhydrite	$CaSO_4$
Gypsum	$CaSO_4.2H_2O$
Ettringite	$Ca_6Al_2(SO_4)_3(OH)_{12}.26H_2O$

2.4 Chemical interaction

Ash water systems in general are very complex and the Sasol Secunda ash water system is no exception. It may be helpful to discuss previous research done on the ash water interaction. It can help to better understand the chemical interaction in the Sasol Secunda Ash disposal system.

The interference of foreign ions has a big influence on the solubility and precipitation of different ions. In almost all the cases the solubility of a precipitate is higher when there are other ions in the solution (NALCO, 1988). An example is Ca, which can precipitate with trace amounts of strontium forming a $CaCO_3$ crystalline form more soluble than calcite. They also found that the ionic strength of a solution, especially that from ions that are not included in the precipitate, influences the solubility of slightly soluble compounds. This makes $CaSO_4$ more soluble in seawater than in fresh water. A high ionic strength increases the solubility of slightly soluble compounds like $CaCO_3$ and $CaSO_4$ (NALCO, 1988).

The electrical conductivity (EC) is a measure of a solution's ability to carry an electrical current. This may differ with the number and type of ions in the solution (Sawyer, 1978). A high EC does, however, show that the mineral phases in the solution is less completely ionised. This decreases the activity coefficient, increasing the solubility of the slightly soluble compounds (NALCO, 1988). There is also a relationship between the conductivity and the TDS in a solution. Care must however be taken because there may be some un-ionised species, which is part of the TDS, that cannot convey a current (Sawyer, 1978).

Sheikholeslami (2001) investigated the effect that different salts have on each other's solubility and the effect of this on the prediction of precipitation. It was found that even small amounts of another precipitating salt affects the thermodynamics and scale structure of all the other precipitating salts. This renders the solubility data of the pure salts useless in complex salty mixtures such as found in the Sasol Secunda ash disposal system.

Singh and Kolay (2001) investigated the influence of the ash water interaction on the physical, chemical and mineralogical characteristics of the ash. The following important findings pertaining to the chemical characteristics were made:

- Activation with NaOH leads to the formation of zeolites, while the KOH activation produces no zeolites. The purpose of the activation is to promote the growth of crystalline zeolites.
- The NaOH activation increased the specific gravity, specific surface area and the cation exchange capacity of the ash.
- Absorption of water also increased and this could be attributed to the increase in the porosity and void ratio. The effect of this is that the compression index of the ash also increases.
- Finally the contact between the ash and the water increases the heavy metal removal ability of the ash.

In conclusion (Singh and Kolay, 2001) found that the ash water interaction changes the physical, chemical and mineralogical characteristics of the ash to such an extent that the ash cannot be used as a fill material. It can still be used for the treatment of polluted water and for the retention of heavy metals.

Pretorius & Nieuwenhuis (2002) developed a conceptual model of the processes in an ash-water contact environment. Figure 2.11 gives a graphic representation of the different processes:

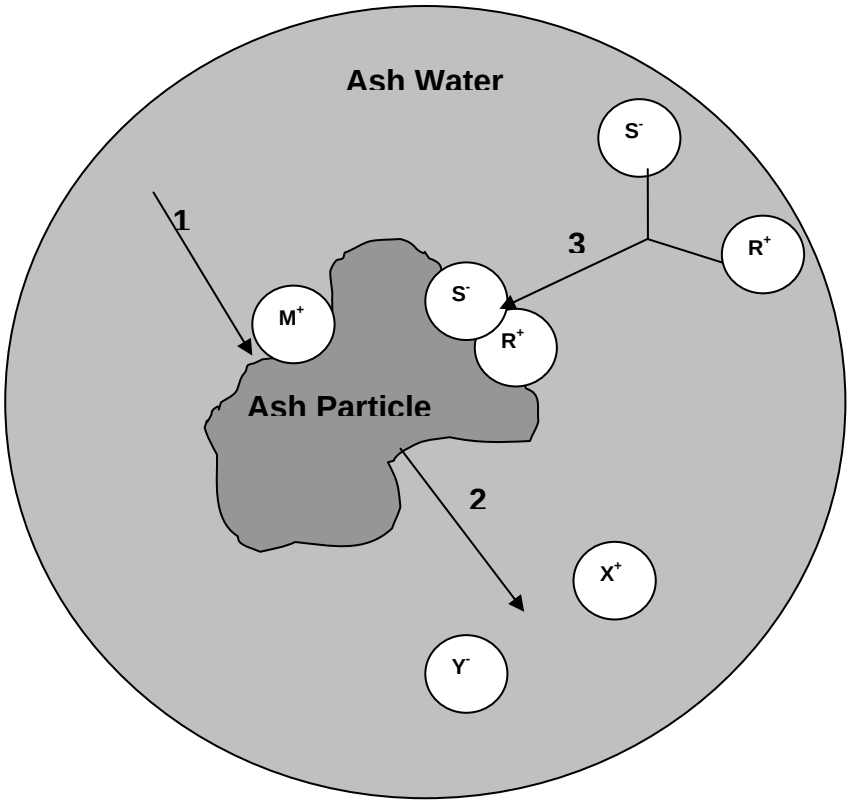

Figure 2.11: Processes occurring in the ash water environment (Pretorius and Nieuwenhuis, 2002)

The different processes can be described as follows:

- Process 1 is adsorption. Electrostatic interactions between the ionic components and the ash particles let ions adsorb onto the ash particles (Singh & Kolay, 2001).

- Process 2 is dissolution. This produces the leaching of the soluble minerals into the liquid phase (Bezuidenhout, 1995).
- Process 3 is precipitation. The changes in the water chemistry after the contact with the ash may result in the precipitation of certain minerals such as CaF_2 and $MnCO_3$ (Nel, 1996).

Roy et.al. (1984) conducted a study to find possible reactions that produce the elements found in fly ash leachate. Figure 2.12 gives the chemical reactions proposed by Roy and Griffin (1984).

Initial contact to 24 hours:

$$MO + H_2O \rightarrow M^{2+} + 2OH^- \quad [2.12]$$
(M = Ca, Mg,...)

$$J_2O + H_2O \rightarrow 2J^+ + 2OH^- \quad [2.13]$$
(J = Na, K,...)

$$Al_6Si_2O_{13} + 19H_2O \rightarrow 6Al(OH)_4^- + 2H_4SiO_4^0 + 6H^+ \quad [2.14]$$

$$6Al(OH)_4^- \rightarrow 6AlO(OH) + H_2O + 6OH^- \quad [2.15]$$

Figure 2.12: Proposed chemical reactions for initial contact (Roy et.al., 1984)

The reactions described in Figure 2.12, especially [2.12] and [2.13] are an indication of the initial leaching experienced when the fine ash is mixed with the ash water in the Sasol Secunda ash disposal system. This leaching contributes to the increase in the Ca, Na and TDS concentrations in the ash water.

Jones (1995) found that processes with fast reaction kinetics control the reactions during the initial mixing of the ash and the liquid phase. In systems where the transport medium is recycled and already saturated with respect to secondary mineral phases, these could precipitate on the surface of the ash

particles. The Sasol Secunda ash disposal system is a system where the transport medium is recycled and this may be a reason for the decrease in some of the elements in the ash water. This is discussed in Chapter 3.

2.4.1 Calcium

Calcium is one of the most important elements in the ash water system. A lot of the chemistry is focused around calcium as discussed in Koch (2002). Reactions pertaining to calcium are described in section 2.3.1 reactions 2.1, 2.2 and 2.3.

This is a very simple representation of the chemical reactions for the formation of calcite, which is the main factor for the removal of calcium from the ash water in the Sasol Secunda ash disposal system. Increasing the calcite formation will increase the Ca precipitation in the system. It may be done through the introduction of CO_2 into the system which will be discussed in a later section.

Calcium also reacts with the sulphate in the effluent to produce mineral phases like anhydrite and gypsum. The chemical reactions are given in the discussion of sulphate interactions.

2.4.2 Sulphate

The chemical interaction, which involves sulphate usually, involves calcium as well. Reactions in which anhydrite and gypsum are formed are as follows:

$$Ca^{2+} + SO_4{}^{2-} \leftrightarrow CaSO_4 \qquad [2.16]$$

$$Ca^{2+} + SO_4{}^{2-} + 2H_2O \leftrightarrow CaSO_4.2H_2O \qquad [2.17]$$

It is possible for these reactions to take place at the mixing of the ash and effluent in a wet ash disposal system (Jones, 1995).

Another form of sulphate reduction was reported by Drever (1988). He found that if there is sufficient suitable organic matter in the sediments, anaerobic bacteria can reduce sulphate ions to form sulphide species. Iron containing minerals then react with the sulphide species. The process is described by the following reaction:

$$2Fe_2O_3 + 8SO_4^{2-} + 15C + 7H_2O \leftrightarrow 4FeS_2 + 14HCO_3^{-} + CO_3^{2-} \qquad [2.18]$$

At the Sasol Secunda ash disposal system the concentration of Fe in the ash and ash water are very low, therefore this reaction may only take place in concentrations which may be too small to measure.

2.4.3 CO_2 addition

In order to understand the formation of calcite and the reason of pure CO_2 addition to an ash disposal system the CO_2-water chemistry needs to be understood. Bezuidenhout (1995) gives a detailed series of the reactions pertaining to the reaction between water and CO_2:

$$CO_2(g) + H_2O \leftrightarrow CO_2(aq) + H_2O \qquad [2.19]$$

$$CO_2(aq) + H_2O \leftrightarrow H_2CO_3 \qquad [2.20]$$

$$H_2CO_3 \leftrightarrow H^+ + HCO_3^{-} \qquad [2.21]$$

$$HCO3^{-} \leftrightarrow H^+ + CO_3^{2-} \qquad [2.22]$$

The carbonate ions then react with the calcium to form calcite as shown in the calcium section. These reactions are pH dependant. At pH < 4 reaction 2.20 takes place which turns the CO_2 into H_2CO_3. If the pH is between 4 and 8.2, reaction 2.21 is the main reaction that takes place. When the pH gets above 8.2, reaction 2.22 is the main reaction. For a pH above 12 all the CO_2 is converted into CO_3^{2-} ions (NALCO, 1988).

2.4.4 Le Châtelier's principle

Le Châtelier's principle states that for reaction equilibrium in a dilute solution, addition of a small amount of a solute species that participates in the reaction, will shift the equilibrium in the direction that uses up some of the solute (McGraw-Hill, 1987).

This principle plays an important part in the precipitation of calcite in the Evaporation and CAE dams of the Sasol Secunda Ash disposal system. An increase in the concentration of Ca in the CAE will have the same effect as the addition of a small amount of solute and will therefore, force the precipitation reaction to the right and increase the calcite precipitation.

2.5 Previous experimental work

Most of the bench-scale experimental work that was previously done on the Sasol Secunda ash disposal system concentrated on simulating the ash dam operation and was therefore column experiments. The addition of CO_2 and the mixing of brines with the ash were also investigated, but on a much smaller scale as performed in this project. The experiments discussed in the next section are work done on the Sasol Secunda ash disposal system and also other experimental work performed on the ash disposal systems in general.

2.5.1 Column experiments

Many investigations used columns to determine the amount of salt leaching into the wet ash disposal systems. It is also important to note that these investigations cannot provide enough information about the kinetic, thermodynamic and geochemical processes that occurs in the actual ash disposal system (Koch, 2002). Care must therefore, be taken in applying

results from small-scale experiments to the real system. This is confirmed by Peterson (1998), who states that slow reaction mechanisms may not be noticeable in laboratory experiments, but may be visible in the ash disposal system over an extended time.

Roy et al. (1984) and Jones (1995) investigated alkaline ash systems with column experiments and found that there was a decrease in Ca and SO_4 concentrations. It was suggested through thermodynamic modeling that $CaSO_4$ and $CaCO_3$ controlled the Ca^{2+} concentration.

The most important work pertaining to the Sasol Secunda ash disposal system was done by Koch (2002) and Pretorius and Nieuwenhuis (2002). Koch (2002) found that the most important elements in the ash disposal system are Ca, Na, Cl, and SO_4. It was also found that SO_4 is retained in a stable phase in the ash and that the system may be used as a salt sink for SO_4. Ca is initially leached from the ash to the ash water and later removed from the effluent through calcite precipitation.

It was found that there are more radical changes taking place in the ash water than in the ash. Mullite, quartz, calcite, sillimanite and small amounts of hematite are the main mineral phases in the ash (Koch, 2002). The main immediate change that takes place in the ash of the Sasol Secunda ash disposal system is the conversion of CaO (lime) to $CaCO_3$ (calcite).

Pretorius and Nieuwenhuis (2002) also did column tests on the Sasol Secunda ash disposal system. It were found that the mixing of brines and ash lead to the removal of salts from the brines. The salts were remobilised by rainwater percolating through the ash beds. The $CaCO_3$ precipitation was the only form of permanent retention found (Pretorius and Nieuwenhuis, 2002).

2.5.2 CO_2 addition

Exposing the columns under different atmospheres was also investigated by Pretorius and Nieuwenhuis (2002). The results obtained for the CO_2

atmosphere show a much larger decrease in the TDS and Ca^{2+} concentration of the effluent in comparison with the air and N_2 atmospheres. They also concluded that the active addition of CO_2 to the system could be used to increase salt retention because of the prevention of Ca leaching through calcite precipitation.

Yasuda et al. (1996) used CO_2 on municipal incinerator fly ash to convert the heavy metal salts into insoluble carbonates. These carbonates were then removed and immobilised in a slag.

2.5.3 Brine addition

De Villiers (2001) investigated the effect of the mixing of TRO brine with the fine ash slurry, fine ash dam (FAD) overflow and evaporation dam water. These experiments were conducted on a bench scale. No significant changes in the composition of the water or precipitation were observed in the first 24 hours. Small amounts of calcite precipitation were observed in the fine ash slurry and TRO mixture.

2.5.4 Liquid:Solids ratio

The Liquid:Solids (L:S) mass ratio plays an important role in the controlling of the pH and the leaching of different elements (Hassett et al., 1985). They found that low L:S ratios produced high pH values and vice versa. In experiments done by Koch (2002) a L:S ratio of 5:1 was used. This was to simulate the actual conditions at the Sasol Secunda ash disposal system. The pH of the leachate was around 12.

Hasset et al. (1985) achieved a pH of around 13 with a L:S ratio of 2:1 and a pH of around 10 with a L:S ratio of 10:1. This is in accordance with the values that Koch (2002) found. In order to keep to the industrial conditions at the Sasol Secunda ash disposal system, a L:S ratio of 5:1 was used for this project.

The L:S ratio influences the pH by increasing or decreasing the amount of salts leaching into the ash water. The pH has an effect on the solubility of the different elements in the ash water. It is important to keep that in mind when making changes to the L:S ratio of an ash disposal system.

2.5.5 pH

As mentioned previously, the pH is an important factor in the ash system chemistry. Shen-Yu and Zwane (2001) found it to be a main factor in influencing the solubility of a great array of solids.

Coal that is used for combustion in South Africa has a low sulphur content and therefore the leachate that is produced, is an alkaline one (Bezuidenhout, 1995). The fine ash slurry at Sasol Secunda ash disposal system has a pH value of about 12 and this is confirmation of the low sulphur content of South African coal. Almost 70% of fly ashes produce a neutral or alkaline leachate (Koch, 2002).

The ash slurry at the Sasol Secunda ash disposal system has a very high pH. A decrease in the pH of the ash slurry at Sasol Secunda ash disposal system occurs as it moves through Phase 2 and Phase 3 of the Sasol Secunda ash disposal system and this can be attributed to the recarbonation of the CaO to form $CaCO_3$ (Koch, 2002).

2.6 Experimental design

According to Montgomery (1984) experiments are done to investigate the effect of several factors on a system or to discover something new about a particular system. The objective of the experiment may either be the confirmation of existing knowledge or the exploration of something new.

Montgomery (1984) also states that the statistical design of the experiment is a process of planning the experiment so that appropriate data are collected. This data can then be used in the statistical analysis to produce valid, objective and representative conclusions.

2.6.1 Phase 1

A mixture experiment is classified as an experiment in which two or more ingredients are mixed or blended together to form an end product (Ghosh, 1990). The characteristics of this end product are used as the measure to evaluate the different mixtures.

Different mixtures are used in the Phase 1 experiments and the design of mixture experiments was used as basis for the design of the Phase 1 experiments. The mixtures in these experiments contain three components. These components are CAE, fine ash and brine.

A simple design to investigate the response of different components over the entire simplex region is one where the points are positioned uniformly over the simplex factor space (Ghosh, 1990). In the case of the Phase 1 experiments the simplex factor space is a triangle with the three components on the three corners of the triangle.

Figure 2.13 (Ghosh, 1990) is a graphic demonstration of the different combinations that have to be investigated in a mixture experimental design. The numbers in the boxes indicate the fraction of each substance for each experiment. In this case the first number is the fraction ash, the second the fraction brine and the third the fraction CAE. A limit can be put on each component to decrease the area over which the experiments needs to be done.

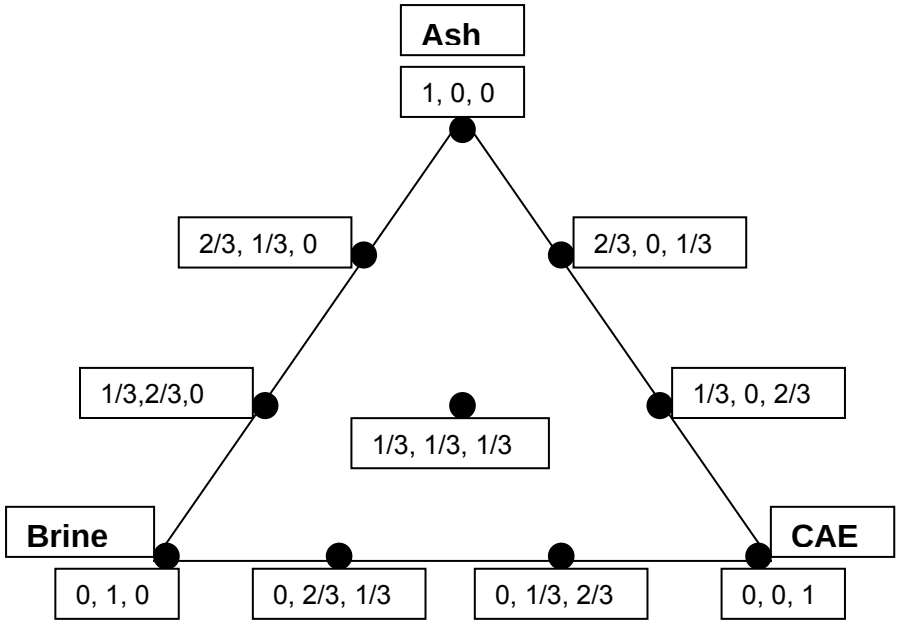

Figure 2.13: Experimental design for the whole simplex region

2.6.2 Phase 3

The Phase 3 experiments involve the investigation of the effects of different treatments on the Sasol Secunda ash disposal system and also combinations of these treatments. When two or more factors are investigated in an experiment, a factorial design is the most efficient type of experimental design.

Factorial design is also useful when there is interaction between the different factors in the experiment. A problem with factorial designs is that an increase in the number of factors investigated greatly increases the number of experiments that have to be done to completely replicate the design (Montgomery, 1984). These multi-factor experiments can be simplified by only allowing two levels for each of the factors (Garcia-Diaz & Philips, 1995). Unfortunately the problem with regards to the number of experiments is not solved with this.

The most commonly used method to decrease the number of experiments is by neglecting the higher order interactions and to focus only on the lower order interactions. This is called a fractional factorial design (Montgomery, 1984). Only a fraction of the experimental conditions is sampled and main effects are estimated under the assumption that the higher order interactions are negligible (Garcia-Diaz & Philips, 1995).

Experiments like this are also known as screening experiments (Montgomery, 1984). This type of design is the most suitable experimental design for the Phase 3 experiments. Through the screening process the main factors that influence the system can be identified and the focus can then shift to these factors in more detailed experiments.

All the above was taken into account in designing the experiments for Phase 3. The factors will only be investigated on two levels and the third order interactions are not taken into account.

The following factors are investigated in the experiments:

(a)	Evaporation rate	(High/Low)
(b)	Adding a chemical substance	(Addition/No addition)
(c)	CO_2 addition through air	(Addition/No addition)
(d)	Adding nets to enhance precipitation	(Addition/No addition)

In a normal factorial design 16 experiments will have to be done to investigate 4 different factors. With the fractional factorial design these the amount of experiments can be reduced to 8.

Table 2.8 shows the implementation of the factors.

Table 2.8: Phase 3 experimental design

a	b	c	d = abc	Combination
-	-	-	-	(1)
+	-	-	+	ad
-	+	-	+	bd
+	+	-	-	ab
-	-	+	+	cd
+	-	+	-	ac
-	+	+	-	bc
+	+	+	+	abcd

(+ = High/Addition - = Low/No addition)

2.7 Statistics

The experimental design is done to ensure that the data from the experiments can be used statistically. To comply with the experimental design, the statistical calculations used in mixture and fractional factorial experiments are discussed.

2.7.1 Mixture experiments

The mixture experiments are a combination of 3 different substances. In the design, a triangle is used to represent the whole experimental space and the different combinations are indicated on this triangle.

The data can be fitted with a linear (2.23), quadratic (2.24) or cubic (2.25) model as it is given below (Ghosh, 1990):

$$\eta = \sum_{i=1}^{q} \beta_i x_i \qquad [2.23]$$

$$\eta = \sum_{i=1}^{q} \beta_i x_i + \sum \sum_{i<j}^{q} \beta_{ij} x_i x_j \qquad [2.24]$$

$$\eta = \sum_{i=1}^{q} \beta_i x_i + \sum \sum_{i<j}^{q} \beta_{ij} x_i x_j + \sum \sum_{i<j<k} \sum^{q} \beta_{ijk} x_i x_j x_k \qquad [2.25]$$

The amount of points that must be investigated is given by the formula $2^q - 1$, where q is the number of substances in the mixture.

2.7.2 Fractional factorial experiments

The experiments on Phase 3 are fractional factorial experiments. These are usually used as screening experiments to identify the main factors that have an influence on a certain system. In these experiments the higher order interactions are not taken into account (Montgomery, 1984). Table 2.9 shows the design:

Table 2.9: Phase 3 statistical experimental design

a	b	c	d = abc	Combination	Result
-	-	-	-	(1)	A
+	-	-	+	ad	B
-	+	-	+	bd	C
+	+	-	-	ab	D
-	-	+	+	cd	E
+	-	+	-	ac	F
-	+	+	-	bc	G
+	+	+	+	abcd	H

(+ = High/Addition - = Low/No addition)

The influences that each factor (ℓ_A) and second order interaction (ℓ_{AB}) have can then be calculated as follows:

$$\ell_A = \tfrac{1}{4}(-A + B - C + D - E + F - G + H) \quad [2.26]$$

$$\ell_{AB} = \tfrac{1}{4}(A - B - C + D + E - F - G + H) \quad [2.27]$$

The other factors can be calculated in the same way. With these results, the factors and combination of factors that have the biggest influence can be identified.

2.8 Summary

The literature review gives an overview of the general conditions in a wet ash disposal system. Previous experimental work was also discussed. This work includes experimental work performed on the Sasol Secunda ash disposal system and also experimental work performed on similar ash disposal systems. The focus in this project is on the Sasol Secunda ash disposal system and therefore most of the literature discussion focused on the conditions in this system. The main aspects of the Sasol Secunda ash disposal system is the following:

- Ca, Na, Cl and SO_4 are the main elements in the ash water (CAE) of the ash disposal system.
- The formation of $CaCO_3$ is the main product formed in precipitation of insoluble solids in the ash disposal system.
- Previous experimental work conducted on the system showed a decrease in the Ca and SO_4 ions in solution.

After investigating the chemical interaction, which has an influence on the chemistry in the ash disposal system, the following main factors came to the fore:

- Fast reaction kinetics dominates the initial leaching of salts into the ash water.

- The prediction of solubilties is complicated by the presence of foreign ions and high ionic strengths.
- The addition of CO_2 might be the best way to increase $CaCO_3$ precipitation at the initial mixing.

The experimental design and statistics was also discussed.

In the next chapter the experimental work done on Phase 1 of the Sasol Secunda ash disposal system is discussed. The focus is on the mixing of the TRO and EDR brine with the ash and the addition of CO_2 to the system.

Chapter 3

Phase 1 Experiments:

Brine, CAE and ash mixing

As mentioned previously, Phase 1 represents the first contact point between the ash and the CAE at the Power Station (Figure 3.1). This is where close interaction between the ash and CAE takes place because of the high turbulence in the flows of the CAE and ash slurry. The fact that the ash is hot (~260°C) enhances these interactions. It is therefore, also the ideal place to enhance the salt removal/retention or immobilisation capabilities of the ash system. This is especially advantageous because solids are separated at the Inside Ash plant in thickeners.

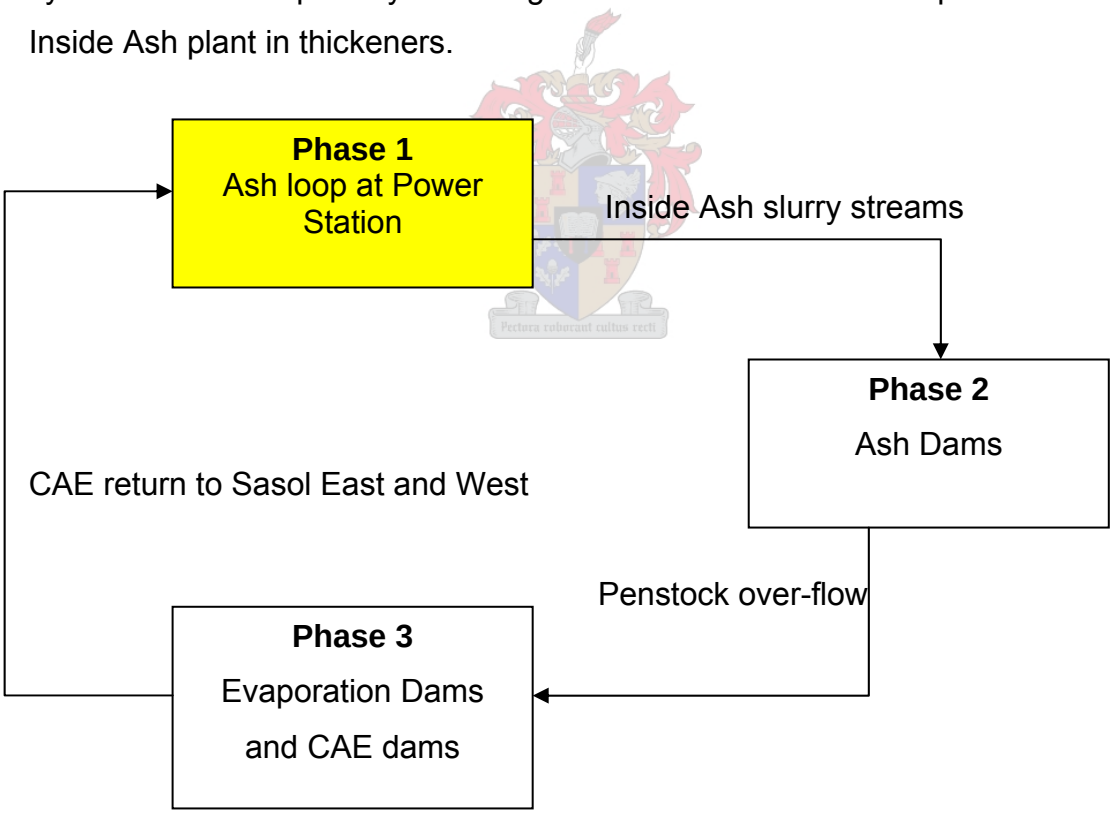

Figure 3.1: Phase 1 indication diagram

Factors that were investigated included the following:

- Effect of mixing of salt solutions (brines) with the ash.

- The effect of CO_2 addition at the mixing point.
- Effect of different durations for the CO_2 addition.

The main aim is to investigate what will happen when brines and ash are directly mixed. Previous studies on the Sasol Secunda ash disposal system found that large amounts of calcium are leached from the ash into the system. The effect of CO_2 addition was evaluated to prevent the Ca leaching through $CaCO_3$ precipitation.

The experimental results obtained through these experiments give an indication of what may happen in the ash system. Care must be taken when using this information, because the real ash disposal system is much more complex.

3.1 Experimental design

The Phase 1 experiments included 3 different substances. These substances were the CAE, a salt solution (brine) and ash. The experiments could therefore, be seen as mixture experiments. Ghosh (1990) provided a design for mixture experiments.

3.1.1 Mixture experiment design

A mixture experiment is classified as an experiment in which two or more ingredients are mixed or blended together to form an end product (Ghosh, 1990). Usually the characteristics of the end product are used to determine the best mixture. In these experiments the amount of salt removal or the prevention of leaching was used as the measure to evaluate the different mixtures.

Different mixtures were used in the Phase 1 experiments and the design of mixture experiments was used as basis for the design of the Phase 1 experiments. The mixtures in these experiments contain three components. These components are CAE, ash and TRO/EDR brine.

The design that was discussed in the literature review was changed to suit the Phase 1 experiments. Limits were introduced on the amount of liquid and the amount of ash to keep the Liquids:Solids ratio at 5:1.

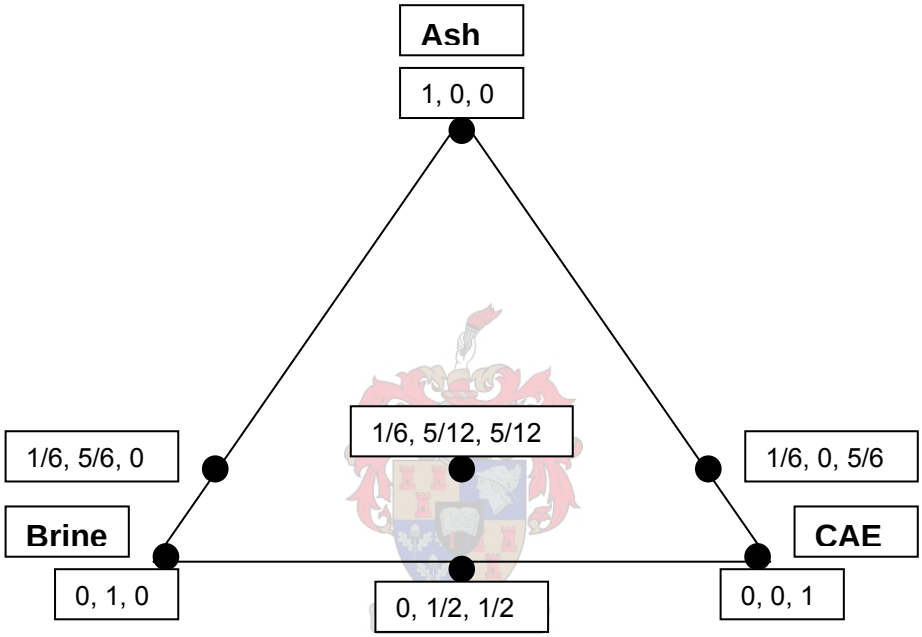

Figure 3.2: Experimental design for the Phase 1 experiments

Figure 3.2 is a graphic demonstration of the different combinations that were investigated. The first number in each box indicates the fraction ash, the second number indicates the fraction TRO/EDR brine and the third number the fraction CAE in the mixture.

3.1.2 Statistics

The changes to the experimental design made it impossible to use simple analysis methods for the statistical analyses and therefore, a computer program, Design-Expert, were used to evaluate the experimental data. This

made it possible to identify outliers and also to use the best model for the predictions.

The number of points that should be investigated is given by the formula $2^q - 1$, where q is the number of substances in the mixture. In this design seven points had to be investigated.

3.2 Experiments

3.2.1 Experimental procedure

The experiments conducted for Phase 1 involved the mixing of different brines, CAE and fine ash. It also included the addition of CO_2 at this mixing point. The main aim was to enhance the salt retention/removal capabilities of the ash system. The following was done during a typical experiment:

1. 1 kg fine ash was heated in an oven at 260ºC for 2.5 hours before the experiment was started. This is to ensure that the ash was at 260ºC. A sample of the ash was taken for analysis before it was heated.
2. The liquid phase was prepared. This involved the correct amount of brine or CAE or both being mixed. The liquid phase consisted of 5 kg of liquid. The EDR/TRO brine or CAE or a 50/50 mixture of the two made up this liquid phase. This was put into the CSTR and the stirrer started. A sample of the liquid phase was taken.
3. CO_2 was added where applicable at a rate of 6 l/min for 5, 10 or 20 minutes. A 20 minute addition is the maximum possible at the plant. It was decided to test with half and quarter of that time for comparison.
4. The hot fine ash was added quickly so that the effluent could quench it. The mixing was continued for 2.5 hours to keep by industrial conditions.
5. After the 2.5 hours the stirrer was stopped and samples of the ash and liquid phase were taken.

6. A part of the ash sample was washed (three times) with distilled water and the washed and unwashed ash samples were dried in an oven at 80ºC to constant weight.

For the experiments, which did not include ash and CO_2, steps 1, 3, 4 and 6 were omitted. For the experiments that did not include CO_2, step 3 was omitted.

Sasol supplied all the fine ash, CAE, TRO and EDR brines. All the substances are produced at the Sasol Secunda Petrochemical Plant.

3.2.2 Experimental set-up

The experimental set-up (Figure 3.3) consisted of a small SS (stainless steel) container with a stirrer. This container acted like a CSTR and was open to the atmosphere. A pipe with a valve was connected to the bottom of the container to provide a way for samples to be taken. The CO_2 was fed with a small pipe, which was attached to the inside of the container and with the outlet as close as possible to the bottom. This made sure that there was proper mixing of the CO_2 and ash slurry.

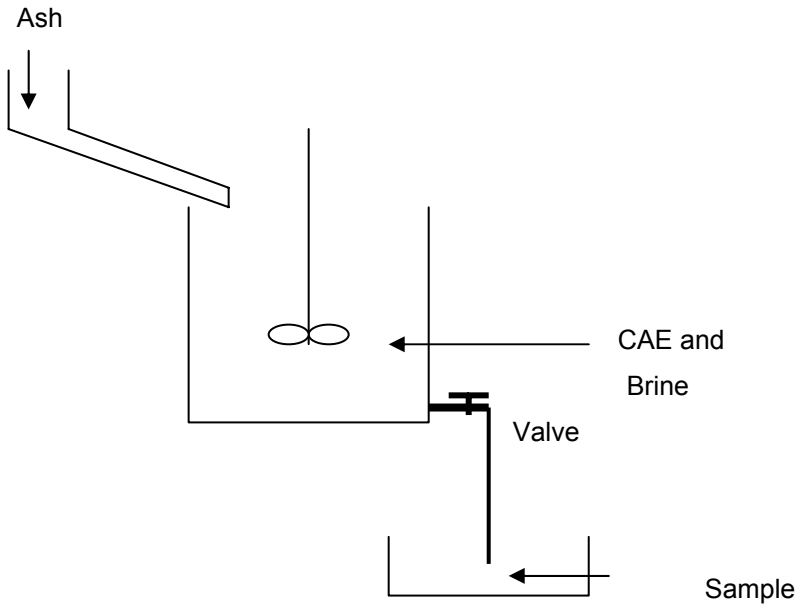

Figure 3.3: Laboratory experimental set-up

The experimental set-up was designed to simulate the initial mixing of the fine ash and the ash water (CAE) at the Power Plant. To make sure that there was a lot of turbulence during the mixing of the effluent and ash, the stirrer was operated at a high speed (~ 2000 rpm).

3.2.3 Experiments performed

All the experiments were performed according to what was needed for the adjusted mixture experimental design. The CO_2 addition experiments were done on their own to test the different addition time and the influence thereof.

All the experiments were repeated three times to test the repeatability of the results. The different experiments that were done are presented in Table 3.1.

The samples that were taken before and after the experiments were analysed for Ca, Na, Cl, SO_4 and TDS concentration. The pH and electrical conductivity (EC) were also measured. The concentrations were used to calculate the amounts (in milligrams) of the different substances in the liquid phase.

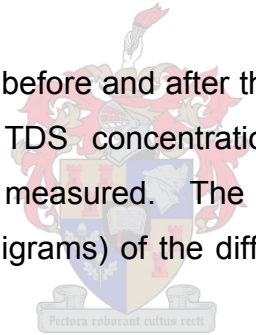

Average values for each of the experimental combinations were obtained and graphs were drawn from these results. The graphs and discussion of the results can be seen in section 3.3. From the statistical analysis (discussed in Section 3.1.2 and Chapter 2) prediction graphs for the leaching/removal of the different elements were drawn.

Ash samples were taken after each of the experiments. These samples was analysed for changes in chemical and mineralogical composition. The average values for these analyses can be seen in Table 3.7.

Table 3.1 : Phase 1 Experiments					
Exp	**Date**	**Combination**	**Exp**	**Date**	**Combination**
1	21-Oct-2003	5kg EDR + 1kg Ash	21	5-Apr-2004	5kg CAE
2	21-Oct-2003	5kg TRO + 1kg Ash	22	5-Apr-2004	5kg CAE
3	22-Oct-2003	2.5kg EDR + 2.5kg CAE + 1kg Ash	23	15-Apr-2004	5kg CAE + 1kg Ash + CO_2 (20 min)
4	22-Oct-2003	2.5kg TRO + 2.5kg CAE + 1kg Ash	24	15-Apr-2004	5kg CAE + 1kg Ash + CO_2 (20 min)
5	18-Feb-2004	5kg CAE + 1kg Ash	25	15-Apr-2004	5kg CAE + 1kg Ash + CO_2 (20 min)
6	18-Feb-2004	5kg TRO + 1kg Ash	26	16-Apr-2004	5kg CAE + 1kg Ash + CO_2 (5 min)
7	19-Feb-2004	2.5kg CAE + 2.5kg TRO + 1kg Ash	27	16-Apr-2004	5kg CAE + 1kg Ash + CO_2 (5 min)
8	19-Feb-2004	5kg CAE + 1kg Ash	28	16-Apr-2004	5kg CAE + 1kg Ash + CO_2 (5 min)
9	19-Feb-2004	5kg TRO + 1kg Ash	29	19-Apr-2004	5kg TRO
10	20-Feb-2004	2.5kg CAE + 2.5kg TRO + 1kg Ash	30	19-Apr-2004	5kg TRO
11	2-Mar-2004	5kg EDR + 1kg Ash	31	19-Apr-2004	5kg TRO
12	2-Mar-2004	5kg CAE + 1kg Ash	32	20-Apr-2004	2.5kg TRO + 2.5kg CAE
13	3-Mar-2004	2.5kg CAE + 2.5kg EDR + 1kg Ash	33	20-Apr-2004	2.5kg TRO + 2.5kg CAE
14	3-Mar-2004	5kg EDR + 1kg Ash	34	20-Apr-2004	2.5kg TRO + 2.5kg CAE
15	3-Mar-2004	5kg CAE + 1kg Ash	35	21-Apr-2004	5kg EDR
16	4-Mar-2004	2.5kg CAE + 2.5kg EDR + 1kg Ash	36	21-Apr-2004	5kg EDR
17	8-Mar-2004	5kg CAE + 1kg Ash + CO_2 (10 min)	37	21-Apr-2004	5kg EDR
18	9-Mar-2004	5kg CAE + 1kg Ash + CO_2 (10 min)	38	23-Apr-2004	2.5kg EDR + 2.5kg CAE
19	9-Mar-2004	5kg CAE + 1kg Ash + CO_2 (10 min)	39	26-Apr-2004	2.5kg EDR + 2.5kg CAE
20	5-Apr-2004	5kg CAE	40	26-Apr-2004	2.5kg EDR + 2.5kg CAE

3.2.4 Analytical methods

3.2.4.1 Calcium

Calcium analyses were performed by means of Atomic Absorption Spectroscopy. Standards were prepared using a 10% nitric acid solution to preserve the standards. The standards used were 250 ppm, 500 ppm, 750 ppm and 1000 ppm. A Varian 250 plus Atomic Absorption Spectrophotometer (AA) was used to analyse the samples. A lamp with a current of 10 mA, as well as a wavelength of 239.9 nm and a spectral band pass of 0.2 nm was used in conjunction with the specific standards mentioned, for all the samples. The fuel used was acetylene, with the support being nitrous oxide. Some of the samples needed to be diluted with distilled water (20 times dilution).

3.2.4.2 Sodium

Sodium was analysed for by means of Atomic Absorption Spectroscopy. Standards were prepared using a 10% nitric acid solution to preserve the standards. The standards used were 100 ppm, 200 ppm, 500 ppm and 1000 ppm. A Varian 250 plus Atomic Absorption Spectrophotometer as used to analyses the samples. A lamp current of 5 mA, a wavelength of 330.3 nm, and a spectral band pass of 0.5 nm were used, in conjunction with the specific standards mentioned, for all the samples. The fuel used was acetylene, with the support being air. Some of the samples needed to be diluted with distilled water (20 times dilution).

3.2.4.3 Sulphate

The sulphate ions were analysed with a Dionex Al450 Ion Chromatograph. Due to the high concentrations of SO_4 present in the ash water and brines, all the samples were diluted using distilled water (20/50 times dilution) before being analysed. Before the samples were injected into the Dionex apparatus they were filtered through a 0.45 µm nylon Millipore filter. The operating

conditions pertaining to the Dionex AI450 Ion Chromatograph are given in Table 3.2.

Table 3.2 Operating conditions for the Dionex AI450 Ion Chromatograph

Sample Loop Volume	Approx. 20 µl
Guard Column	IonPac AG4A-SC 4 mm
Separator Column	IonPac AG4A-SC 4 mm
Eluant	1.80 mM Na_2CO_3, 1.70 mM $NaHCO_3$
Eluant flow rate	2.0 ml/min
Suppressor	Anion Micro Membrane
Regenerant	25 mM H_2SO_4
Regenerant flow rate	3 ml/min
Expected background conductivity	14 to 18 µS

3.2.4.4 Chloride

The chloride ions were also analysed for using a Dionex AI450 Ion Chromatograph. The operating conditions are the same as those for the SO_4 analysis and are shown in Table 3.2. Due to the high concentrations of Cl present in the ash water and brines, all the samples were diluted using distilled water (20/50 times dilution) before being analysed. Before the samples were injected into the DIONEX apparatus they were filtered through a 0.45 µm nylon Millipore filter.

3.2.4.5 Conductivity and pH

The conductivity of the samples was measured using an EC 215 conductivity meter. The probe was made of glass with four corrosion resistant platinum rings and had a built-in temperature sensor that automatically compensated for temperature changes. The pH was measured using a Beckman Φ360 pH meter with automatic temperature compensation (ATC). Each time the pH meter was used it was calibrated using a two-point calibration at pH 7 and pH 10.

3.2.4.6 Ash analysis

The chemical composition of the ash samples were analysed through X-ray fluorescence spectroscopy (XRF). To obtain the mineralogical composition of the ash samples, X-ray diffractometry (XRD) analyses were performed.

3.3 Liquid phase results

As mentioned previously, the most important elements in the ash disposal system are Ca, Na, Cl and SO_4. The focus was, therefore, on these elements.

3.3.1 Chemical and physical results

Note that a positive value indicates an increase in the mass concentration of the specific element in the liquid phase and a negative value indicates a decrease in the mass concentration of the specific element in the liquid phase.

To put these results in perspective the CAE, TRO brine and EDR brine are compared with each other in Table 3.3.

Table 3.3 CAE and brines comparison

Comparison between brines and CAE			
	TRO	**EDR**	**CAE**
Ca (mg/l)	844	566	645
Na (mg/l)	2743	3582	1962
Cl (mg/l)	1746	983	1250
SO_4 (mg/l)	5716	11055	3768
TDS (mg/l)	9593	11933	7110
EC (mS/m)	1582	1744	1075
pH	6.84	6.99	11.69

The main differences between the brines and the CAE are the high SO_4 and TDS concentrations in the brines compared to the CAE. The pH of the brines are also much lower than that of the CAE.

Figure 3.4 shows the influence that the different combinations had on the elements in the liquid phase. The values in Figure 3.4 indicate the mass increase (positive value)/decrease (negative value) of each of the elements in the liquid phase. The results of the 10 minute addition of CO_2 are also shown to indicate the difference that it makes compared to the other combinations. The CO_2 addition will be discussed in more detail in a later section.

Calcium is leached into the liquid phase. The leaching of calcium is between 55% and 65% less for the pure brines and almost 97% less with the CO_2 addition. Large decreases in the amount of sulphate in the pure brines were achieved. This is largely due to the high concentrations of sulphate that were already present from the start of the experiments.

The amount of sodium and chloride shows little or no change with all the different combinations tested. This indicates, as expected, that there is no precipitation, leaching or ion exchange, which involves these elements, occurring during the initial mixing.

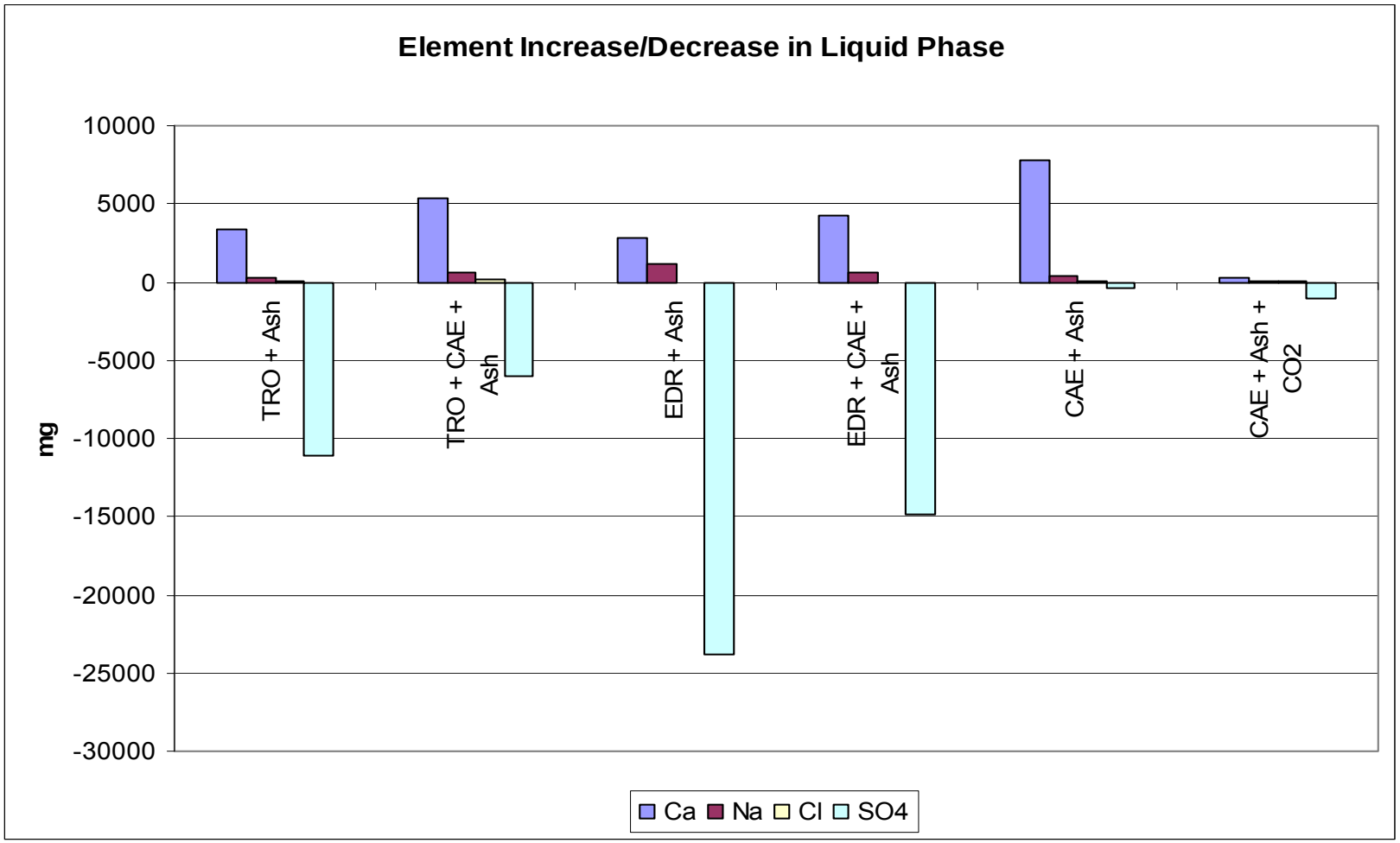

Figure 3.4: Increase/decrease of elements in liquid phase

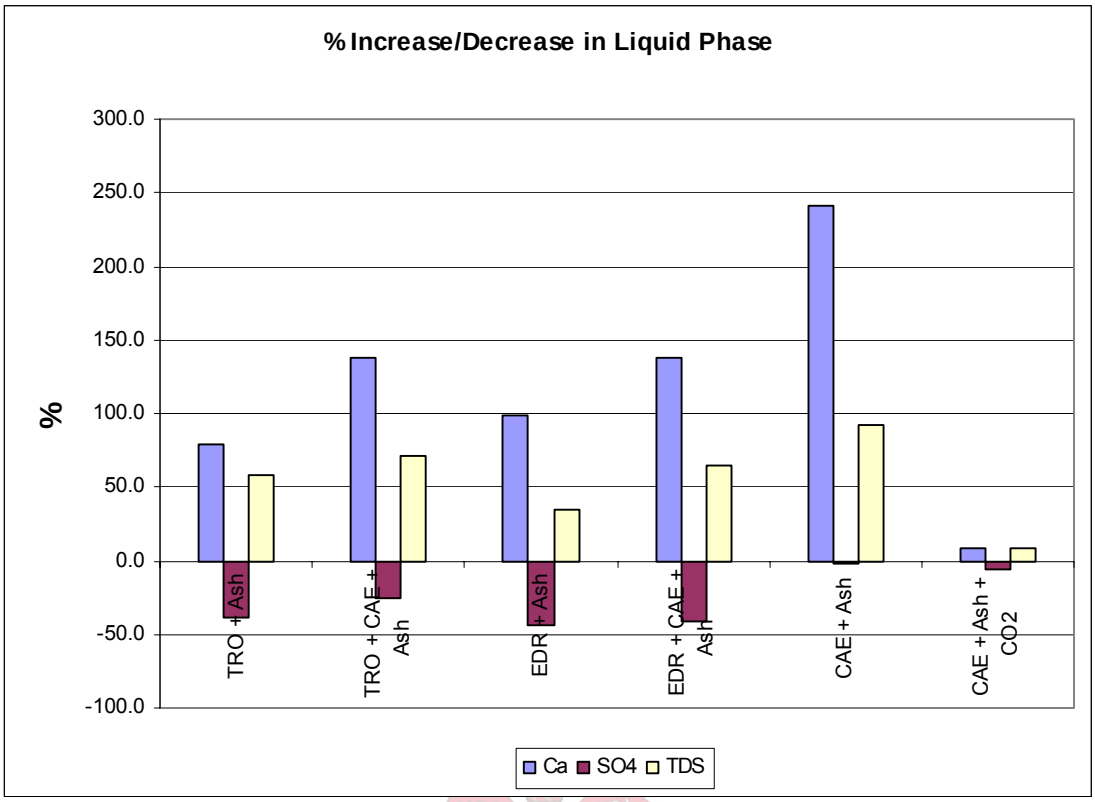

Figure 3.5: Percentage increase/decrease of elements in liquid phase

Figure 3.5 indicates a 240% increase in the mass of calcium in the liquid phase for the mixing of pure CAE and ash. This is much higher than the 79% and 99% increases in the mass of calcium for the TRO and EDR brines and ash mixtures, respectively. The CO_2 addition shows only an 8% increase in the mass of calcium. The decreases in SO_4 for the TRO and EDR brines and ash mixtures are 39% and 43% respectively. The TDS shows the same trend as the Ca for the CO_2 addition. The increase in the mass of TDS in the liquid phase for the pure CAE and ash mixture is 93%. When CO_2 is added to the mixture the increase in the mass of TDS is only 9%.

The leaching of Ca in the TRO brine experiments is less than that of the pure CAE experiments. Figure 3.6 indicates that the TRO brine starts off with a higher amount of Ca but the leaching is much less and in the end the TRO liquid phase contains much less calcium than the CAE liquid phase. This leaching is in accordance with what Roy et.al. (1984) predicted for the initial contact between the ash and water.

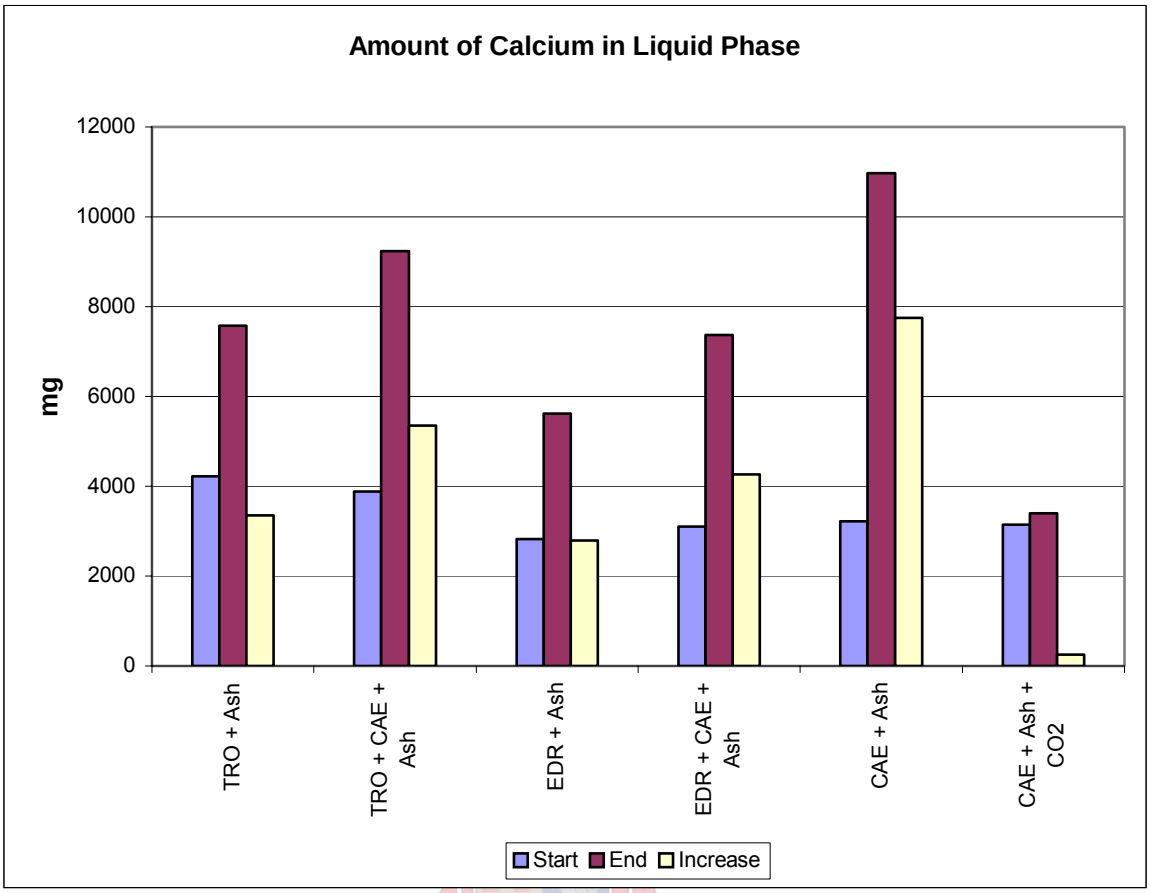

Figure 3.6: Amount of calcium in the liquid phase

Figure 3.6 indicates that the EDR brine contains less Ca than the CAE at the start of the experiments. The leaching of calcium is also much less in the EDR liquid phase than in the CAE liquid phase, which leads to a lower amount of Ca in the liquid phase at the end of the experiments.

The TRO also contains much more SO_4 than the CAE at the start of the experiments (Figure 3.7). The removal of SO_4 from the TRO liquid phase is quite high and in the end the TRO and CAE liquid phases contain almost the same amount of SO_4. It may therefore, be possible to use the TRO brine as carrier medium for the fine ash.

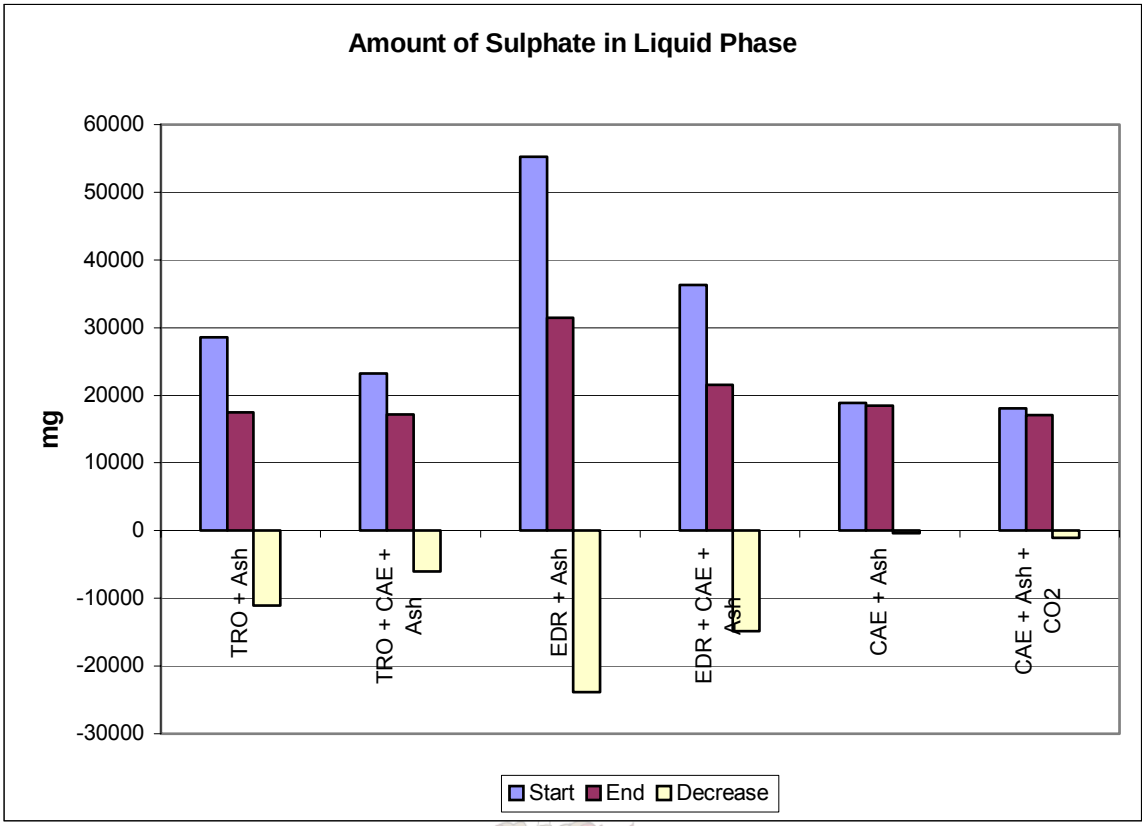

Figure 3.7: Amount of sulphate in the liquid phase

When the SO_4 in the EDR liquid phase is considered, it can be seen that the EDR brine contains a very high amount of SO_4 (Figure 3.7). The removal of SO_4 is also high, but the amount of SO_4 in the liquid phase stays at a much higher level than the amount of SO_4 in the CAE liquid phase. The results indicate that the use of EDR brine as the carrier medium for the fine ash may result in too high salt concentrations in the liquid phase. These high salt concentrations may lead to excessive scaling in the pipes, which transport the slurry from Inside Ash to the FAD.

The SO_4 removal is mainly through the precipitation of $CaSO_4$ and $CaSO_4.2H_2O$. This means that lower concentrations of Ca may prevent large scale SO_4 removal.

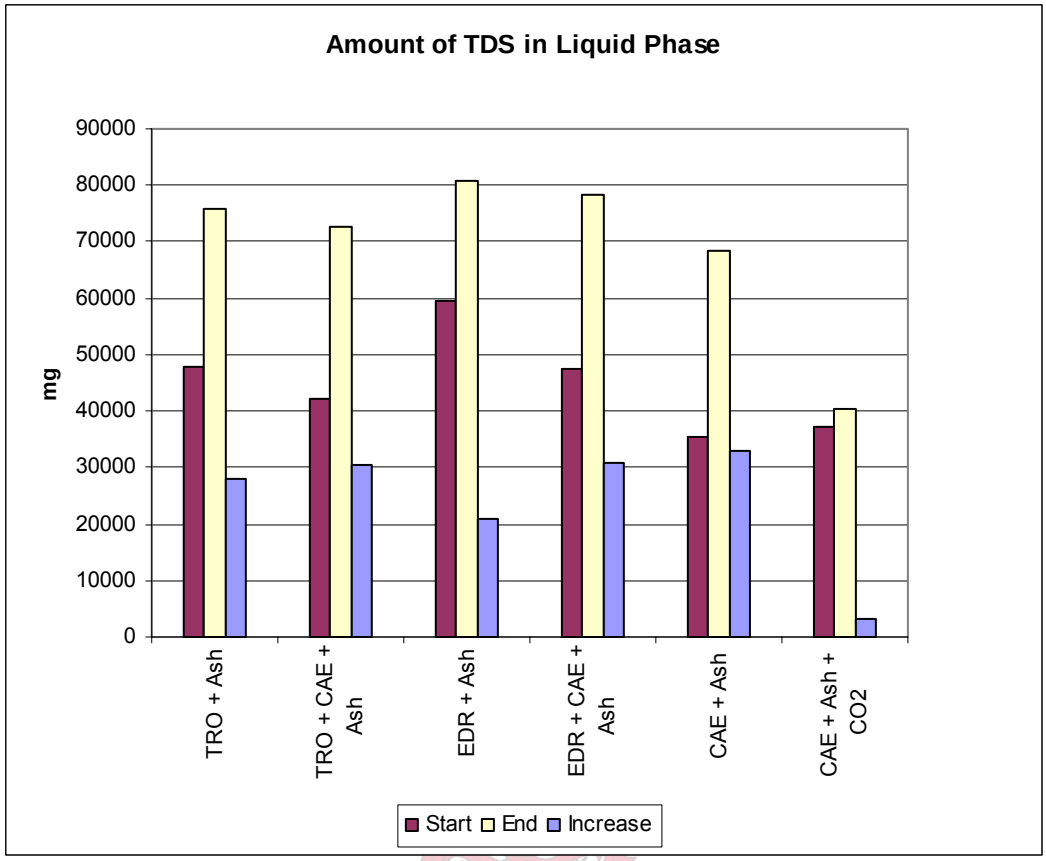

Figure 3.8: Amount of TDS in liquid phase

Figure 3.8 shows the change of the mass of total dissolved solids (TDS) in the liquid phase for the different combinations tested. The EDR and TRO brines again show a smaller increase in TDS values than the 50/50 mixtures of brine and CAE and also less than the pure CAE. This could be attributed to the higher TDS concentration of the brines at the start of the experiments. After the initial mixing the TRO brine has about 9% more dissolved solids than the CAE. The EDR brine has 20% more dissolved solids than the CAE. This confirms that the TRO might be suitable to use as carrier medium because the final salt concentrations in the TRO brine liquid phase is almost the same as those in the pure CAE liquid phase. The CO_2 addition not only prevents the leaching of calcium but also keeps the increase of TDS in the liquid phase to a minimum.

To test the consistency of the results, the ratio between the electrical conductivity and the total dissolved solids were calculated. Table 3.4 indicates that this ratio is consistently between 6.5 and 7.

Table 3.4: TDS:EC Ratio for mixture experiments

TDS:EC Ratio	
TRO + Ash	6.54
TRO + CAE + Ash	6.76
EDR + Ash	6.81
EDR + CAE + Ash	7.01
CAE + Ash	6.53

The conductivity of the liquid phase for the different combinations can be seen in Figure 3.9. In accordance with the previous results, the conduction increases by approximately the same amount for all the combinations except for the CO_2 addition. The conductivity is higher in the brines because of the higher ion concentrations. In accordance with what NALCO (1988) and Sheikholeslami (2001) found, the high conductivity values indicate the presence of a high number of different ions. This influences the precipitation of the slightly soluble salts and may prevent $CaCO_3$ and $CaSO_4$ from forming.

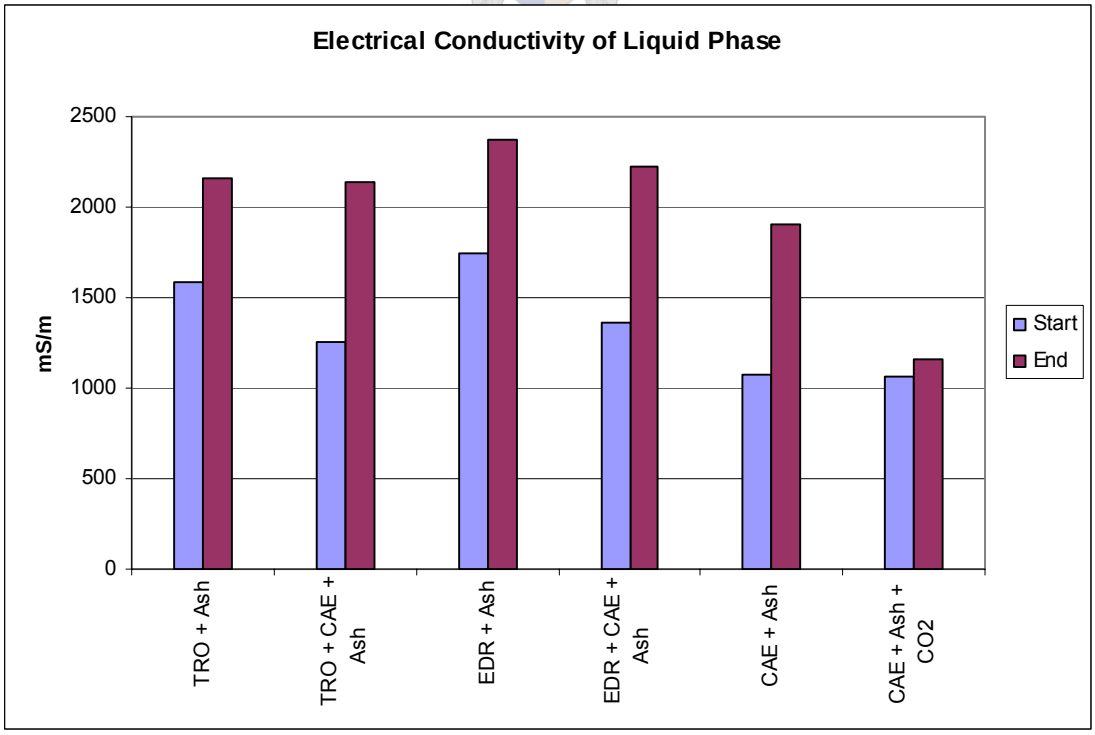

Figure 3.9: Electrical conductivity of liquid phase

The pH (Figure 3.10) of the liquid phase increases to above 12 for all the different combinations. For the EDR and TRO brines the pH increases from ~7 to >12. Adding CO_2 to the mixture does not make the liquid phase acidic as can be seen from the results. The results show that the addition of the ash makes the slurry a totally alkaline environment because of the leaching of salt (principally Ca, Figure 3.6) that occurs during the initial mixing.

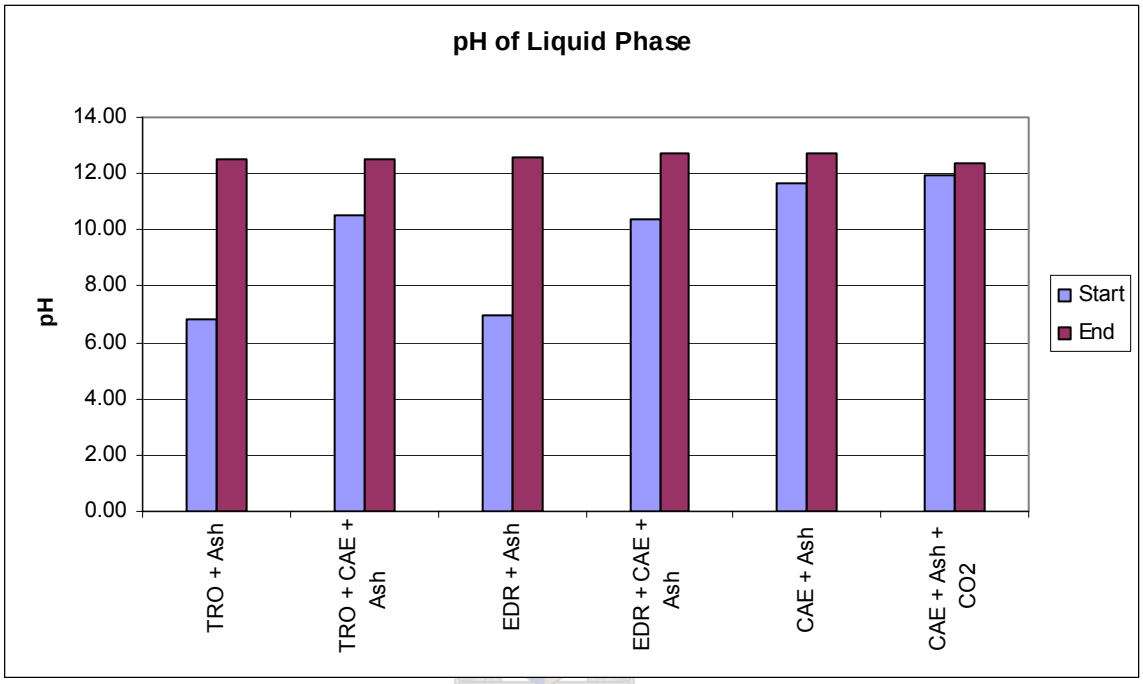

Figure 3.10: pH of liquid phase

3.3.2 CO_2 addition

According to previous studies on wet ash disposal systems in general, the active addition of CO_2 was not tested for the removal of salts from ash effluents. In this study not only the influence of CO_2 addition was tested but also the effect that different addition times have. The results for the different addition times are shown in Figures 3.11 to 3.14 for comparison.

Figure 3.11 indicates the increase of TDS for the different durations. The increases are much smaller than that of the CAE liquid phase without CO_2 addition. It can also be seen that the longer the addition, the less the increase in TDS. With 20 minutes of CO_2 addition the increase is almost negligible.

The influence of the CO_2 as found in Bezuidenhout (1995) shows that CO_2 addition will increase the $CaCO_3$ precipitation. Pretorius and Nieuwenhuis (2002) also found that a CO_2 atmosphere decreases the Ca and TDS concentrations in the effluent.

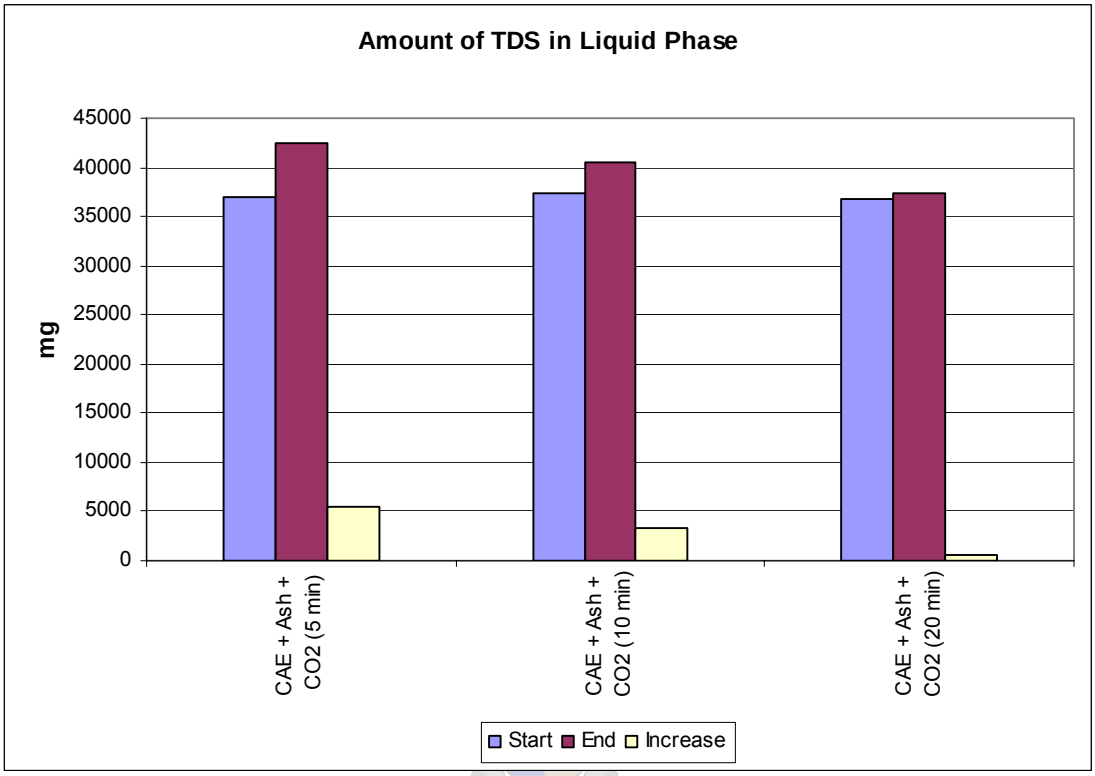

Figure 3.11: TDS increase in liquid phase for CO_2 addition

These results also indicate that increasing the addition time do have an influence on the prevention of leaching. Longer addition times lead to better prevention of leaching.

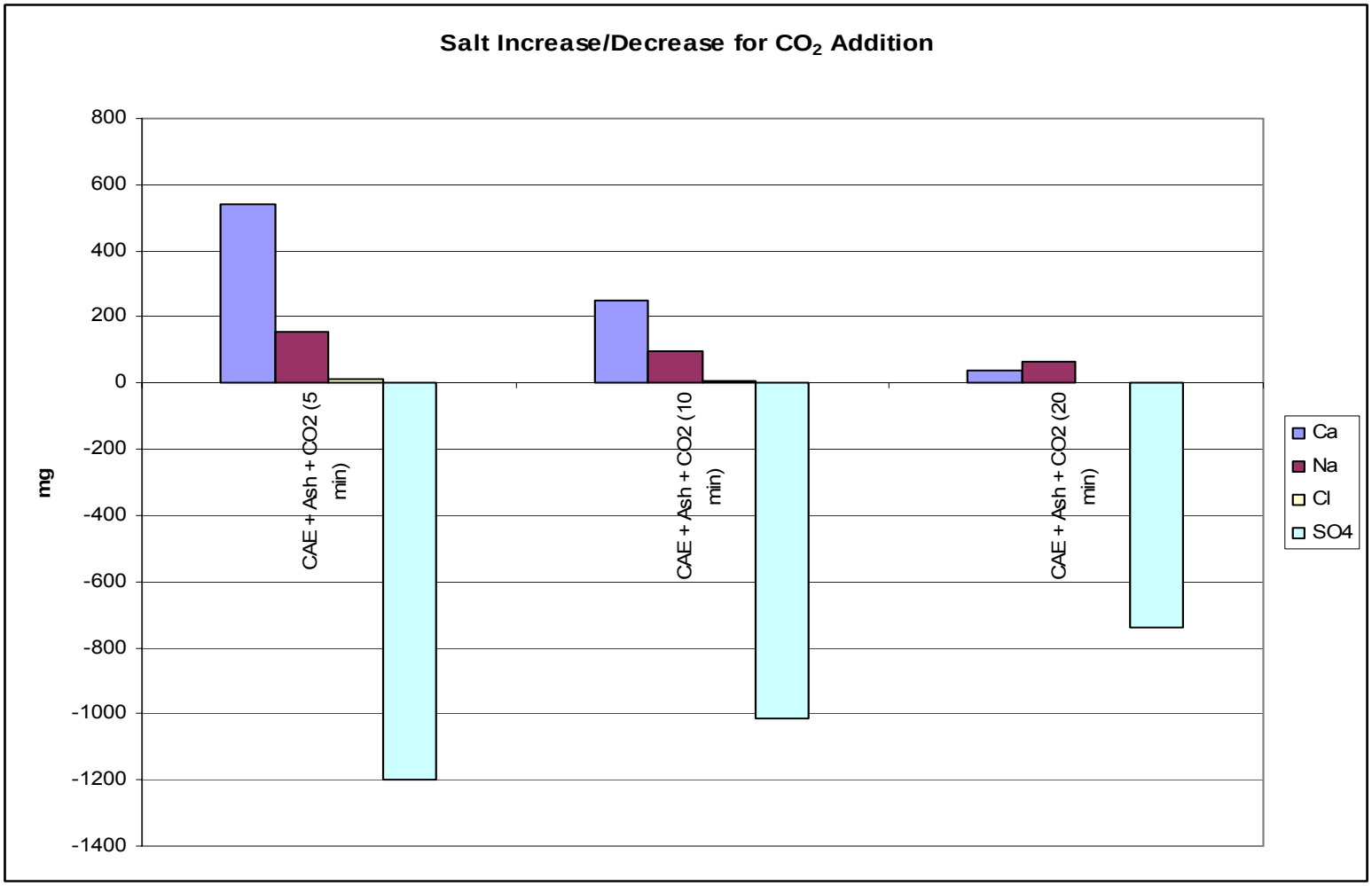

Figure 3.12: Salt increase/decrease in liquid phase for CO_2 addition

For the CO_2 addition experiments, the TDS:EC ratio was also calculated and the ratio stays almost exactly the same for the different addition times (see Table 3.5). This indicates good consistency in the results and it also compares well to the ratios found for the brine mixing experiments.

Table 3.5: TDS:EC Ratio for CO_2 addition

TDS:EC Ratio	
CAE + Ash + CO_2 (5 min)	7.00
CAE + Ash + CO_2 (10 min)	6.98
CAE + Ash + CO_2 (20 min)	7.00

Conductivity results (Figure 3.13) also show the largest increase at the 5 minute addition where most of the leaching takes place. For the 10 minute addition the conductivity shows lesser of an increase and the conductivity stays relatively constant for the 20 minute addition. Less dissolved substances will lessen the effect that ions have on each other's solubility.

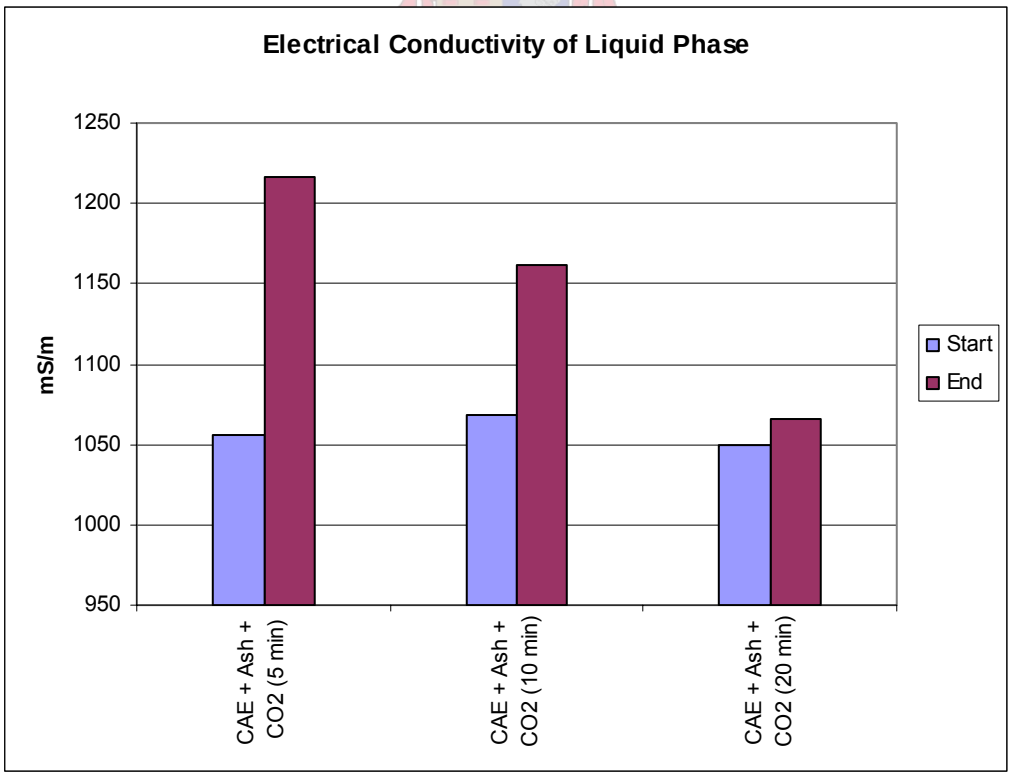

Figure 3.13: Electrical conductivity of liquid phase for CO_2 additions

Figure 3.14 indicates that the CO_2 addition prevents the large scale leaching of Ca. The SO_4 removal from the pure CAE is less than that of the TRO and EDR brines, but that is due to the relative low SO_4 concentration in the CAE liquid phase. Sodium is also removed and the only explanation may be the co-precipitation of the sodium with the calcite. In accordance with the TDS results, the 20 minute addition prevents the leaching to a negligible scale.

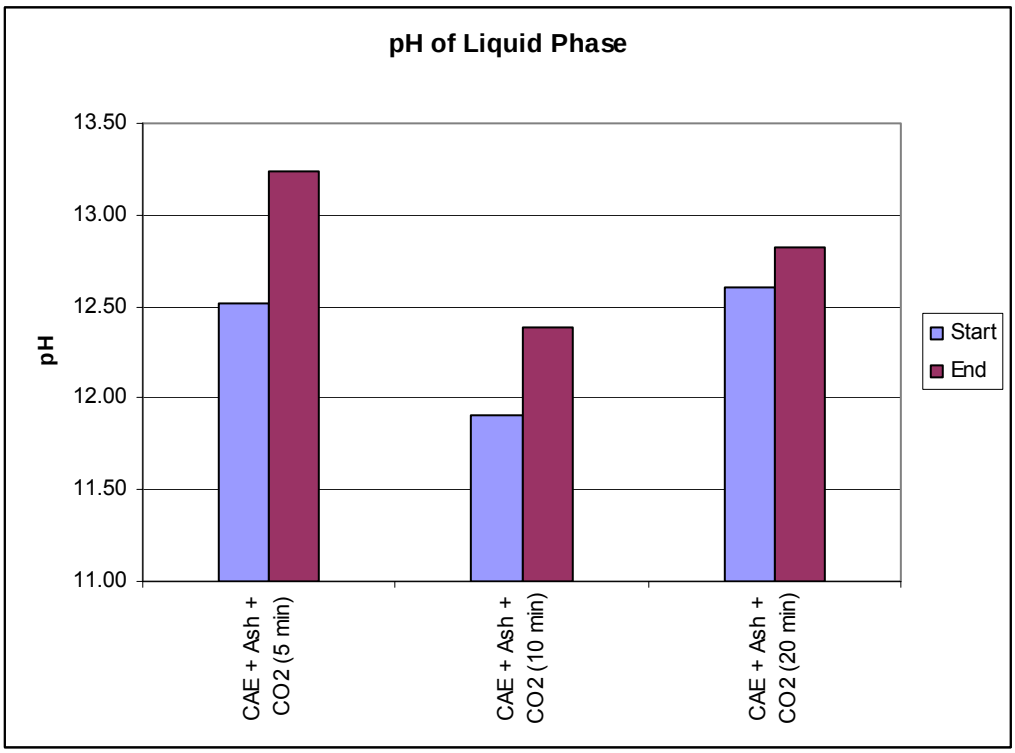

Figure 3.14: pH of liquid phase for CO_2 additions

The pH results (Figure 3.14) show that the addition of CO_2 does not make the liquid phase acidic. If the liquid phase became acidic it will enhance the leaching of the salts in the ash and that will increase the salt concentrations again.

3.3.3 Statistical analysis

The statistical analysis done on the Phase 1 experiments was discussed earlier in this chapter. The statistical computer program, Design-Expert was

used to evaluate the mixture experiment data. A quadratic model as it is given below was the model that fitted the data the best:

$$\eta = \sum_{i=1}^{q} \beta_i x_i + \sum \sum_{i<j}^{q} \beta_{ij} x_i x_j \qquad [3.1]$$

Through the analysis prediction graphs of the increase/decrease of salts for the different ratios of brine and CAE could be obtained. The details of the statistical analysis can be found in Appendix B.

Figure 3.15 is an indication of how the graph should be read. The ash amount is set at 16.7% (to keep the liquid:solids ratio at 5:1). The graph should be read parallel to the X-axis. A reading should be taken as shown by the dashed line. Point A indicates the amount of TRO brine in the mixture as a percentage. Point B indicates the percentage of CAE in the mixture. Point C is the amount of calcium leaching that is predicted for this specific mixture. In this example a mixture consisting of 16.7% ash, 23.3% TRO brine and 60% CAE would produce calcium leaching of around 6200 mg (1240 mg/l) for the experiment.

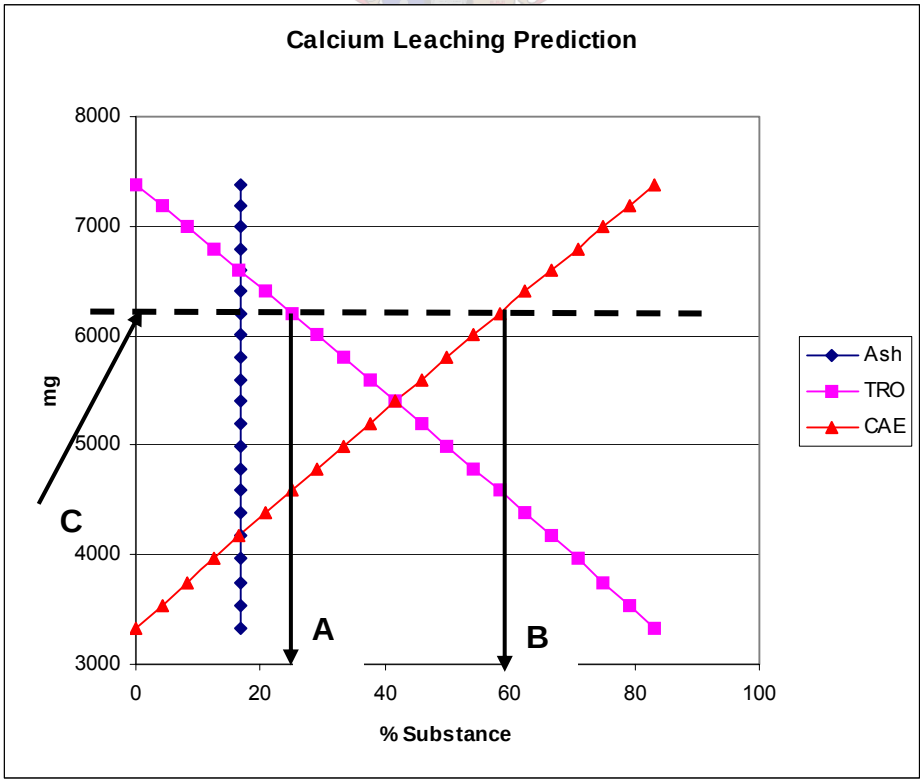

Figure 3.15: How to read the prediction graphs

These predictions give an indication of the type of leaching, which may be expected in a brine/CAE mixture. To obtain the amount per litre of effluent concentration divide the predicted amount by 5.

Ca, SO_4 and TDS were chosen to perform the statistical analysis on. It was done for the TRO and EDR brine mixtures with CAE.

3.3.3.1 TRO brine

Table 3.6 indicates the values for the constants that were obtained for the prediction formulas of the Ca, SO_4 and TDS. These prediction formulas were used to draw the graphs that can be used to predict the leaching/removal of salts for the different effluent mixtures.

As mentioned earlier in this chapter, quadratic models were fitted to the data.

Table 3.6: Statistical analysis for TRO brine

TRO brine statistical analysis					
Ca		SO_4		TDS	
Constants	Values	Constants	Values	Constants	Values
b_1	37210000	b_1	27469100	b_1	30519400
b_2	33	b_2	-103	b_2	-11
b_3	-107	b_3	-187	b_3	0
b_{12}	-44630000	b_{12}	-33043500	b_{12}	-36419000
b_{13}	-44600000	b_{13}	-32970000	b_{13}	-36388100
b_{23}	253	b_{23}	1847	b_{23}	1655

Equation 3.2 is the prediction formula for the calcium leaching in the TRO brine experiments. The R^2 for this prediction is 0.9884, which indicates that the model fits the data well.

$$Y = 37210000x_1 + 33x_2 - 107x_3 - 44630000x_1x_2 - 44600000x_1x_3 + 253x_2x_3 \quad [3.2]$$

$R^2 = 0.9884$

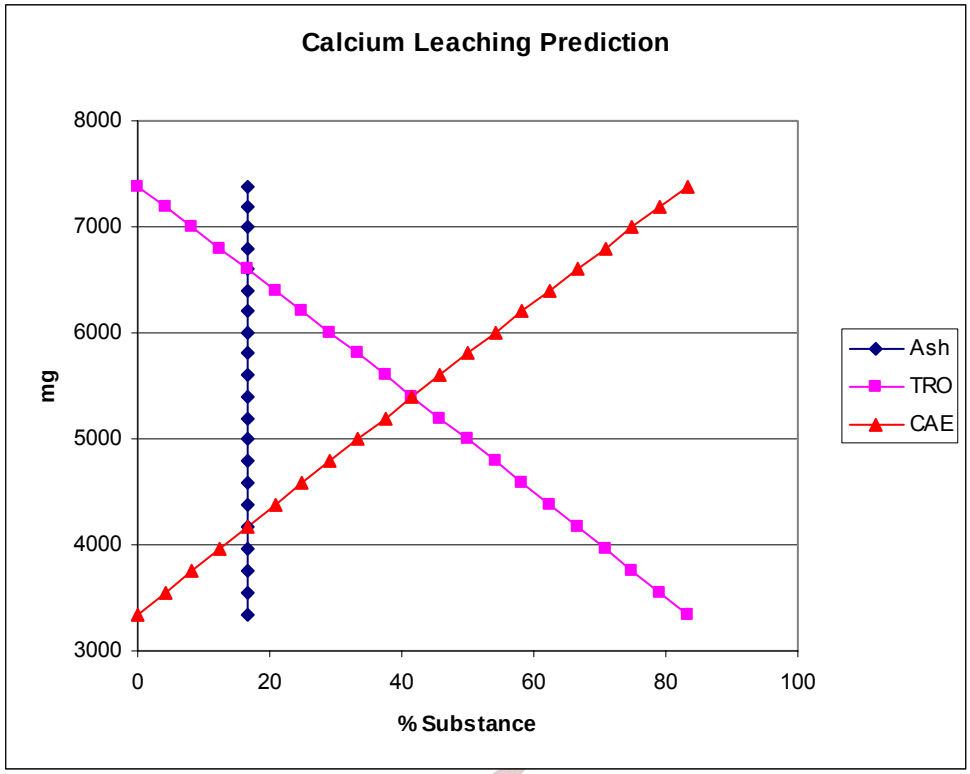

Figure 3.16: Calcium leaching prediction for TRO brine

Figure 3.16 indicate that mixtures with large amounts of TRO will lead to a decrease in the amount of calcium leaching. The pure TRO brine and also a 50/50 mixture of the CAE and TRO brine will lead to decreased calcium leaching.

Equation 3.3 is the sulphate removal prediction formula for the TRO brine. In Figure 3.17 it can be seen that the sulphate removal for the pure TRO brine is high. It is important to keep in mind that the TRO brine contains much more sulphate than the CAE. It would therefore, predict higher values of removal.

$$\mathbf{Y = 27469100x_1 - 103x_2 - 187x_3 - 33043500x_1x_2 - 32970000x_1x_3 + 1847x_2x_3} \quad [3.3]$$

$R^2 = 0.9619$

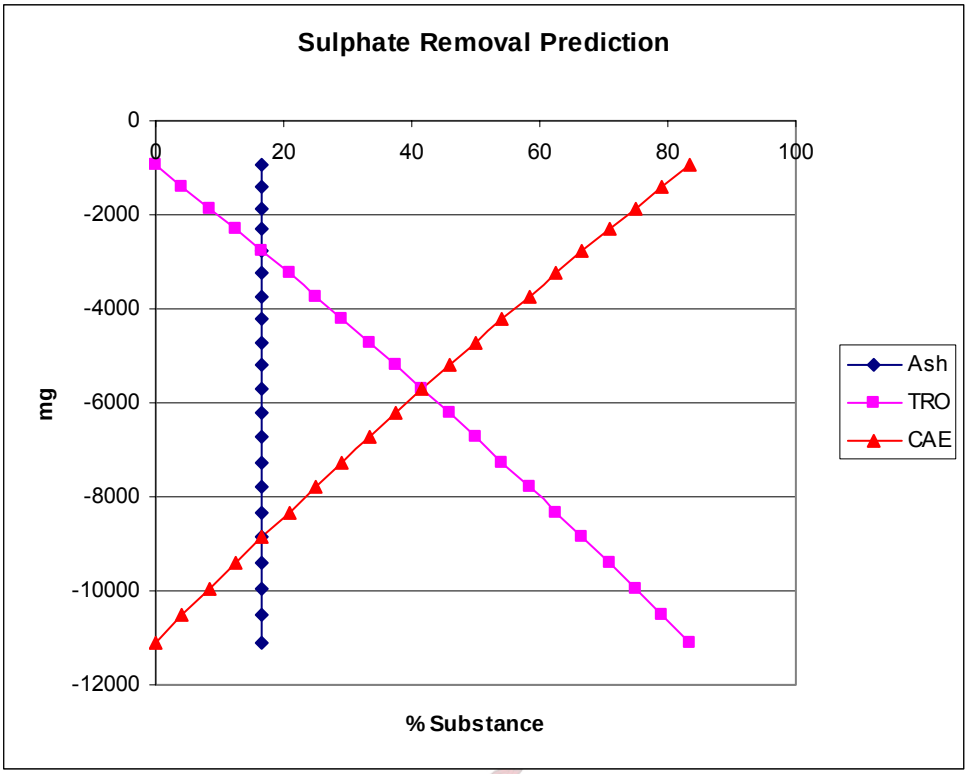

Figure 3.17: Sulphate removal prediction for TRO brine

The prediction also indicates that the ash has high sulphate removal capabilities. This will also be discussed when looking at the EDR brine prediction formulas.

The TDS leaching prediction can be seen in Figure 3.18 and Equation 3.4. In this case the difference between the values predicted for the pure TRO brine and the pure CAE is less severe. There is still the same trend as for the calcium and sulphate, but it must again be noted that the TDS concentration of the TRO brine is larger than that of the CAE and therefore, the concentration of TDS after the leaching will be more or less the same.

$$Y = 30519400x_1 - 11x_2 - 217x_3 - 36419000x_1x_2 - 36388100x_1x_3 + 1655x_2x_3 \quad [3.4]$$

$R^2 = 0.9991$

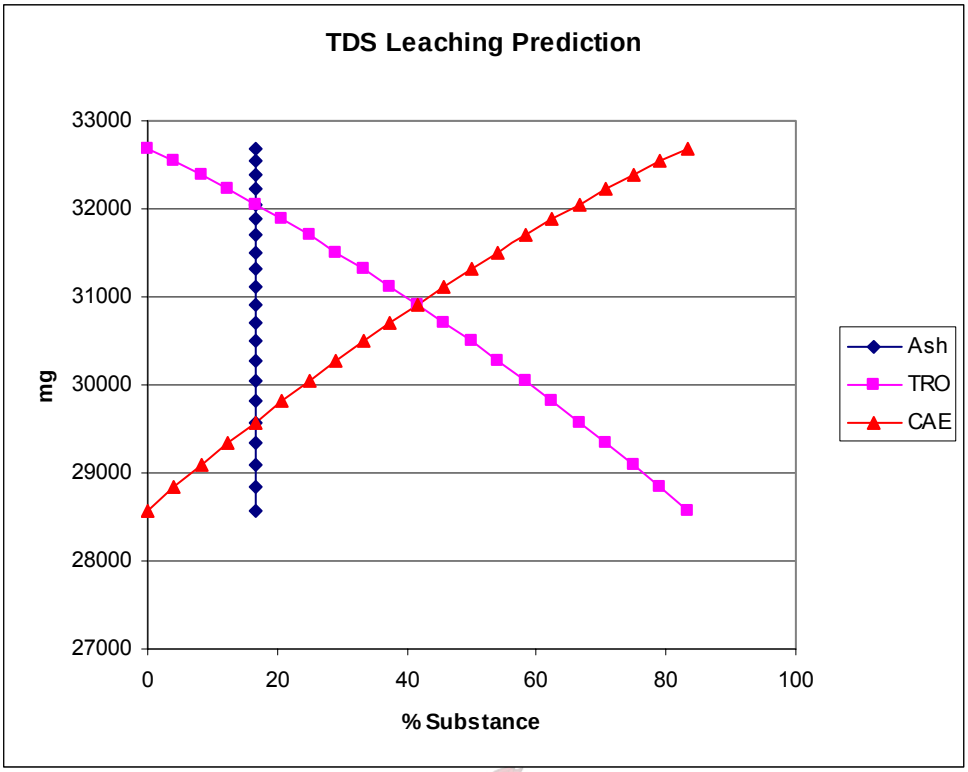

Figure 3.18: TDS leaching prediction for TRO brine

3.3.3.2 EDR brine

Table 3.7 indicates the prediction formula constants for the EDR brine. This is also for quadratic models fitted to the mixture experiment data. The EDR brine contains much more sulphate than both the CAE and TRO brine.

Table 3.7: Statistical analysis for EDR brine

EDR brine statistical analysis					
Ca		SO_4		TDS	
Constants	Values	Constants	Values	Constants	Values
b_1	30396600	b_1	47539300	b_1	75680000
b_2	-165	b_2	0	b_2	0
b_3	-107	b_3	0	b_3	-218
b_{12}	-36445600	b_{12}	-57242200	b_{12}	-90610000
b_{13}	-36420200	b_{13}	-57051600	b_{13}	-90580000
b_{23}	537	b_{23}	1573	b_{23}	2033

Equation 3.5 and Figure 3.19 indicate the predictions made for the calcium leaching using EDR brine in combination with CAE. The leaching is slightly higher than that predicted when using the TRO brine. The trends observed in the leaching prediction are similar to that of the TRO brine with an increase in the EDR brine content of the mixture, and thus decreasing the overall amount of leaching.

$$Y = 30396600x_1 - 165x_2 - 107x_3 - 36445600x_1x_2 - 36420200x_1x_3 + 537x_2x_3 \quad [3.5]$$

$R^2 = 0.9401$

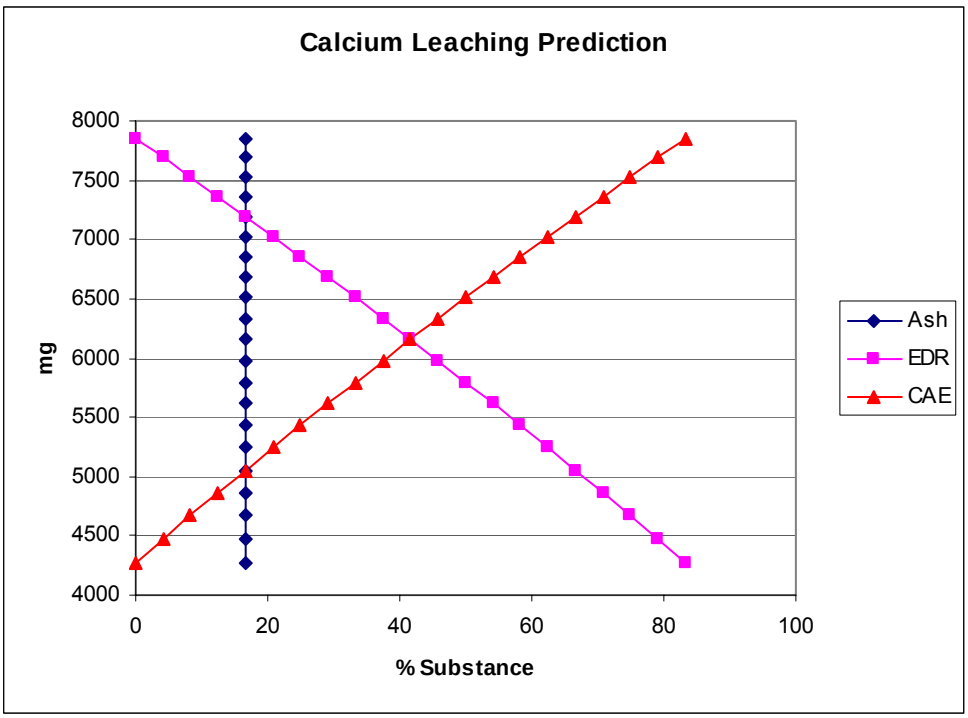

Figure 3.19: Calcium leaching prediction for EDR brine

The EDR brine contains very high concentrations of sulphate. This is clearly visible in the prediction of sulphate removal (Equation 3.6 and Figure 3.20) obtained for the EDR brine experiments. The removal is almost three times that of the TRO brine experiments. This confirms the ability of the fine ash to act as a salt sink for sulphate as found by Koch (2002).

$$Y = 47539300x_1 - 1333x_2 - 187x_3 - 57242200x_1x_2 - 57051600x_1x_3 + 1573x_2x_3 \quad [3.6]$$

$R^2 = 0.9937$

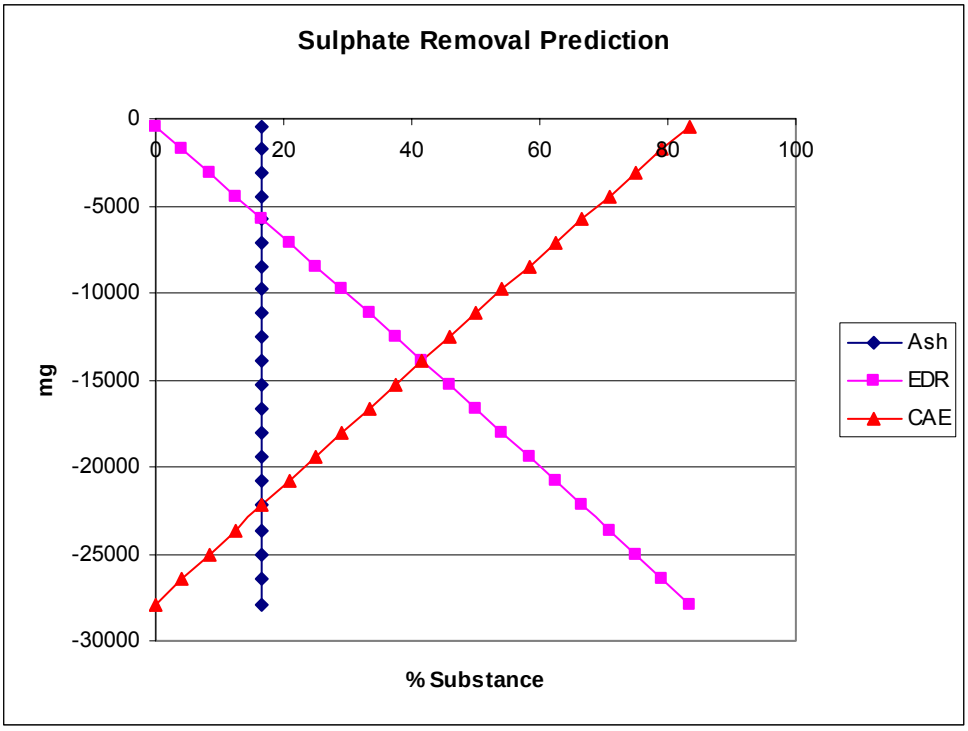

Figure 3.20: Sulphate removal prediction for EDR brine

As was the case with the calcium leaching, the observed trends in the removal of sulphate are the same for the TRO and EDR brines.

The increase in TDS predicted when using the EDR brine does not differ much from using the CAE, but the EDR contains more dissolved solids and will therefore, lead to a high TDS concentration in the effluent.

Figure 3.21 and Equation 3.7 indicate the increases that can be expected when using the EDR brine.

$$Y = 75680000x_1 + 1400x_2 - 218x_3 - 90610000x_1x_2 - 90580000x_1x_3 + 2033x_2x_3 \quad [3.7]$$

$R^2 = 0.996$

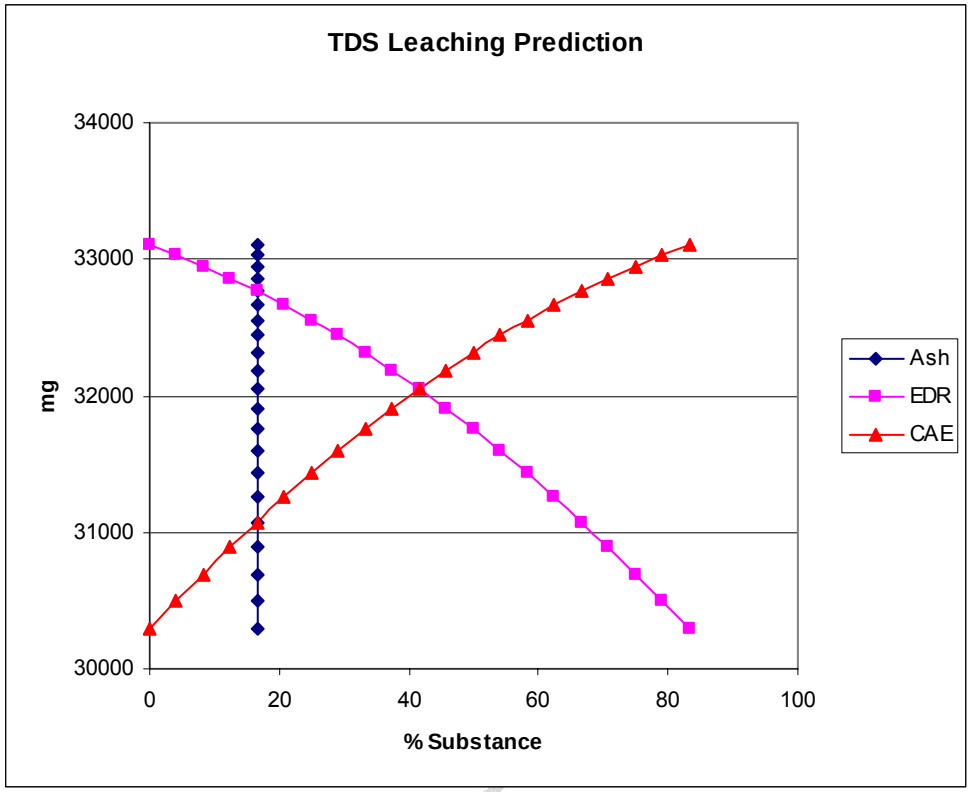

Figure 3.21: TDS leaching prediction for EDR brine

These predictions were made from the different experimental combinations tested during the Phase 1 experiments. They can be used in feasibility studies to predict what can be expected when using the TRO and EDR brines in combination with the CAE as carrier medium.

Changes in the composition of these brines may, however, influence the results and care must be taken when using these predictions. The Sasol Secunda ash disposal system is also much more complicated and test work on this system can be used to enhance the predictions.

3.4 Ash results

3.4.1 Chemical composition

XRF analyses were done on the ash after each experiment to determine the chemical composition of the ash and to investigate any large changes that may occur in the ash due to the mixing of the TRO brine, EDR brine, CAE and ash.

Table 3.8 indicates the average values for the initial composition of the ash and also the composition of the ash after it have been mixed with the TRO, EDR and CAE. The values indicated are the percentages of the total composition of the ash. No major changes can be seen. There is a slight decrease in the amount of CaO. This is in accordance with the leaching of the Ca from the ash. A decrease in the Al_2O_3 may contribute to the increase in the TDS of the liquid phase. There is an increase in the MgO percentage in the ash and also an increase in the percentage SiO_2.

With the addition of CO_2 more radical changes were noticed. There is a big increase in the amount of CaO. This is in accordance with calcite precipitation that takes place and also the prevention of Ca leaching. The decrease in the Al_2O_3 amount is also much larger than the decrease observed with no CO_2 addition.

Table 3.8: Chemical composition of the ash

Chemical Composition of Ash									
Phase	**Fresh ash**	**TRO + Ash**	**% change**	**EDR + Ash**	**% change**	**CAE + Ash**	**% change**	**CAE + Ash + CO2**	**% change**
	%								
LOF	1.93	2.34	0.43	2.17	0.22	2.26	0.34	2.18	0.25
Al_2O_3	26.71	24.88	-1.68	24.57	-2.34	24.81	-1.82	22.26	-4.48
CaO	11.81	10.76	-0.99	11.18	-0.72	11.71	-0.06	16.96	5.15
Cr_2O_3	0.01	0.01	0.00	0.00	-0.01	0.01	0.00	0.01	0.00
Fe_2O_3	3.64	3.38	-0.25	3.78	0.11	3.59	-0.04	4.26	0.61
K_2O	1.00	0.98	-0.01	1.02	0.02	0.97	-0.03	0.99	-0.01
MgO	1.62	2.10	0.49	2.35	0.71	2.01	0.40	1.10	-0.52
MnO	0.08	0.08	0.00	0.09	0.00	0.08	0.00	0.09	0.01
Na_2O	0.66	0.41	-0.24	1.62	0.96	0.68	0.03	0.44	-0.21
NiO	0.02	0.02	0.00	0.02	0.00	0.02	0.00	0.02	0.00
P_2O_5	0.79	0.73	-0.05	0.73	-0.07	0.72	-0.07	0.64	-0.15
SiO_2	50.00	52.06	2.39	51.59	1.20	51.14	1.32	49.58	-0.45
TiO_2	1.46	1.36	-0.09	1.38	-0.09	1.38	-0.07	1.26	-0.20
Total	**99.72**	**99.11**		**100.49**		**99.38**		**99.78**	

3.4.2 Mineralogical composition

XRD analysis alone revealed that there is no formation of $CaSO_4$ or $CaSO_4.H_2O$ in the ash. These minerals may form but were not immobilised in the ash. There are also no traces of ettringite, but that is because of the long time it takes to form. Calcite ($CaCO_3$) did show up in the XRD analysis of the washed and unwashed ash for the CO_2 addition. It can, therefore, be concluded that the calcite that is formed during the CO_2 addition is immobilised in the ash. Figure 3.22 shows the XRD analysis of the ash before mixing and Figures 3.23 and 3.24 shows the washed and unwashed ash after the mixing with the CAE and CO_2 addition. The main mineral phases found in the ash are mullite, quartz and hematite.

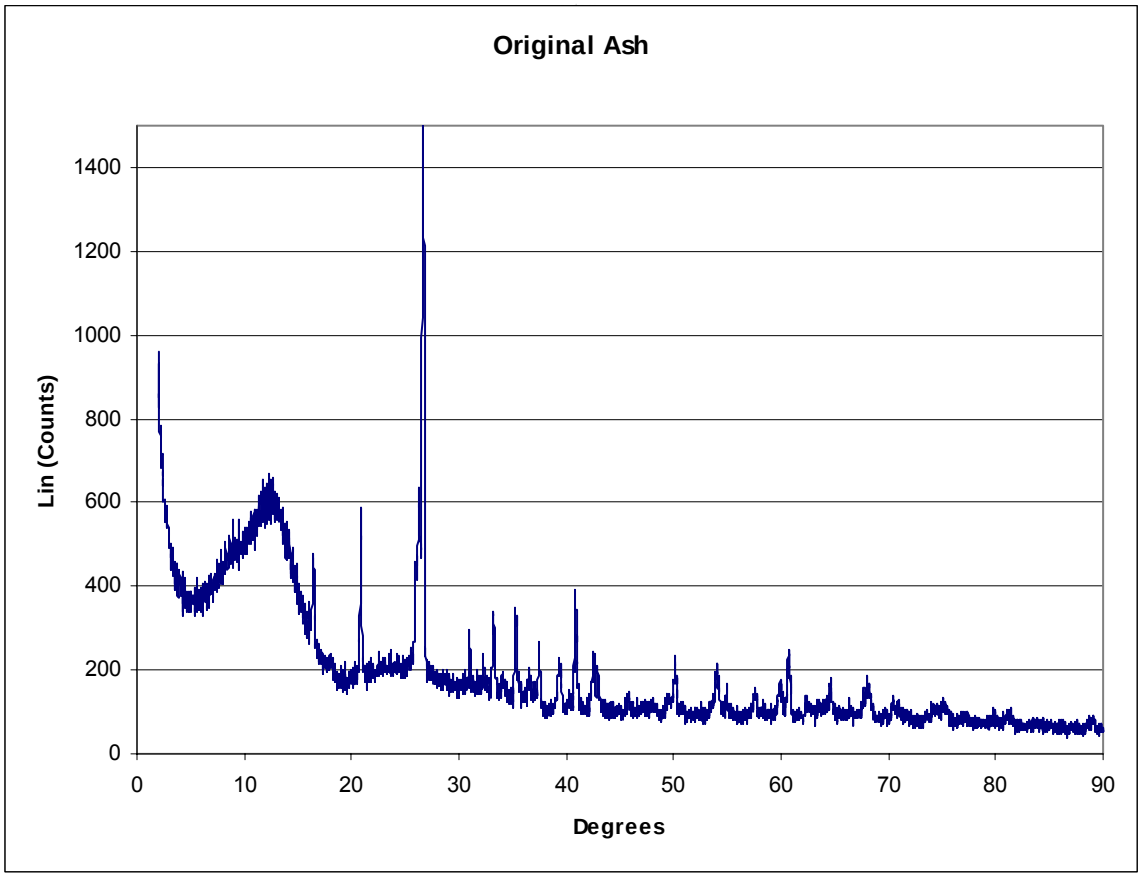

Figure 3.22: Diffractogram of ash before mixing

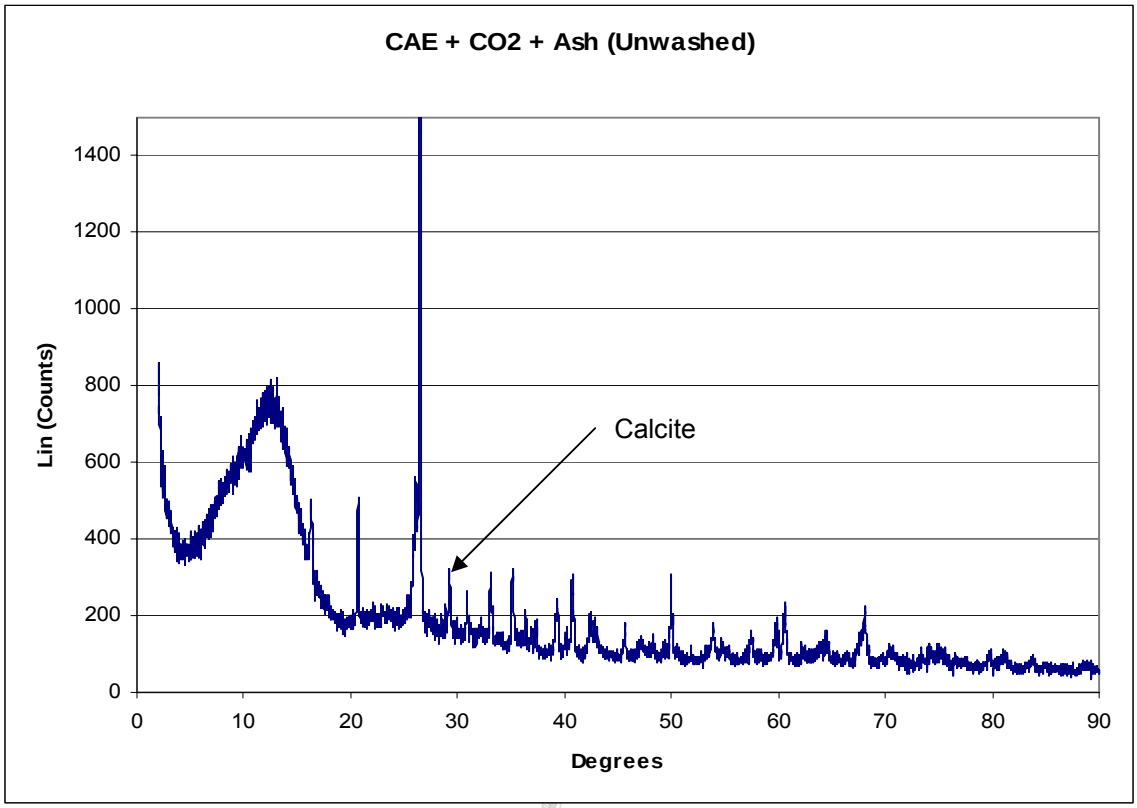

Figure 3.23: Diffractogram of unwashed ash

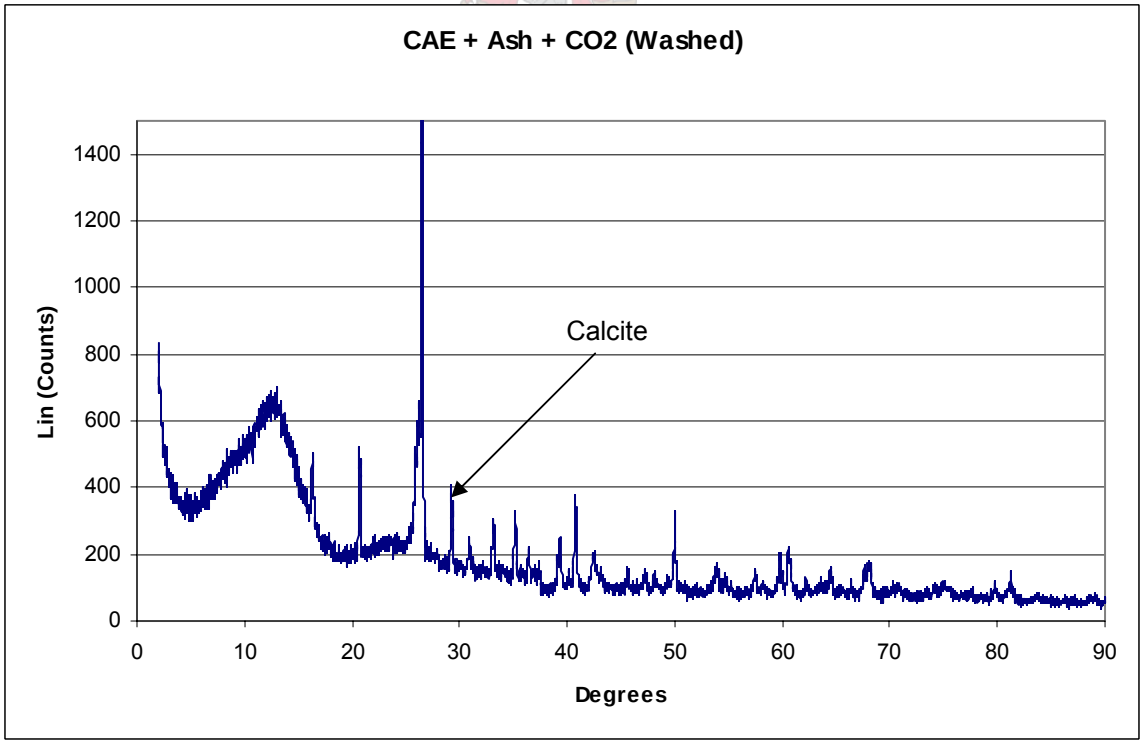

Figure 3.24: Diffractogram of washed ash

Figure 3.23 is a diffractogram of the unwashed fine ash after the CO_2 addition experiments. The arrow indicates a peak, which is visible on this small figure that can be attributed to the presence of calcite in the ash. This shows that the leached calcium is immobilised as calcite in the ash.

The calcite can also still be seen in the washed ash diffractogram (Figure 3.24), confirming that the calcium was not leached from the ash when it was washed with the distilled water.

3.5 Summary

The following is a summary of the results obtained from the Phase 1 experiments:

3.5.1 Liquid phase

- Salts are leached from the ash into the liquid phase.
- The mixing of pure brines does not produce a larger increase in leaching of salts into the liquid phase than the addition of CAE. The brines do, however, have higher salt concentrations to start with.
- Calcium is the main element that is leached (TRO brine = 79% increase, EDR brine = 99% increase and CAE = 240% increase) and sulphate the main element that is removed from the liquid phase. The amount of sodium and chlorine in the liquid phase stays almost constant throughout all the experiments.
- The ash disposal system can be used as a salt sink for sulphate. 39% and 43% sulphate precipitate for the TRO and EDR brines, respectively. Koch (2002) also found that the fine ash dams can be used as a salt sink for sulphates.
- The conductivity and pH of the liquid phase increases to approximately the same level for the different combinations tested. This indicates that the brines produced the same kind of interaction as the CAE.

- Adding CO_2 to the system decreases the leaching of the TDS (only a 9% increase compared to a 93% increase without addition) and especially calcium considerably. Sulphate is still removed from the liquid phase, but with less calcium leached there is also less sulphate removed.
- The pH and conductivity stay relatively constant with the CO_2 addition.
- CO_2 addition can, therefore, be used to prevent excessive leaching of soluble minerals into the liquid phase.
- The TRO brine can be used as carrier medium on its own or in combination with the CAE.
- Using the EDR brine as carrier medium will lead to even larger salt concentration in the ash system and also increased scaling.

3.5.2 Ash phase

- No major changes in the chemical composition of the ash were found for the different combinations tested. There was an increase in the calcium content with the addition of CO_2.
- The XRD analyses also show no real changes to the mineral content of the ash except in the case of the CO_2 addition. $CaCO_3$ can be seen in the washed and unwashed ash. This indicates the immobilisation of the formed calcite in the ash.
- $CaSO_4$ formation may be the reason for the SO_4 decrease but the ash analyses do not show any traces of $CaSO_4$. It may be formed but is not immobilised in the ash.

The influence of different factors on the precipitation and salt removal of the Evaporation and CAE dams of the Sasol Secunda ash disposal system is investigated in the next chapter.

Chapter 4

Phase 3 experiments:

CAE and evaporation dams

Previous research work by Koch (2002), found that a great deal of salt precipitation occurs in the Evaporation and CAE dams of the ash disposal system at Sasol Secunda. These dams are shown as Phase 3 in the ash disposal system (Figure 4.1). The precipitation in these dams is mainly calcite precipitation (Koch, 2002).

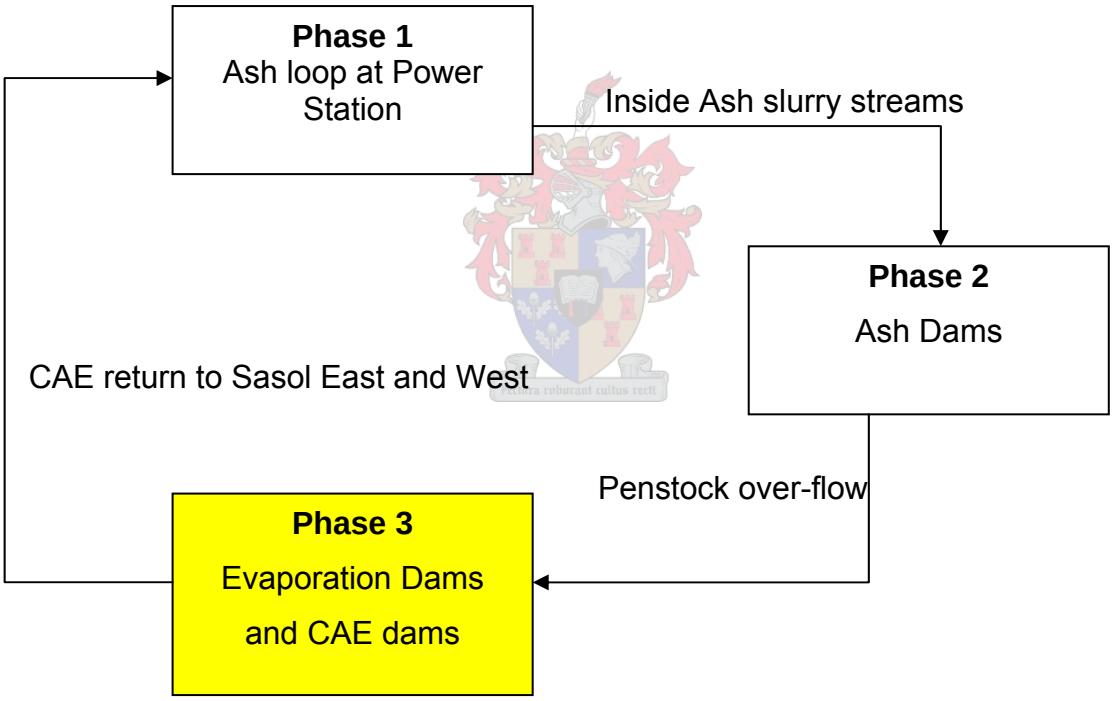

Figure 4.1: Phase 3 indication diagram

The focus in this part of the study was to test the influence that different factors have on the precipitation of salts in the evaporation and CAE dams. The salt removal capabilities of the system would be enhanced if the precipitation in Phase 3 could be increased.

In a closed ash disposal system the water is recycled to transport the ash to the ash heaps on the outskirts of the Sasol Secunda Petrochemical Plant. The ash system at Sasol Secunda also acts as a salt sink and buffers the salt concentration variations of the inlet streams. Over the past 17 years there has been an increase in the salt concentration of the CAE that transport the ash. To combat the increase in the salt concentration the main aim is to find ways to remove more salt through the system and in this case through the Evaporation and CAE dams.

The following factors were investigated:

- The addition of air to the system.
- Adding nets to enhance precipitation.
- The addition of a chemical substance.
- Increasing the evaporation rate.

These factors can all be implemented in some way or another in the Sasol Secunda Evaporation and CAE dams. The experiments were conducted as screening experiments to find the factor with the most influence.

Figure 4.2 indicates the evaporation and CAE dams' part of the Sasol Secunda ash disposal system, which this study focused on. The evaporation and CAE dams are located on the northern side of FAD 1 and 3. Ash water from the penstock overflow of FAD 3 enters from the northern side into evaporation dam 1. The overflow from FAD 5 enters from the northwestern side into evaporation dam 2. Water from FAD 4 and U69 also enter evaporation dam 2. From there it flows through the set of evaporation dams (the flow direction is indicated). From the evaporation dams it flows to the three CAE dams (CAE dam 1-3). The CAE dams are interconnected so that the water can disperse between them. The clear ash effluent is then pumped from the CAE dams to Sasol East and Sasol West for re-use as ash carrier medium, and also to the TRO (U67) and evaporation (U66) plants. A diagram of the entire FAD, evaporation and CAE dam system can be found in Appendix A.

CAE and Evaporation dams

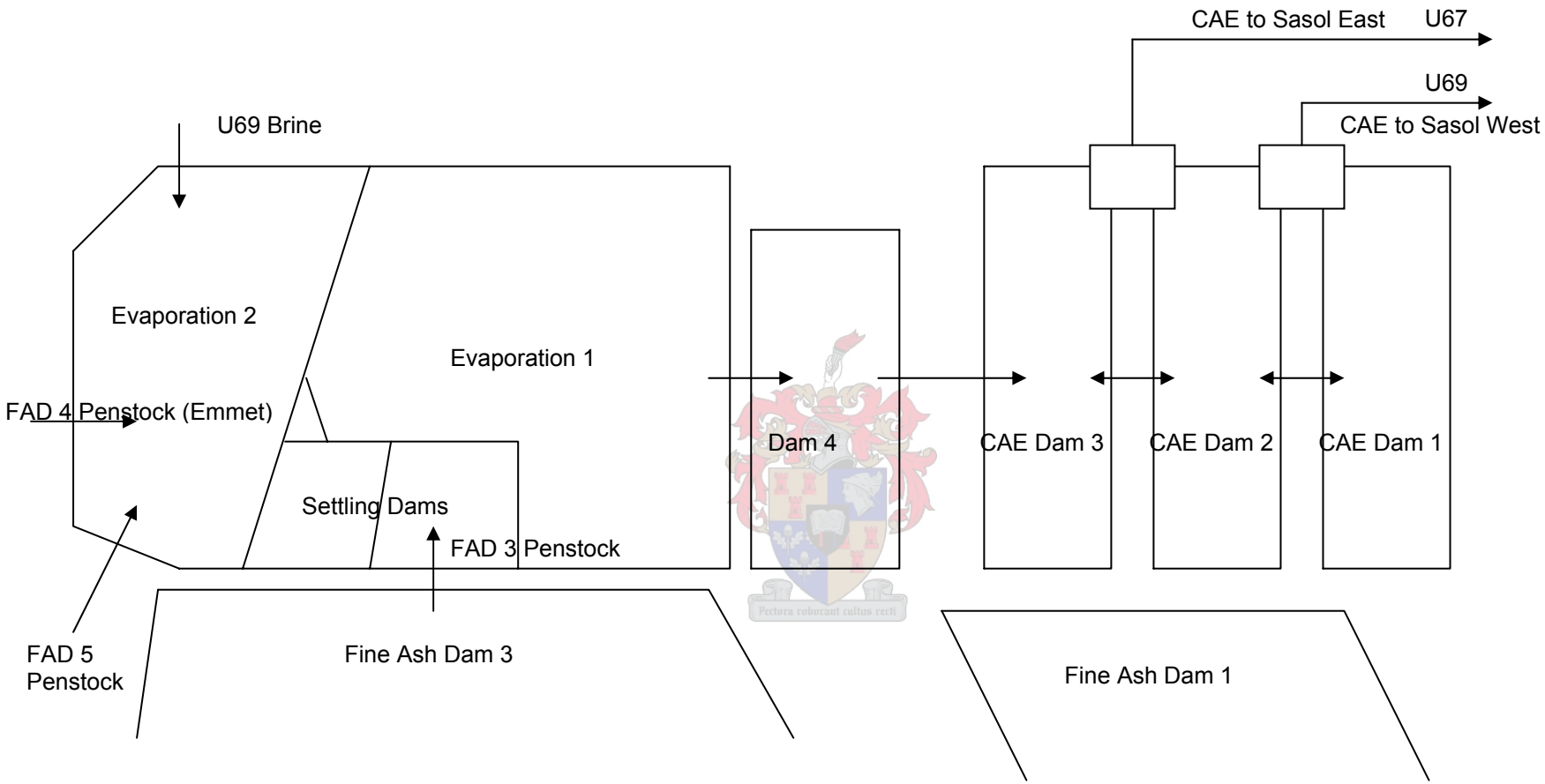

Figure 4.2: Evaporation and CAE dams investigated in this study

Figure 4.3 shows the evaporation dams from the coarse ash heap. Figure 4.4 is the CAE dams.

Figure 4.3: Evaporation dams

Figure 4.4: CAE dams

4.1 Experimental design

4.1.1 Fractional factorial design

The Phase 3 experiments involve the investigation of the effects of different treatments on the system and also combinations of these treatments to evaluate the effect on the enhancement of salt precipitation. When two or more factors are investigated in an experiment, factorial designs are the most efficient type of experimental design.

Factorial designs are also useful when there is interaction between the different factors in the experiment. A problem with factorial designs is that an increase in the number of factors to be investigated greatly increases the number of experiments that have to be done to completely replicate the design (Montgomery, 1984). These multi-factor experiments can be simplified by only allowing two levels for each of the factors (Garcia-Diaz & Philips, 1995). Unfortunately, the problem with the number of experiments is not solved with this.

The most commonly used method to decrease the number of experiments is by neglecting the higher order interactions and to focus only on the lower order interactions. This is called a fractional factorial design (Montgomery, 1984). Experiments like these are also known as screening experiments (Montgomery, 1984). This fractional factorial design is the most suitable design for the Phase 3 experiments in this study.

All the above was taken into account in designing the experiments for Phase 3. The factors were investigated on two levels and the third order interactions were not taken into account. The implementation of the design on the different factors is shown in Table 2.9.

The following factors were investigated in the experiments:

(a) Evaporation rate (High/Low)
(b) Adding a chemical substance ($Ca(OH)_2$) (Addition/No addition)
(c) CO_2 addition through air addition (Addition/No addition)
(d) Adding nets to support the precipitation (Addition/No addition)

In a normal factorial design 16 experimental combinations will have to be done to investigate 4 different factors. With the fractional factorial design, the amount of experiments can be reduced to 8.

Table 2.9: Phase 3 statistical experimental design

a	b	c	d = abc	Combination	Result
-	-	-	-	(1)	A
+	-	-	+	ad	B
-	+	-	+	bd	C
+	+	-	-	ab	D
-	-	+	+	cd	E
+	-	+	-	ac	F
-	+	+	-	bc	G
+	+	+	+	abcd	H

(+ = High/Addition - = Low/No addition)

4.1.2 Statistics

From the results obtained through the experiments the effect that each of the factors has can be statistically calculated. The calculations for each factors' salt removal effect (ℓ_A) and the second order interaction's salt removal effect (ℓ_{AB}), are shown in equations 2.26 and 2.27.

$$\ell_A = \tfrac{1}{4}(-A + B - C + D - E + F - G + H) \quad [2.26]$$

$$\ell_{AB} = \tfrac{1}{4}(A - B - C + D + E - F - G + H) \quad [2.27]$$

The effects of the other factors can be calculated in the same way. With these results, the factors and combination of factors, which have the biggest salt removal effect, can be identified.

4.2 Experiments

4.2.1 Experimental set-up

Phase 3 is the CAE and Evaporation dams. The dams were simulated in an evaporation room. The trays used were 1800mm long, 800mm wide and 100mm deep. These trays were made with stainless steel and had an opening at the one end for emptying the tray at the end of each experiment.

Figure 4.5: Phase 3 experimental setup

A pipe was attached to the bottom of each tray to feed air into the system. The trays were in a room that was exposed to the atmosphere but prevented rain and wind from influencing the experiments.

4.2.2 Experimental procedure

The general experimental procedure for the phase 3 experiments was as follows:

75 litres of CAE was pumped into each of the trays (see 4.2.1). Before the experiment was started a sample of the CAE was taken. The depth of the CAE in each of the trays was measured. The experiment was started and samples and depth measurements were taken on day 3 and day 6 of the experiment. After 6 days the experiment was stopped. The temperature of the air and water was measured every 2 hours throughout the daytime. The influence of the following factors was studied:

- Different evaporation rates.
- Addition of a chemical substance to enhance the precipitation ($Ca(OH)_2$.
- Addition of air to the system.
- Addition of nets to encourage precipitation.

The different evaporation rates were studied to investigate how large the influence of an increase in the evaporation would be on salt removal of the CAE and evaporation dams. Adding a chemical substance had the same influence as the increased evaporation rate, because it would increase the concentration of the Ca in the CAE and evaporation dams. According to Le Chatelier's principle (McGraw-Hill, 1987) this should lead to increased precipitation of calcite.

The CO_2 addition (through the addition of air) is also a way to enhance the precipitation of calcite. The air was added through a pipe with a single opening at the end, connected to the bottom of the tray (Figure 4.10). From

site visits it was observed that extra precipitation formed around reeds on the sides of the dams. It was, therefore, decided to test the influence of nets that could enhance the precipitation in the same way. The nets were hung just below the surface of the water over the entire area of the tray.

Table 4.1 indicates how the different factors were incorporated in the experiments.

Table 4.1: Factors applied to Phase 3 experiments

Factor	High	Low
Addition of air	Air added through pipe ($6l.min^{-1}$)	No addition of air
Evaporation	Evaporation increased with a fan (~$9mm.day^{-1}$)	Normal evaporation (~$3mm.day^{-1)}$
Addition of nets	Nets added to enhance precipitation (4mm mesh size)	No nets added
Chemical substance addition	$Ca(OH)_2$ solution added to increase Ca conc. (100 $mg.l^{-1}$)	No chemical substance added.

Samples of the liquid phase were taken at the start and end of each experiment. These samples were analysed for the following:

- Concentration of Ca, Na, Cl, SO_4 and TDS and
- the electrical conductivity and pH

4.2.3 Experiments performed

Calcite precipitation is the most prominent chemical reaction that takes place in the CAE dams. The atmospheric CO_2 reacts with the $Ca(OH)_2$ in the CAE to form $CaCO_3$ according to reactions 2.1, 2.2 and 2.3 found in Section 2.3.1 in Chapter 2. The factors investigated were those that could enhance this precipitation and be implemented in the Sasol Secunda ash disposal system.

The fractional factorial design determined the combinations that needed to be tested and Table 4.2 indicates the experiments performed on Phase 3.

Table 4.2: Experiments performed on Phase 3

Exp	Treatment
1	Addition of air and nets
2	Increased evaporation rate and addition of air
3	Addition of a $Ca(OH)_2$, air, nets and increased evaporation rate
4	Addition of $Ca(OH)_2$ and air
5	Addition of $Ca(OH)_2$ and nets
6	Increased evaporation rate and addition of nets
7	Increased evaporation rate and the addition of $Ca(OH)_2$
8	Only CAE (Nothing added and no increased evaporation rate)

4.2.4 Analysis methods

The analysis methods are discussed in Section 3.2.3 of Chapter 3.

4.3 Results

4.3.1 Chemical and physical results

Note that a positive value indicates the removal of the element from the effluent and a negative value indicates an increase in the effluent.

The salt concentrations obtained through the analysis were used to calculate the total amount of each of the substances remaining in the effluent at the end of the test. This was done by calculating the amount of water in the trays by means of the height of the water in the tray. The removal of salts from the effluent, the pH and conductivity of the effluent are plotted on graphs for the different combinations tested.

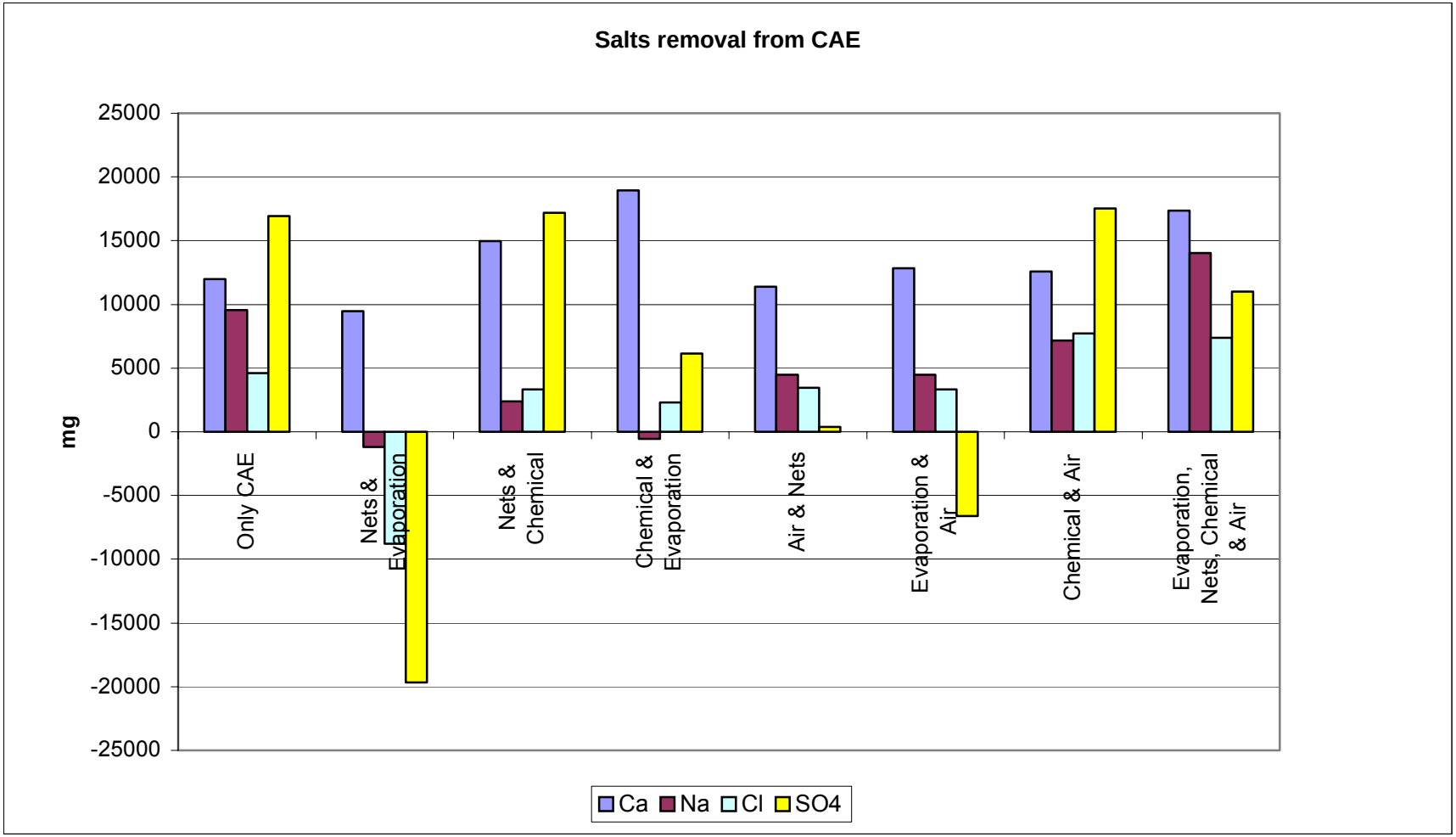

Figure 4.6: Salts removal from CAE

Figure 4.6 shows that calcium is removed throughout all the experiments. This is expected, because of the calcite precipitation found by Koch (2002) and Pretorius and Nieuwenhuis (2002) in their experiments. Sulphate is also removed from the effluent in all, but two of the experiments. In these two experiments there is an increase in the amount of sulphate in the effluent, but this is not possible, because no sulphate is added to the solution. These discrepancies are in experiments where an increased evaporation rate is investigated. The increased evaporation causes very high salt concentrations, which requires large dilution when analysed. Errors in the analysis may be responsible for the increases seen in the amount of sulphate in the effluent. Sodium and chlorine are also removed from the CAE, but in smaller amounts than the calcium and sulphate. This removal can be attributed to very high salt concentrations for which the saturation concentrations of the sodium and chlorine salts were surpassed. The TDS analysis (Figure 4.7) indicates large removal of dissolved solids from the CAE for all the combinations.

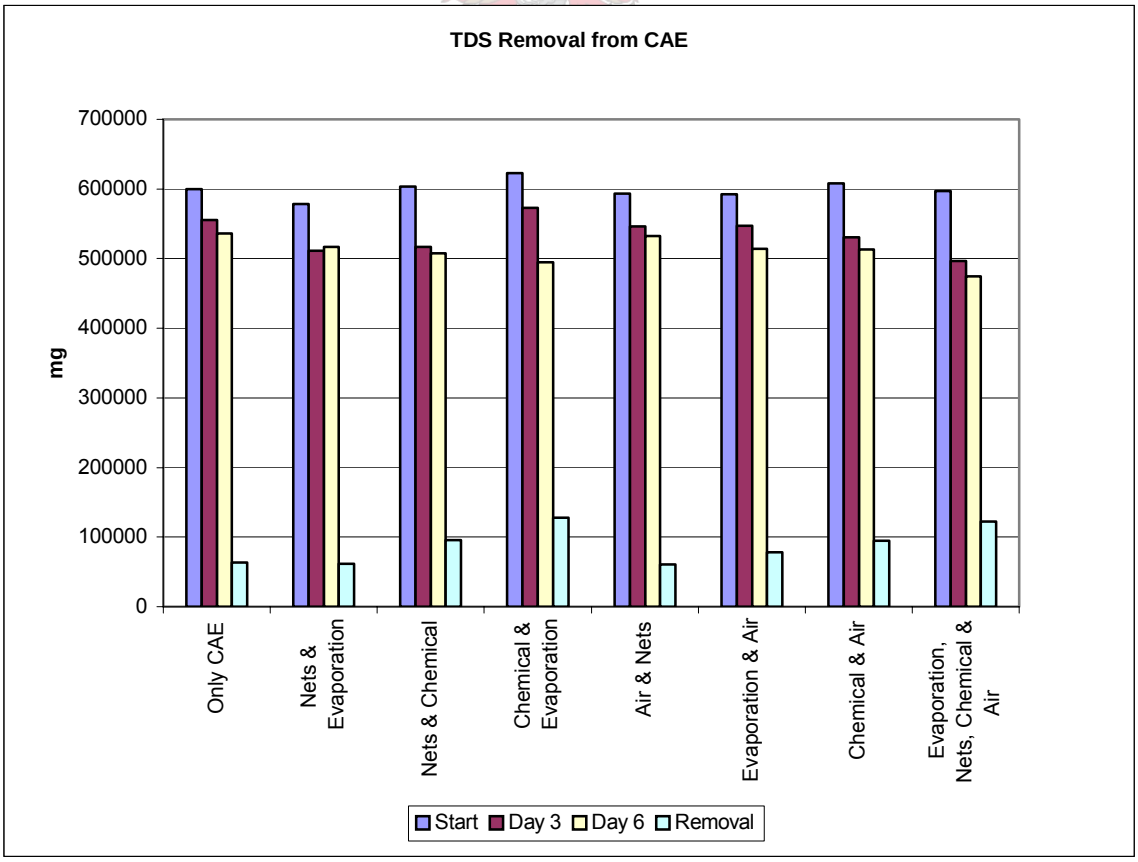

Figure 4.7: TDS removal from CAE

The largest decreases in the amount of TDS occurred in the combinations which investigated the increased evaporation rate and the $Ca(OH)_2$ addition. These factors increase the salt concentration in the CAE, which forces the precipitation reactions to the right hand side according to Le Châtelier's principle (McGraw-Hill, 1987).

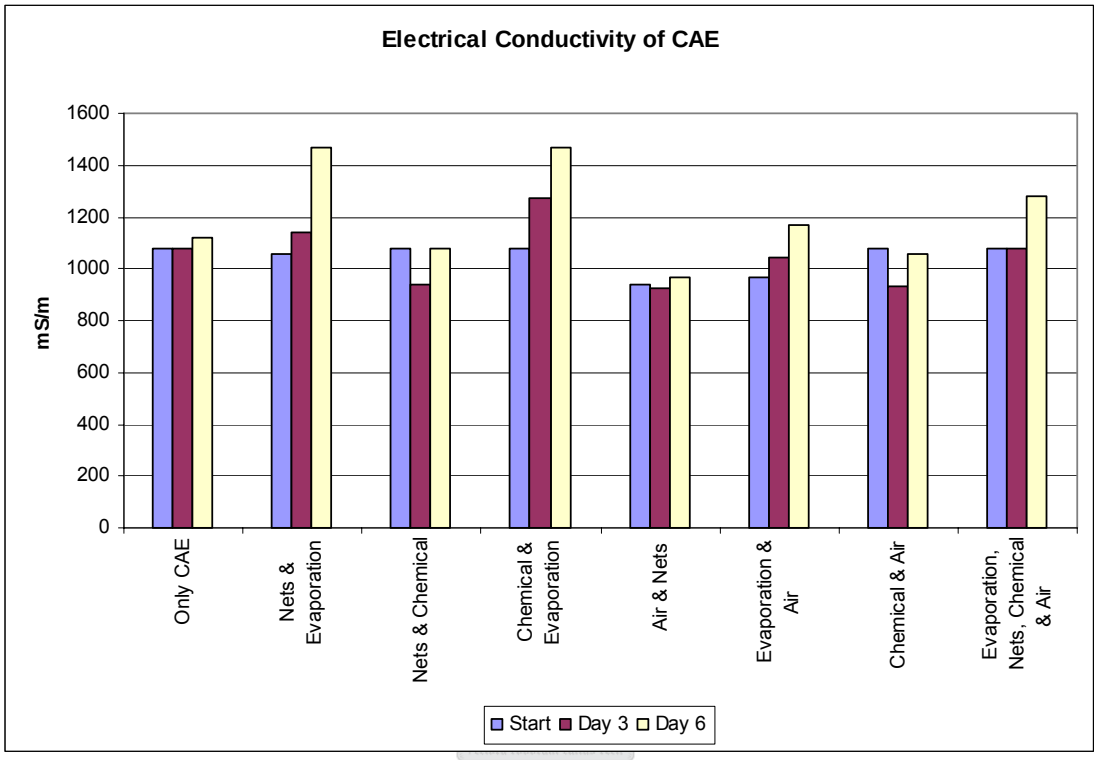

Figure 4.8: Electrical conductivity of CAE

As expected the conductivity of the CAE (Figure 4.8) increases over time. The increase is the highest in the experiments where an increased evaporation rate is investigated. This is due to the high salt concentrations in the effluent that are caused by the high evaporation. The increases in conductivity indicate that the ions are packed more closely together. This decreases the activity coefficient and increases the solubility of the slightly soluble compounds like calcite (NALCO, 1988). The increased evaporation rate on the one hand encourages precipitation by increasing the concentration of the salts in the solution but on the other hand it may also increase the solubility of the calcite.

Most of the precipitation occurs during the first 3 days as deducted from the results of the TDS and pH. It may therefore, be this increase in the solubility of the calcite that prevents more of it to precipitate.

The pH of the CAE (Figure 4.9) is relatively high at the start of the experiments. It drops sharply after the first 3 days, which is due to the precipitation of the calcite. The calcite precipitation lessens the amount of CO_3^{2-} and HCO_3^- in the effluent, which in turn decreases the alkalinity and the pH of the CAE. In the next 3 days, this drop is less severe. This could be due to most of the calcium already being precipitated as calcite during the first 3 days of the experiments or the CAE could be saturated with respect to $CaCO_3$. It appears that the air (CO_2) addition does not influence the pH. The level of the pH on day 6 stay more or less around 8 for all the different combinations tested.

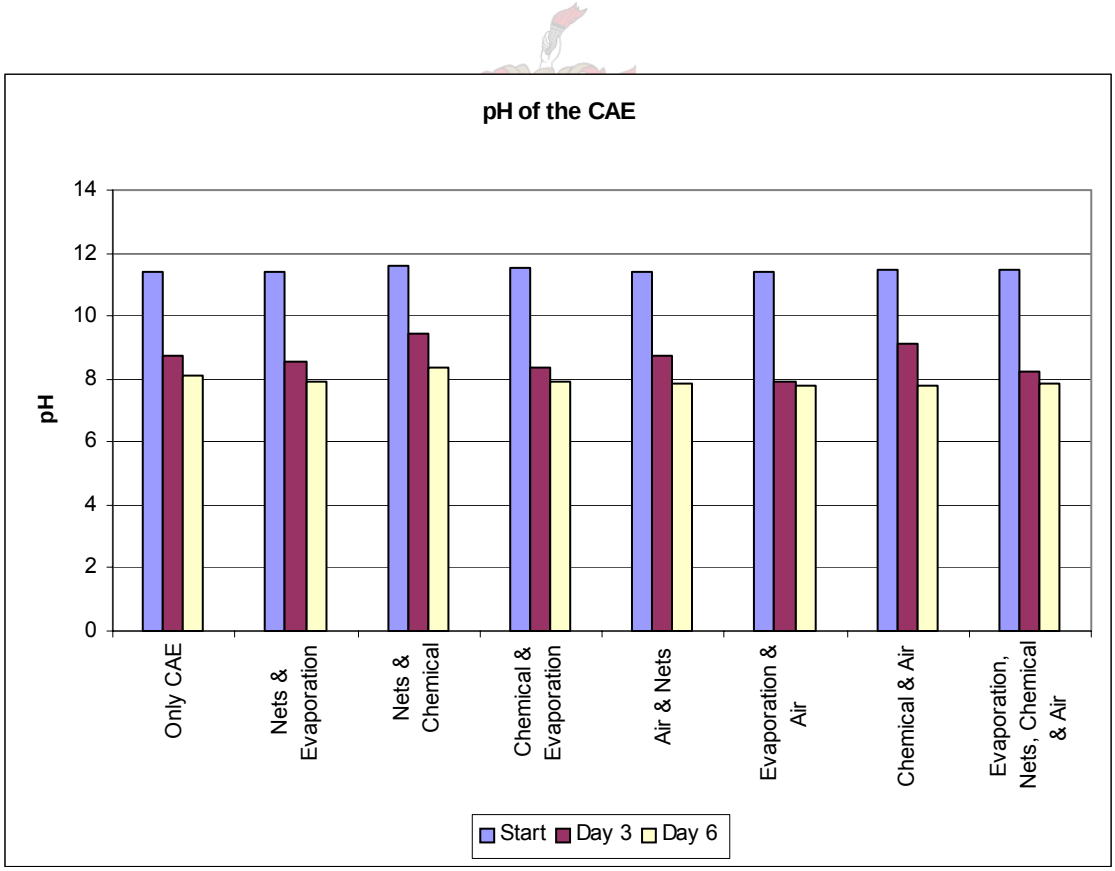

Figure 4.9: pH of the CAE

Figure 4.10: Calcite precipitation in the Phase 3 experiments

Figure 4.10 and 4.11 indicate the calcite precipitation that was observed around the outlets of the air into the CAE during the combinations that investigated the addition of air.

From the observation it may seem as if a lot of calcite precipitated during these experiments. The results, however, tell a different story and the salt removal effect of the air is much less than expected as can be seen in the discussion of the statistical analysis.

Figure 4.11: Calcite precipitation in the Phase 3 experiments (close up)

Table 4.3 indicates the ratio between the amount of TDS in the effluent and the electrical conductivity. This was done to test consistency of the results for the different combinations. Only two of the combinations show a slightly higher ratio than that of the other but it is not alarmingly high. The rest of the combinations compare well to the ratios found in Chapter 3.

Table 4.3: TDS:EC ratio for CAE

TDS:EC Ratio	
Only CAE	7.47
Nets & Evaporation	7.30
Nets & Chemical	7.31
Chemical & Evaporation	7.48
Air & Nets	8.36
Evaporation & Air	8.45
Chemical & Air	7.41
Evaporation, Nets, Chemical & Air	7.12

4.3.2 Statistical Analysis

The statistical analysis for the Phase 3 experiments was discussed in Chapter 2 and an overview was given at the start of this chapter.

Each result from the different combinations is assigned a letter from A to H. The assignment can be seen in Table 4.4. This is done to simplify the explanation of the statistical analysis.

Table 4.4: Experimental results for statistical analysis

Experiments	Result
Only CAE	**A**
Nets & Evaporation	**B**
Nets & Chemical	**C**
Chemical & Evaporation	**D**
Air & Nets	**E**
Evaporation & Air	**F**
Chemical & Air	**G**
Evaporation, Nets, Chemical & Air	**H**

In Table 4.5 it can be seen how the results were manipulated to present the statistical results. After the addition each column had to be divided by 4. This calculated figure was then used to analyse the salt removal effect of each individual factor and also the interaction between the factors as indicated. The statistical analyses were done on the calcium and TDS results, as they were the most constant results. In the statistical results a large positive value indicates a large salt removal effect and a large negative value indicates little or no salt removal effect.

Table 4.5: Statistical analysis for Phase 3

Statistical Analysis						
Factors						
Evap	**Chem**	**Air**	**Nets**	**Evap+Chem**	**Evap+Air**	**Chem+Air**
-A	**-A**	**-A**	**-A**	**+A**	**+A**	**+A**
+B	**-B**	**-B**	**+B**	**-B**	**-B**	**+B**
-C	**+C**	**-C**	**+C**	**-C**	**+C**	**-C**
+D	**+D**	**-D**	**-D**	**+D**	**-D**	**-D**
-E	**-E**	**+E**	**+E**	**+E**	**-E**	**-E**
+F	**-F**	**+F**	**-F**	**-F**	**+F**	**-F**
-G	**+G**	**+G**	**-G**	**-G**	**-G**	**+G**
+H	**+H**	**+H**	**+H**	**+H**	**+H**	**+H**

Table 4.6 shows the statistical results for the calcium. The addition of $Ca(OH)_2$ and the increased evaporation rate have the largest positive effects and therefore, the largest salt removal capabilities. The negative values of the addition of air and nets indicate that these factors have little salt removal capabilities.

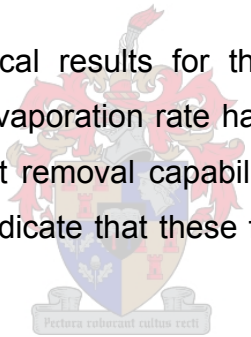

Table 4.6: Statistical results for calcium

Statistical Analysis	
Calcium	
Factors	**Relative effect**
Evaporation	1922.2
Chemical addition	4560.7
Air addition	-308.3
Nets	-789.8
Evaporation + Chemical addition	2446.4
Evaporation + Air addition	1186.4
Chemical addition + Air addition	-1677.1

Results for the TDS statistical analysis (Table 4.7) compare well to the results from the statistical analysis on the calcium. Increases in concentration through increased evaporation rate and $Ca(OH)_2$ addition are the factors with the biggest salt removal capabilities. The salt removal capabilities of the air addition and nets addition are again very small.

Table 4.7: Statistical results for TDS

Statistical Analysis	
TDS	
Factors	**Relative effect**
Evaporation	18683.5
Chemical addition	44151.5
Air addition	1986.5
Nets	-5961.5
Evaporation + Chemical addition	11171.5
Evaporation + Air addition	3896.5
Chemical addition + Air addition	-4865.5

From the statistical analysis it is clear that the increased evaporation rate and the addition of $Ca(OH)_2$ to the CAE are the factors that have the biggest salt removal ability. This is conformation of what was seen in the salt and TDS removal analyses.

4.4 Mass Balances

To quantify the salt removal of Phase 3 of the Sasol Secunda ash disposal system, one has to look at the mass balance around the whole system. The influence that this research will have on the Sasol Secunda ash disposal system, will be discussed in detail in Chapter 5. The results presented here are only to give an indication of the expected precipitation that the investigated factors will produce.

4.4.1 Calcium

Table 4.8 indicates the precipitation of calcium, which is primarily in the form of calcite. Large increases in the precipitation are experienced with the addition of $Ca(OH)_2$ and the increasing of the evaporation rate, but good precipitation is also achievable without the addition of anything.

Table 4.8: Calcium Mass Balance

Mass Balance				
Calcium				
Combination	**Start**	**End**	**Loss**	
	mg			**g/l**
Air & Nets	52425	41052	**11373**	**0.152**
Evaporation & Air	51825	39000	**12825**	**0.171**
Evaporation, Nets, Chemical & Air	53898	36533	**17365**	**0.223**
Chemical & Air	53040	40440	**12600**	**0.162**
Nets & Chemical	53196	38214	**14982**	**0.192**
Nets & Evaporation	48600	39120	**9480**	**0.126**
Chemical & Evaporation	54990	36036	**18954**	**0.243**
Only CAE	51225	39245	**11980**	**0.160**

4.4.2 TDS

Although the calcite is one of the main precipitants in the CAE dams the decreases in the TDS values are much larger than the decreases in the calcium concentration. Table 4.9 indicates that there are other mechanisms that may be occurring in the CAE because of the large amounts of TDS that are removed.

Table 4.9: TDS Mass Balance

Mass Balance				
TDS				
Combination	**Start**	**End**	**Loss**	
	mg			**g/l**
Air & Nets	593250	532620	**60630**	**0.808**
Evaporation & Air	592500	514500	**78000**	**1.040**
Evaporation, Nets, Chemical & Air	596700	474204	**122496**	**1.570**
Chemical & Air	607620	512914	**94706**	**1.214**
Nets & Chemical	603720	508200	**95520**	**1.225**
Nets & Evaporation	578250	516960	**61290**	**0.817**
Chemical & Evaporation	622440	495000	**127440**	**1.634**
Only CAE	600000	536364	**63636**	**0.848**

Due to the complexity of the CAE and the influence that foreign ions have on precipitation prediction (NALCO, 1988), it is very difficult to theoretically predict what is happening in the system. The precipitation of calcite is the only mechanism that can be explained chemically.

These mass balances only give an indication of the amount of calcium and TDS that was removed during the experiments. The main aim of the experiments was to identify possible salt removal enhancements that may be used in the Evaporation and CAE dams.

4.5 Summary

After analysing the results that were obtained from the experiments replicating Phase 3 it can be summarised as follows:

- Increases in the concentration of the CAE through $Ca(OH)_2$ addition and an increased evaporation rate, had the biggest influence on increasing salt precipitation. This is in accordance with Le Chatelier's principle (McGraw-Hill, 1987).

- A cost effective way to increase the precipitation in the evaporation and CAE dams system would be to increase the evaporation rate. This may be possible to do by installing a sprinkler system.
- A constant decrease in the calcium concentrations and a decrease in the pH for all combinations confirm the formation of calcite in Phase 3.
- The constant reduction in the TDS of the CAE, which is much larger than the reduction in calcium, indicates that there may be other minerals that co-precipitate with the calcite.
- The addition of the air (CO_2 in low concentrations) and nets had little or no effect on increasing the precipitation of salts in the CAE.

In the next chapter the focus will be on the Evaporation and CAE dams in the Sasol Secunda ash disposal system. The results of the flow measurements done on the ash disposal system will be used to analyse the salt removal capabilities of the Sasol Secunda ash disposal system at the moment.

Chapter 5

CAE and evaporation dams:

Salt balances and residence time

As discussed in Chapter 4, calcite precipitation is the main mechanism of salt removal in the Evaporation and CAE dams. In this chapter the focus is on what is happening at the Evaporation and CAE dams at Sasol Secunda (Figure 4.1).

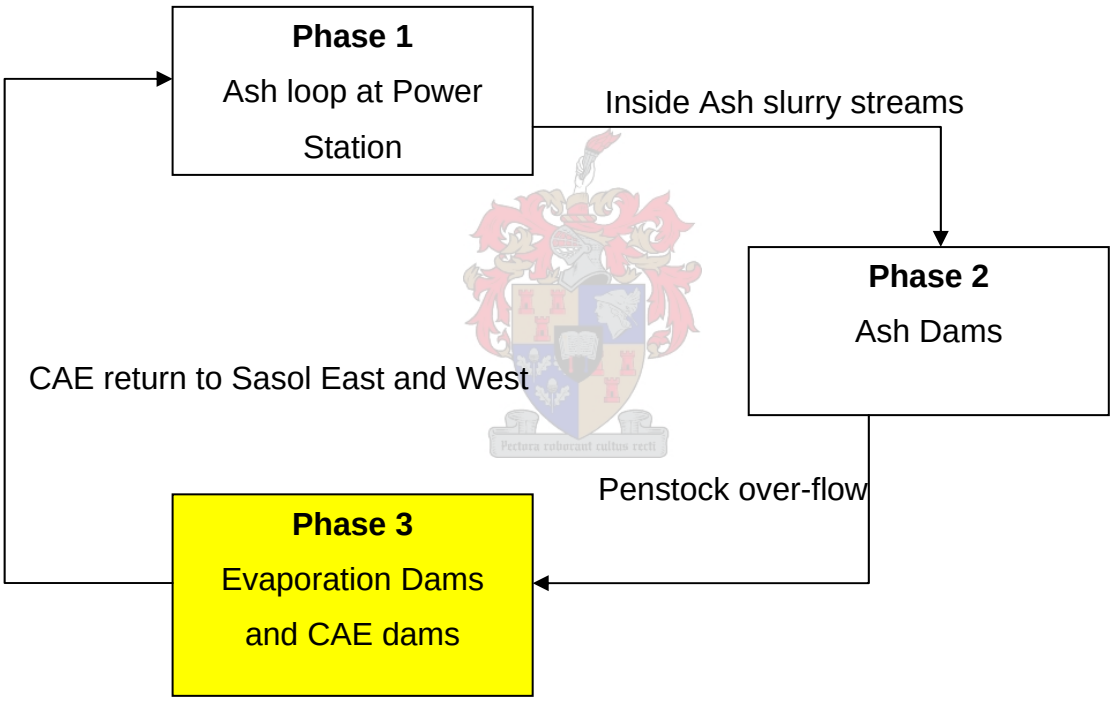

Figure 4.1: Phase 3 indication diagram

This part of the study was deemed necessary to supplement the findings of the precipitation enhancement tests done in the previous chapter. It was decided to investigate the salt removal and residence time of the water in the CAE and Evaporation dams.

To achieve this, the following was done:

- Identifying all the inlet and outlet streams to the CAE and Evaporation dams.
- Taking flow measurements.
- Analysing the water entering and exiting the dam system.
- Calculating a mass balance across the Evaporation and CAE dams.

The amount of salt removal found by this study can be used to make predictions of the increases that may be expected if the precipitation enhancement factors, studied in the previous chapter, were implemented.

5.1 Evaporation and CAE dams system

This system was also discussed in Chapter 4. Reviewing Figure 4.2 (duplicated on the next page) one can see that there are four main streams entering the Evaporation and CAE dams. There are also four main streams exiting the system. The focus will therefore, be on these streams.

There are other smaller streams also entering the system. This will be discussed at a later stage. The rainfall and evaporation must also be taken into account. This study was conducted during the months of late August and beginning of September. Strong winds make evaporation an important factor to consider. Although the rainfall is very little during that time, it was also considered.

5.1.1 Inlet streams

Slurry is pumped from Inside Ash inside the Sasol Secunda Petrochemical Plant to the ash dams on the outside of the plant. An estimation of the amount of water in this slurry is 1968 m^3/h (Moller, 2002).

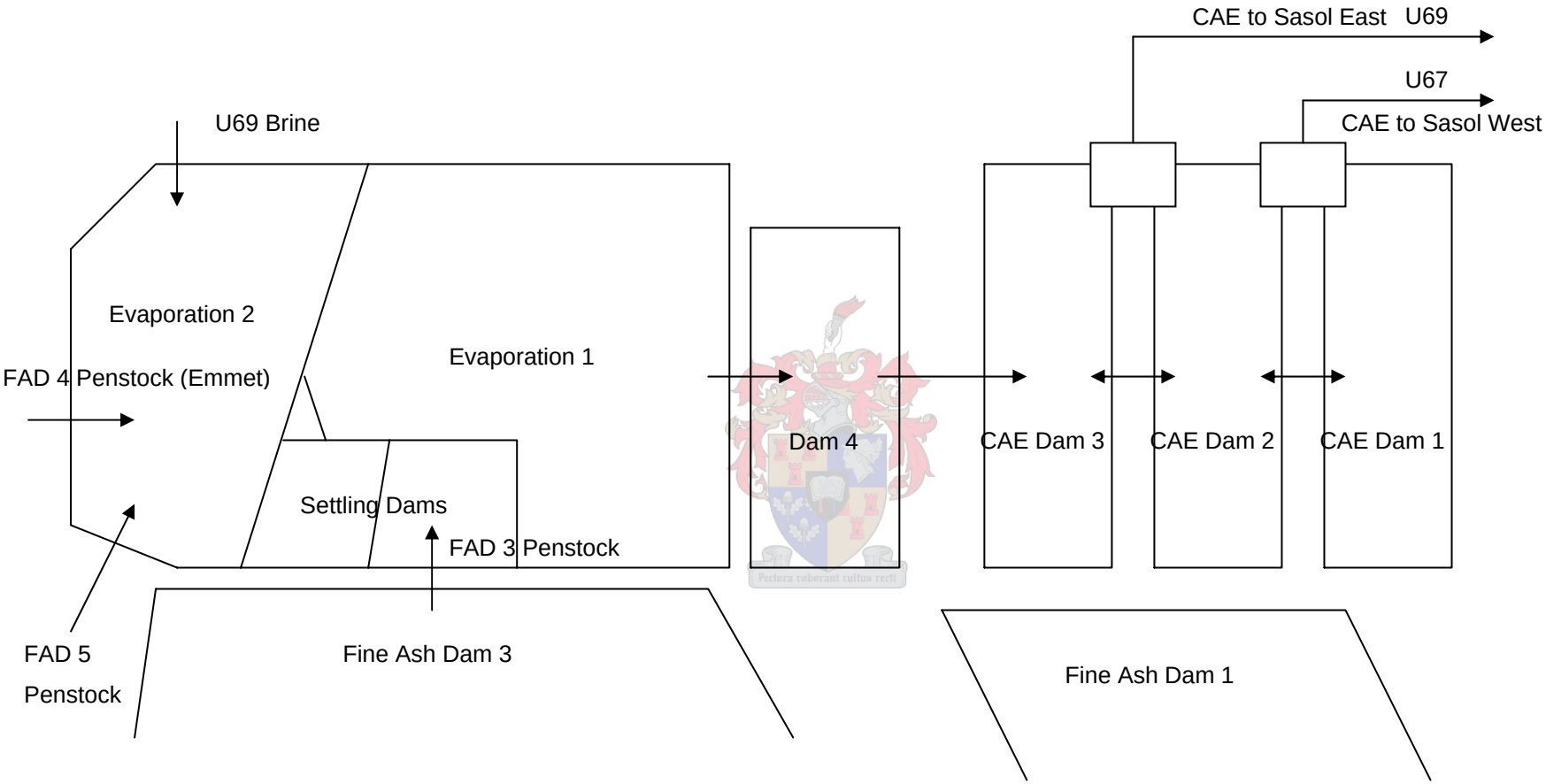

Figure 4.2: Evaporation and CAE dams investigated in this study

This slurry is pumped onto FAD 3, FAD 4, and FAD 5. A fine coal slurry is pumped from time to time to fine coal dam 5 (FCD 5). The slurry pumped to FCD 5 is normally such a small amount that it was decided to leave it out in this investigation.

The water that is not withheld in these ash dams then flows through the penstock overflow into Evaporation dam 2 (FAD 4 and FAD 5) or Evaporation dam 1 (FAD 3). There is also brine from U69 (TRO), which is pumped into Evaporation dam 2.

The following can now be classified as the inlet streams:

- Penstock from FAD 3,
- Penstock from FAD 5,
- Penstock from FAD 4 (Emmet),
- Brine form U69 (TRO), and
- Other

Other streams that enter the evaporation and CAE dams include water contained in the coarse ash and mine water that is pumped to the outside ash system. These flows are combined into a category named “Other”. The flow rates for other streams are estimated from the work done by Moller (2002).

5.1.2 Outlet streams

The outlet streams from the evaporation and CAE dams are comprised of the following:

- CAE to Sasol West,
- CAE to Sasol East,
- CAE to U67, and
- CAE to U69

The flow rates of these streams are measured or will be estimated from previous work done on the evaporation and CAE dams.

5.1.3 Evaporation and rainfall

Data for the evaporation and rainfall of the Secunda region were obtained. This data in conjunction with the areas of the Evaporation and CAE dams was used to estimate the amount of evaporation.

5.2 Flow measurements

In the work done by Moller (2002), most of the flows that were measured at Outside Ash at the Sasol Secunda ash disposal system had to be done by primitive means or by estimations. From previous site visits to the Sasol Secunda ash disposal system it was decided to measure the flows where possible. This will give better estimations of the salt holding capabilities of the evaporation and CAE dams.

Weirs to measure the flow from FAD 3 and FAD 5 were designed at the University of Stellenbosch. These weirs were manufactured and installed by Sasol during a site visit in the month of August. The weir design for the FAD 3 weir was done from information found in Binnie & Partners (1987).

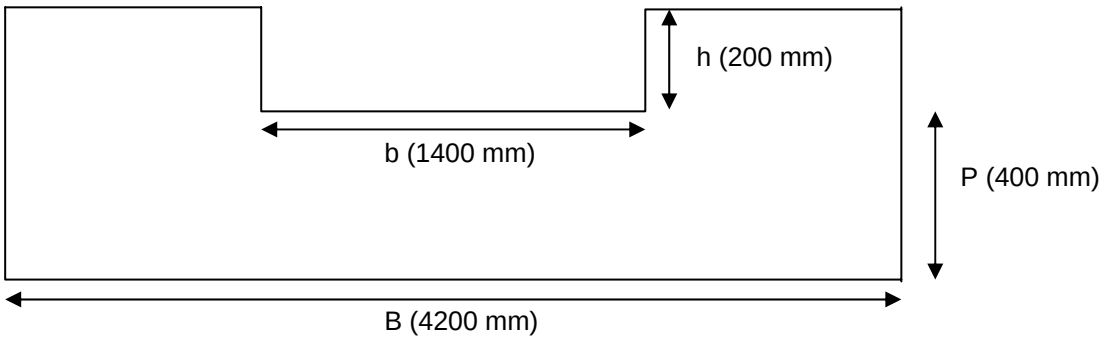

Figure 5.1: FAD 3 weir design

The head of water over the weir (h) is measured and then formulas 5.1 and 5.2 were used to determine the flow:

$$\mathbf{Q} = C_e*2/3*b*(2g)^{1/2}*h^{3/2} \quad [5.1]$$

$$\mathbf{C_e} = 0.616*(1-0.1*h/b) \quad [5.2]$$

Q = flow rate	[m^3/s]
C_e = discharge coefficient	
b = width of weir	[m]
g = gravitational acceleration	[m/s^2]
B = base width of weir	[m]
P = height of weir from ground	[m]
h = head of water over weir	[m]

The FAD 5 weir is a suppressed weir design (ASTM, 1993).

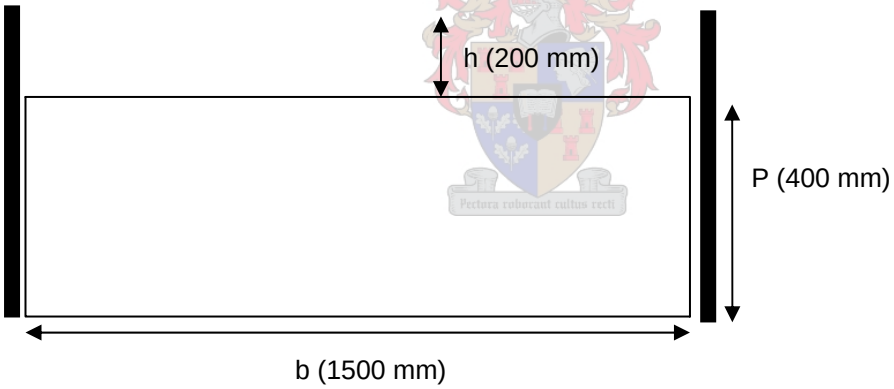

Figure 5.2: FAD 5 weir design

To determine the flow rate, the head of water over the weir is also measured and then used in formulas 5.3 and 5.4:

$$\mathbf{Q} = C_e*2/3*b*(2g)^{1/2}*h^{3/2} \quad [5.3]$$

$$\mathbf{C_e} = 0.605+1/1000h+0.08h/P \quad [5.4]$$

Q = flow rate [m^3/s]

C_e = discharge coefficient
b = width of weir [m]
g = gravitational acceleration [m/s^2]
P = height of weir from ground [m]
h = head of water over weir [m]

5.2.1 Inlet streams

The flow rates were measured over a two week period and the average values are given here.

The average of measured flow rate from the FAD 3 penstock is 458.67 m^3/h. This is less than the average measured flow rate from the FAD 5 penstock, which is 537.35 m^3/h.

The flow of the inlet streams classified as “other” can be estimated with information found in Moller (2002). The coarse ash transported to the coarse ash heaps contains water. Some of this water enters the ash system and the flow rate is estimated at 30 m^3/h (Moller, 2002). There is also mine water entering the CAE and evaporation dams and Moller (2002) estimated this flow at 97 m^3/h.

The flow from FAD 4 (Emmet dam) is 425 m^3/h and the TRO brine entering the system, 539.4 m^3/h.

5.2.2 Outlet streams

The outlet streams are all combined in one flow measurement. It consists of water fed to units 03, 203, 67 and 69. The total flow is 2070.3 m^3/h.

Figure 5.3: FAD 3 weir after installation

Figure 5.4: FAD 5 weir after installation

5.2.3 Evaporation and rainfall

From the evaporation data it could be calculated that the average evaporation per day is ~ 4 mm/day for the time the flow measurements were taken. This translates into an average evaporation rate of 92 m^3/h. The rainfall for the same period was only 2 mm. This is an average rate of only 2.3 m^3/h.

5.2.4 Residence time

Table 5.1 indicates the different inlet and outlet streams. The average volume of the evaporation and CAE dam system was also calculated. This was used to determine the time the CAE spends in the evaporation and CAE dams. The assumption that no short circuiting takes place was made.

Table 5.1: Residence time calculation

Residence time	
Inlet streams	**Flowrate (m^3/h)**
FAD 5	537.35
FAD 4 (Emmet)	425
FAD 3	458.67
U69 Brine	539.4
Other	127
Rainfall	2.3
Total In	**2089.72**
Outlet streams	**Flowrate (m^3/h)**
Sasol 2	2070.3
Sasol 3	
U69	
U67	
Evaporation	92
Total Out	**2162.3**
Dam volumes	**m^3**
Volume (Start)	1856000
Volume (End)	1790000
Volume (Avg)	**1823000**
Time (h)	**843**
Time (days)	**35**

The outlet streams are slightly higher than the inlet streams and that led to a decrease in the dam volumes. A residence time of approximately 35 days was calculated.

5.3 Salt balance

A salt balance over the Evaporation and CAE dam system was done for the main components investigated in this study. The calculations for each of the components can be found in Appendix D.

Table 5.2 indicates a summary of the results obtained for the salt balance. A positive value indicates that the salts are retained in the Evaporation and CAE dams. A negative value indicates a salt increase in the ash water.

Table 5.2: Overall salt balance

Overall Salt Balance			
	IN	**OUT**	**Increase/Decrease**
	t/h		
Ca	1.077	0.803	**0.274**
Na	3.408	3.145	**0.263**
Cl	2.003	1.855	**0.148**
SO_4	7.224	8.323	**-1.098**
TDS	15.723	13.362	**2.361**

Calcium is retained in the CAE and Evaporation dams, as expected. Sodium and chlorine are also retained. There is an increase in the sulphate concentration of the ash water. Overall there is a 2.4 tons per hour decrease in the amount of TDS in the ash water, amounting to salt removal of approximately 57.6 ton/day. This is 15% of the total salt load per day.

Table 5.3: Salt balance comparison

Overall Salt Balance		
	Van den Berg (2004)	**Moller (2002)**
	Increase/Decrease	
	t/h	
Ca	0.274	0.388
Na	0.263	-0.629
Cl	0.148	-0.101
SO_4	-1.098	-1.069
TDS	2.361	1.971

Comparing the results of this investigation with those of the investigation done by Moller (2002) some similarities can be seen. In both cases there is retention of calcium and TDS. An increase in the sulphate concentration is also found in both cases. The sodium and chlorine results do not compare well. A reason for the changes could be the addition of the TRO brine.

5.4 Summary

The results obtained in this chapter can be summarised as follows:

- The residence time of the CAE in the Evaporation and CAE dams is approximately 35 days. This is assuming no short circuiting occurs which would shorten the residence time.
- Calcium is retained in the Evaporation and CAE dams. This is further proof that the $CaCO_3$ precipitation is the main mechanism of salt removal in the Evaporation and CAE dams.
- An increase in the sulphate concentration in the Evaporation and CAE dams indicates that most of the sulphate removal occurs during the ash-water interaction in Phase 1. The increase may however also be due to the addition of the TRO brine to the CAE and Evaporation dams.

Chapter 6
Conclusions and Recommendations

The aim of this study was to find means to enhance the salt removal capabilities of the ash disposal system. The initial mixing of the effluent and fine ash and the CAE and evaporation dams of the system were investigated. The main conclusions drawn from the study are presented here.

6.1 Conclusions

6.1.1 Phase 1 experiments (Ash loop at Power Station)

The following conclusions could be drawn after studying the results obtained from the experiments:

6.1.1.1 Liquid phase

- The mixing of brines (TRO and EDR) and ash only, does not produce more leaching of salts into the liquid phase than the mixing of CAE and ash.
- Calcium is the main element that is leached and sulphate the main element that is removed from the liquid phase. The amount of sodium and chloride in the liquid phase stays almost constant throughout all the experiments.
- The increase in the amount of calcium in the liquid phase is less than 100% for the TRO and EDR brine and ash mixtures, but more than 240% for the CAE and ash mixture.
- For the TRO and EDR brine and ash mixtures, 39% and 43% of the sulphate is removed, respectively.
- The ash disposal system can be used as a salt sink for sulphate. This is in accordance with results obtained by Koch (2002).

- The conductivity of the liquid phase increases to approximately the same level for the different combinations tested. This indicates that the brines produce the same kind of interaction as the CAE.
- There is virtually no difference in the final value of the pH for the different combinations tested. This also confirms that the interaction of the brines and ash and that of the CAE and ash do not differ.
- Adding CO_2 to the system decreases the leaching of the TDS (an 8% increase compared to a 93% increase without addition) and especially calcium, considerably. Sulphate is still removed from the liquid phase, but with less calcium leached there is also less sulphate removed. The sulphate is mainly removed through $CaSO_4$ precipitation, therefore, if there is less calcium to react with, less $CaSO_4$ can form to precipitate sulphate from the liquid phase.
- CO_2 addition can, therefore, be used to prevent excessive leaching of soluble minerals into the liquid phase.
- The TRO brine can be used as carrier medium for the ash. Either on its own or in combination with the CAE.

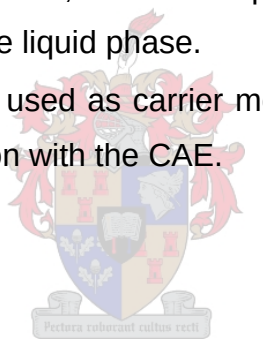

6.1.1.2 Ash phase

- No major changes in the chemical composition of the ash are found for the different combinations of brine, CAE and ash tested. There is an increase in the calcium content with the addition of CO_2.
- The XRD analyses also show no real changes to the mineral content of the ash except in the case of the CO_2 addition. $CaCO_3$ can be seen in the washed and unwashed ash. This indicates the immobilisation of the formed calcite in the ash.
- $CaSO_4$ formation is the reason for the SO_4 decrease in the liquid phase around the ash, but the ash analyses do not show any traces of $CaSO_4$. This indicates that the $CaSO_4$ formed, is not immobilised in the ash.

6.1.2 Phase 3 experiments (Evaporation and CAE dams)

After analysing the results that were obtained from the experiments the following conclusions can be drawn:

- The most cost effective way (tested in this study) to increase the precipitation in the evaporation and CAE dams system would be to increase the evaporation rate. This may be possible to do by, for example installing sprinklers.
- A constant decrease in the calcium concentrations and a decrease in the pH for all combinations confirm the formation of calcite in Phase 3.

6.1.3 Salt balances and residence time

The following could be concluded from the salt balance and residence time calculations:

- The residence time of the CAE in the Evaporation and CAE dams is approximately 35 days. This is assuming that no short circuiting occurs which would shorten the residence time.
- Calcium is retained in the Evaporation and CAE dams. This is further proof that the $CaCO_3$ precipitation is the main mechanism of salt removal from the liquid phase in the Evaporation and CAE dams.
- An increase in the sulphate concentration in the Evaporation and CAE dams indicates that the sulphate removal from the liquid phase occurs during the ash-water interaction in Phase 1.

6.1.4 General conclusions

This study focussed on multiple aspects of the Sasol Secunda ash disposal system. In this section the influence of the different findings on the larger research project regarding the salt problem at the Sasol Secunda ash disposal system will be discussed.

The Phase 1 experiments (initial mixing of ash, brine and CAE) showed that SO_4 can be precipitated during the initial contact between the ash and the TRO and EDR brines. This is in accordance with the results obtained by Koch (2002) for the usage of the ash dams as a salt sink for SO_4. The investigation into the influence of CO_2 addition yielded the following:

- Ca leaching is reduced from a 240% increase to only an 8% increase in the liquid phase.
- TDS leaching is also reduced.
- $CaCO_3$ is formed, as expected.

Pretorius and Nieuwenhuis (2002) did column test, which simulates the conditions in the ash dams, under a CO_2 atmosphere and also found that the concentrations of the Ca and TDS decreased. This study shows that the CO_2 addition at the mixing point leads to better results.

There may be a trade-off between the Ca and SO_4 removal. The SO_4 needs Ca to form $CaSO_4$ and be removed. If Ca is removed through CO_2 addition it may cause less SO_4 to be removed. At this moment this is only speculation and it still needs to be tested.

The Phase 3 experiments indicated that increased evaporation and the addition of $Ca(OH)_2$ are the best mechanisms to increase the precipitation in the Evaporation and CAE dams. Financial implications were not considered in this study because of it being part of a larger study. Using sprinklers to increase the evaporation may be the most cost effective way to increase the evaporation.

The mass balance indicates that the Evaporation and CAE dams remove approximately 57 tons of salt per day. This is 15% of the salts that enter the Evaporation and CAE dams. This salt removal is mainly through the precipitation of $CaCO_3$.

6.2 Recommendations

Further research should still be done on various areas of the ash system. Recommendations pertaining to follow-up work from this research project are as follows:

6.2.1 Phase 1 experiments (Ash loop at Power Station)

- The addition of CO_2 to the brine and ash mixtures should be investigated.
- Different injectors can be looked at to disperse the CO_2 better and this may totally prevent the leaching of calcium.
- More work needs to be done to enhance the formulas predicting the amount of leaching and salt removal. This can include doing test runs with brines on the Sasol Secunda ash disposal system.
- The TRO brine may be used as carrier medium for the ash.
- Investigate the relationship (trade-off) between Ca and SO_4 removal.

6.2.2 Phase 3 experiments (Evaporation and CAE dams)

- The addition of pure CO_2 to the CAE may increase the calcite precipitation further. Care must be taken not to make the CAE too acidic (pH < 8), which will then prevent calcite precipitation.
- Experiments that run for longer should also be done. For this bigger trays or maybe even small dams would be needed. It would have to sustain up to a month's evaporation.
- The installation of a sprinkler system (or similar evaporation devices) to enhance the evaporation should be investigated.

6.2.3 Salt balances and residence time

- Constant measurement of as many as possible of the flow rates should be done.

- Samples should be taken on a regular basis to determine the salt retaining capabilities of the Evaporation and CAE dams for different times of the year.

References

American Society for Testing and Materials (ASTM), 1993, ASTM D5242, *Standard method for open-channel flow measurement of water with thin-plate weirs*, Available from Global Engineering Documents at http://global.ihs.com

Bezuidenhout, N., 1995, *Chemical and mineralogical changes associated with leachate production at Kriel power station ash dams*, MSc Thesis, University of Cape Town, South Africa, pp 2-66.

Binnie & Partners, 1987, *Guide to water and waste-water management in the fruit and vegetable processing industry*, Report for Water Research Commission, Pretoria, South Africa, pp 47-52.

De Villiers, D., 2001, *Bench-scale Investigation into the Blending of TRO Brine with Thickened Fine-ash Slurry, Fine-ash Dam Penstock & Evaporation Dam Water*, Sastech R&D, Water and Environmental Technology Research, Internal Report.

Dhanpat, R., Eary, L.E., Mattigold, S.V., Ainsworth, C.C., and Zachara, J.M., 1986, *Leaching Behavior of Fossil Fuel Wastes: Mineralogy and Geochemistry of Calcium*. In: McCarthy, G.J., Glasser, F.P., Roy, D.M., and Diamond, S., (Eds.) Fly Ash and Coal Conversion By-products: Characterization, Utilisation and Disposal III, Materials Research Society Symposia Proceedings, Boston, vol. 86, pp 3-12.

Drever, J.I., 1988, *The geochemistry of natural waters*, 2nd edition, Prentice Hall, New Jersey, USA, pp 207-208.

Fytianos, K., Tsaniklidi, B., Voudrias, E., 1998, *Leachability of heavy metals in Greek fly ash from coal combustion*, Environment International, 24, (4) In: Fuel and Energy Abstracts, September 1998, pp 393.

Garcia-Diaz, A., Philips, D.T., 1995, *Principles of Experimental Design and Analysis,* Chapman & Hall, New York, USA, pp 197-219.

Ghosh, S., 1990, *Statistical Design and Analysis of Industrial Experiments*, Marcel Dekker, New York, USA, pp 175-207.

Hassett, D.J., Henke, K.R., McCarthy, G.J., and Korynta, E.D., 1984, *Characterization of a lignite ash from the METC gasifier III. Correlation of leaching behavior and mineralogy*. In: McCarthy, G.J., and Lauf, R.J., (Eds.) Fly Ash and Coal Conversion By-products: Characterization, Utilisation and Disposal I, Materials Research Society Symposia Proceedings, Boston, vol. 43, pp 213-226.

Hassett, D.J., Henke, K.R., McCarthy, G.J., 1985, *Leaching Behavior of Fixed-Bed Gasification Ash Derived from North Dakota Lignite*. In: McCarthy, G.J., Glasser, F.P., and Roy, D.M., (Eds.) Fly Ash and Coal Conversion By-products: Characterization, Utilisation and Disposal II, Materials Research Society Symposia Proceedings, Boston, vol. 65, pp 285-299.

Jones, D.R., 1995, The *Leaching of Major and Trace Elements from Coal Ash*. In: Swaine, J. and Goodarzi, F. (Eds.) Environmental Aspects of Trace Elements in Coal, Kluwer Academic Publishers, pp 221-262.

Koch, E.W., 2002, *An Investigation of the Chemistry Involved in the Mixing of an Industrial Effluent with Fine Ash*, MSc thesis, University of Stellenbosch, South Africa, 281 pages.

Lee, S., Hahn, J., 1997, *Geochemistry of leachate from fly ash disposal mounds*. In: Journal of Environmental Science and Health, Part A: Environmental Science and Engineering & Toxic and Hazardous Substance Control, vol. 32, issue 3, pp 649-669.

McGraw-Hill Encyclopedia of Science and Technology, 6th Edition, 1987, McGraw-Hill, New York, USA, Volume 9, pp 655.

Moller, R., 2002, *Evaluation of the Outside Ash system on the water and salt balance*, Sasol Synthetic Fuels, Secunda, Internal Report.

Montgomery, D.C., 1984, *Design and Analysis of Experiments*, John Wiley & Sons, New York, USA, pp 325-349.

NALCO Water Handbook, 1988, McGraw Hill, New York, USA, pp 3.1-4.29.

Nel, M.C., 1996, *A Characterisation of Ash Water Quality and Quality Changes in the SCI system*, Sasol Technology, Internal Report.

Petersen, J., 1998, *Assessment and Modelling of Chromium Release in Minerals Processing Waste Deposits*, PhD Thesis, University of Cape Town, South Africa, pp 92-93.

Pourbaix, M., 1966, *Atlas of Electrochemical Equilibria in Aqueous Solutions*, Pergamon Press, London, UK, pp 150-153.

Pretorius, P.C., and Nieuwenhuis, J.G., 2002, *An investigation into the salt holding capacity of the Secunda ash system*, Sastech R&D, Water and Environmental Technology Research, Internal Report.

Roy, W.R., Griffin, R.A., Dickerson, D.R. and Schuller, R.M., 1984, *Illinois basin coal fly ashes. 1. Chemical characterization and solubility*. Environ. Sci. Technol., 18, pp 734-739.

Sawyer, C.N., 1978, *Chemistry for Environmental Engineering*, McGraw-Hill, New York, USA, pp 65-71.

Sheikholeslami, R., 2001, *Mixed Salts – Scaling Limits and Propensity*, Desalination 154 (2003), pp 117-127.

Shen-Yu, F., and Zwane, S.T., 2001, *Relationship between salinity and metal availability in solid waste leachates*, Internal Report, University of Cape Town, South Africa, 46 pages.

Singh, D.N., Kolay, P.K., 2001, *Simulation of ash-water interaction and its influence on ash characteristics*, Progress in Energy and Combustion Science 28, pp 267-299.

Villaume, J.F., Bell, J.W., and Labuz, L.L., 1987, *Evaluation of Leachate generation at the Montour, Pennsylvania Fly Ash Test Cell*. In: McCarthy, G.J., Glasser, F.P., Roy, D.M., and Hemmings, R.T., (Eds.) Fly Ash and Coal Conversion By-products: Characterization, Utilisation and Disposal IV, Materials Research Society Symposia Proceedings, Boston, vol. 113, pp 325-332.

Yasuda, S. et.al., 1996, *Fly ash treatment for secondary environmental pollution prevention* In: Fuel and Energy Abstracts, September 1998, pp 220.

Appendix A
General information

A1: Definitions

Conductivity: The conductivity of a solution is a measure of its ability to carry an electrical current, and varies both with the number and type of ions the solutions contains. (Sawyer, 1978). According to Hassett (1985), the electrical conductivity (EC) of a solution is an indicator of the total dissolved ionic species.

Loss on ignition: LOI is an effective and simple way to determine the amount of organic matter in the ash. A single gram of ash is heated to 1000ºC to a constant mass and the loss of mass that is measured is indicated as a percentage.

Zeolites: Zeolites are microporous crystalline solids with well-defined structures. Generally they contain silicon, aluminium and oxygen in their framework and cations, water and/or other molecules within their pores. Many occur naturally as minerals, and are extensively mined in many parts of the world. Others are synthetic, and are made commercially for specific uses, or produced by research scientists trying to understand more about their chemistry.

A2: Mineral names

Table A1: Mineral Names and Formulae

Mineral	Formula
Anhydrite	$CaSO_4$
Aragonite	$CaCO_3$
Calcite	$CaCO_3$
Dolomite	$CaMg(CO_3)_2$
Ettringite	$Ca_6Al_2(SO_4)_3(OH)_{12}.26H_2O$
Gypsum	$CaSO_4.2H_2O$
Hematite	Fe_2O_3
Lime	CaO
Maghemite	Fe_2O_3
Magnetite	Fe_3O_4
Melilite	$(Ca,Na)_2(Al,Mg,Fe^{2+})(Si,Al)_2O_7$
Merwinite	$Ca_3Mg(SiO_4)_2$
Mullite	$Al_6Si_2O_{13}$
Periclase	MgO
Portlandite	$Ca(OH)_2$
Pyrite	FeS_2
Quartz	SiO_2
Wollastonite	$CaSiO_3$

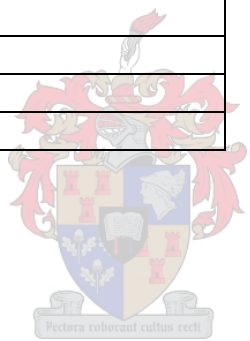

A3
Diagrams of Sasol Secunda Ash disposal system

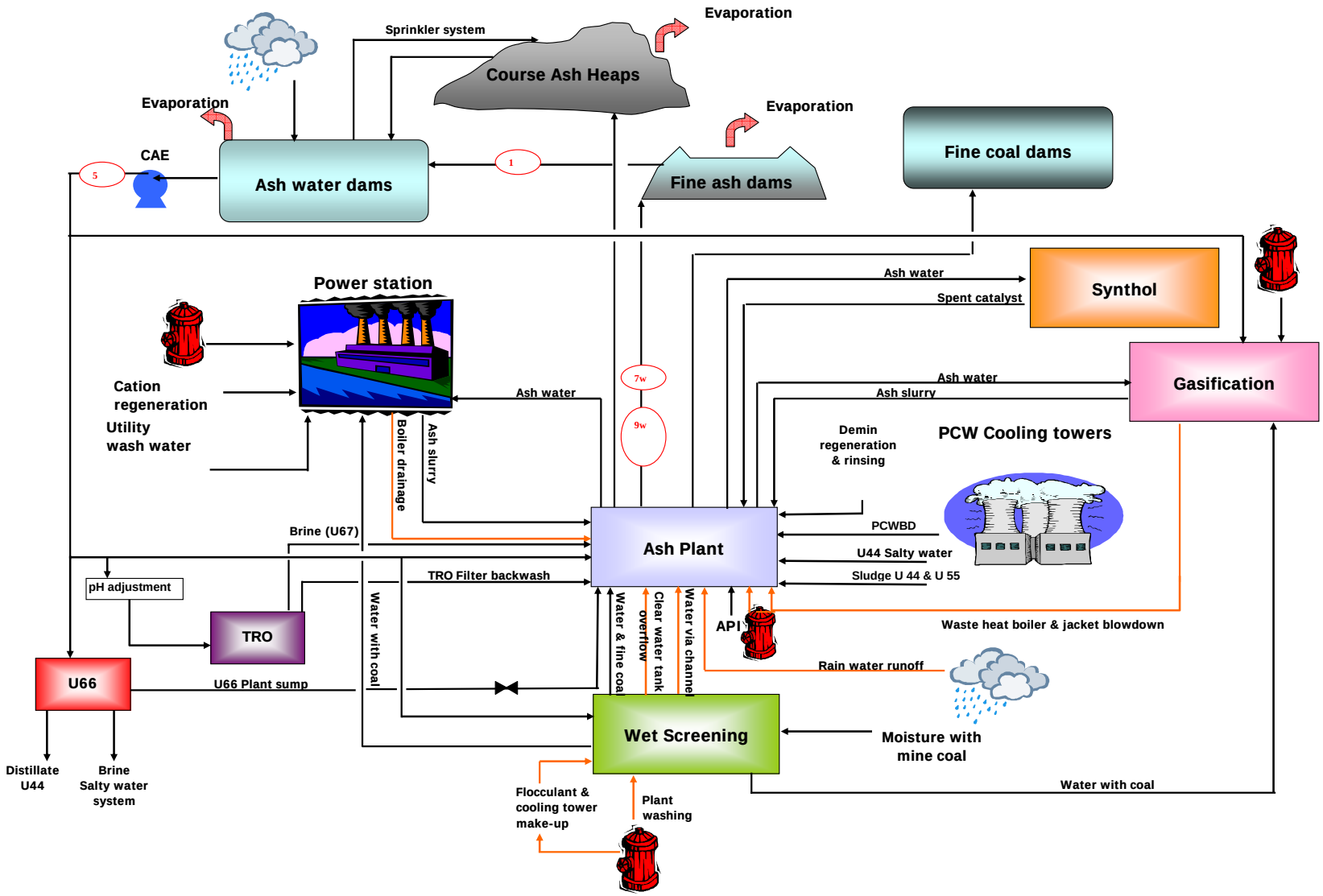

Figure A1: Sasol 2 (West) ash water system

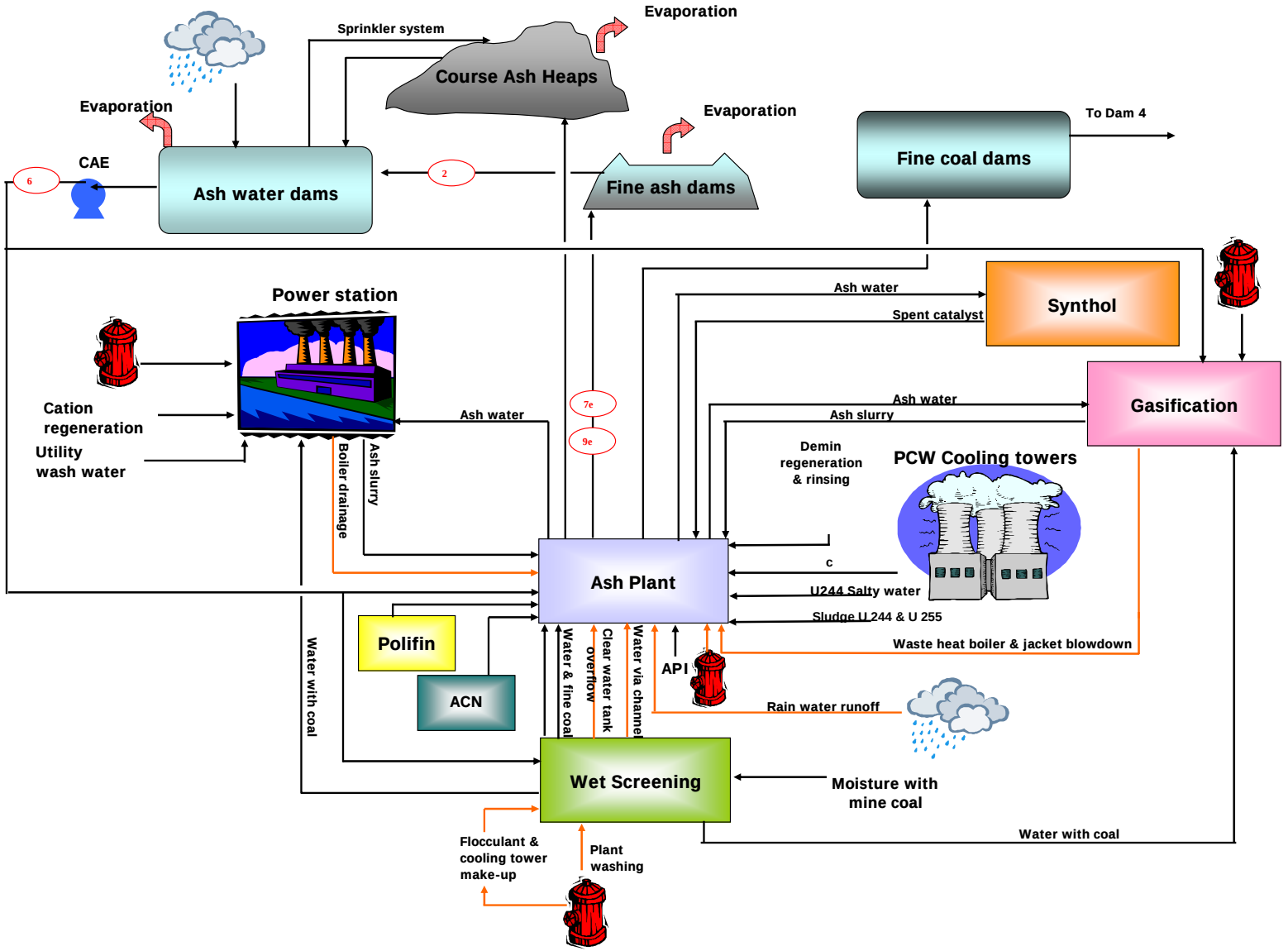

Figure A2: Sasol 3 (East) ash water system

Appendix B

Experimental results

B1: Liquid phase

B1.1: Cl and SO_4 results

Table B1.1: Phase 1 Cl and SO_4 analysis

Sample	Date	Component	Concentration	Dilution	Actual Concentration
			ppm		ppm
Exp 1.1	30-Oct	Cl	15.3	50	**763**
Exp 1.2	30-Oct	Cl	15.3	50	**763**
Exp 2.1	30-Oct	Cl	34.5	50	**1723**
Exp 2.2	30-Oct	Cl	34.7	50	**1735**
Exp 1.1	30-Oct	SO_4^{2-}	213.6	50	**10682**
Exp 1.2	30-Oct	SO_4^{2-}	150.4	50	**7518**
Exp 2.1	30-Oct	SO_4^{2-}	107.6	50	**5379**
Exp 2.2	30-Oct	SO_4^{2-}	68.7	50	**3436**
Exp 3.1	4-Nov	Cl	21.1	50	**1055**
Exp 3.2	4-Nov	Cl	20.6	50	**1030**
Exp 4.1	4-Nov	Cl	30.6	50	**1530**
Exp 4.2	4-Nov	Cl	32.1	50	**1605**
Exp 3.1	4-Nov	SO_4^{2-}	139.4	50	**6970**
Exp 3.2	4-Nov	SO_4^{2-}	79.8	50	**3990**
Exp 4.1	4-Nov	SO_4^{2-}	90.0	50	**4500**
Exp 4.2	4-Nov	SO_4^{2-}	70.6	50	**3530**
Exp 5.1	1-Mar	Cl	62.7	20	**1254**
Exp 5.2	1-Mar	Cl	62.4	20	**1248**
Exp 6.1	1-Mar	Cl	87.5	20	**1750**
Exp 6.2	1-Mar	Cl	88.8	20	**1776**
Exp 7.1	1-Mar	Cl	75.5	20	**1510**
Exp 7.2	1-Mar	Cl	75.8	20	**1516**
Exp 8.1	1-Mar	Cl	62.7	20	**1254**
Exp 8.2	1-Mar	Cl	63.7	20	**1274**
Exp 9.1	1-Mar	Cl	88.3	20	**1766**
Exp 9.2	1-Mar	Cl	89.0	20	**1780**
Exp 10.1	1-Mar	Cl	76.2	20	**1524**

Table B1.1 (Cont)					
Sample	**Date**	**Component**	**Concentration**	**Dilution**	**Actual Concentration**
			ppm		**ppm**
Exp 10.2	1-Mar	Cl	77.1	20	**1542**
Exp 5.1	1-Mar	SO_4^{2-}	186.5	20	**3730**
Exp 5.2	1-Mar	SO_4^{2-}	185.2	20	**3704**
Exp 6.1	1-Mar	SO_4^{2-}	293.5	20	**5870**
Exp 6.2	1-Mar	SO_4^{2-}	173.7	20	**3474**
Exp 7.1	1-Mar	SO_4^{2-}	233.7	20	**4674**
Exp 7.2	1-Mar	SO_4^{2-}	163.3	20	**3266**
Exp 8.1	1-Mar	SO_4^{2-}	189.2	20	**3784**
Exp 8.2	1-Mar	SO_4^{2-}	183.6	20	**3672**
Exp 9.1	1-Mar	SO_4^{2-}	294.9	20	**5898**
Exp 9.2	1-Mar	SO_4^{2-}	179.0	20	**3580**
Exp 10.1	1-Mar	SO_4^{2-}	237.1	20	**4742**
Exp 10.2	1-Mar	SO_4^{2-}	176.1	20	**3522**
Exp 11.1	8-Mar	Cl	32.2	20	**644**
Exp 11.2	8-Mar	Cl	32.4	20	**648**
Exp 12.1	8-Mar	Cl	62.1	20	**1242**
Exp 12.2	8-Mar	Cl	62.3	20	**1246**
Exp 13.1	8-Mar	Cl	47.2	20	**944**
Exp 13.2	8-Mar	Cl	46.9	20	**938**
Exp 14.1	8-Mar	Cl	32.1	20	**642**
Exp 14.2	8-Mar	Cl	31.9	20	**638**
Exp 15.1	8-Mar	Cl	62.5	20	**1250**
Exp 15.2	8-Mar	Cl	62.1	20	**1242**
Exp 16.1	8-Mar	Cl	47.5	20	**950**
Exp 16.2	8-Mar	Cl	47.3	20	**946**
Exp 11.1	8-Mar	SO_4^{2-}	562.4	20	**11248**
Exp 11.2	8-Mar	SO_4^{2-}	285.2	20	**5704**
Exp 12.1	8-Mar	SO_4^{2-}	189.2	20	**3784**
Exp 12.2	8-Mar	SO_4^{2-}	186.6	20	**3732**
Exp 13.1	8-Mar	SO_4^{2-}	373.7	20	**7474**
Exp 13.2	8-Mar	SO_4^{2-}	231.1	20	**4622**
Exp 14.1	8-Mar	SO_4^{2-}	561.8	20	**11236**
Exp 14.2	8-Mar	SO_4^{2-}	281.3	20	**5626**
Exp 15.1	8-Mar	SO_4^{2-}	188.7	20	**3774**
Exp 15.2	8-Mar	SO_4^{2-}	183.5	20	**3670**
Exp 16.1	8-Mar	SO_4^{2-}	368.3	20	**7366**
Exp 16.2	8-Mar	SO_4^{2-}	214.8	20	**4296**
Exp 17.1	12-Mar	Cl	60.6	20	**1212**
Exp 17.2	12-Mar	Cl	59.7	20	**1194**
Exp 18.1	12-Mar	Cl	59.7	20	**1194**
Exp 18.2	12-Mar	Cl	60.6	20	**1212**
Exp 19.1	12-Mar	Cl	60.5	20	**1210**
Exp 19.2	12-Mar	Cl	60.7	20	**1214**
Exp 17.1	12-Mar	SO_4^{2-}	181.1	20	**3622**
Exp 17.2	12-Mar	SO_4^{2-}	168.7	20	**3374**

Table B1.1 (Cont)					
Sample	**Date**	**Component**	**Concentration**	**Dilution**	**Actual Concentration**
			ppm		**ppm**
Exp 18.1	12-Mar	SO_4^{2-}	179.7	20	**3594**
Exp 18.2	12-Mar	SO_4^{2-}	172.3	20	**3446**
Exp 19.1	12-Mar	SO_4^{2-}	181.8	20	**3636**
Exp 19.2	12-Mar	SO_4^{2-}	171.2	20	**3424**
Exp 20.1	23-Apr	Cl	60.5	20	**1210**
Exp 20.2	23-Apr	Cl	60.5	20	**1210**
Exp 21.1	23-Apr	Cl	59.6	20	**1192**
Exp 21.2	23-Apr	Cl	59.6	20	**1192**
Exp 22.1	23-Apr	Cl	59.9	20	**1198**
Exp 22.2	23-Apr	Cl	60.1	20	**1202**
Exp 23.1	23-Apr	Cl	60.5	20	**1210**
Exp 23.2	23-Apr	Cl	60.7	20	**1214**
Exp 24.1	23-Apr	Cl	60.9	20	**1218**
Exp 24.2	23-Apr	Cl	60.7	20	**1214**
Exp 25.1	23-Apr	Cl	59.1	20	**1182**
Exp 25.2	23-Apr	Cl	59.2	20	**1184**
Exp 26.1	23-Apr	Cl	60.0	20	**1200**
Exp 26.2	23-Apr	Cl	60.5	20	**1210**
Exp 27.1	23-Apr	Cl	60.1	20	**1202**
Exp 27.2	23-Apr	Cl	60.4	20	**1208**
Exp 28.1	23-Apr	Cl	60.7	20	**1214**
Exp 28.2	23-Apr	Cl	60.2	20	**1204**
Exp 20.1	23-Apr	SO_4^{2-}	182.8	20	**3656**
Exp 20.2	23-Apr	SO_4^{2-}	181.5	20	**3630**
Exp 21.1	23-Apr	SO_4^{2-}	180.2	20	**3604**
Exp 21.2	23-Apr	SO_4^{2-}	177.4	20	**3548**
Exp 22.1	23-Apr	SO_4^{2-}	181.9	20	**3638**
Exp 22.2	23-Apr	SO_4^{2-}	180.4	20	**3608**
Exp 23.1	23-Apr	SO_4^{2-}	182.6	20	**3652**
Exp 23.2	23-Apr	SO_4^{2-}	176.3	20	**3526**
Exp 24.1	23-Apr	SO_4^{2-}	181.5	20	**3630**
Exp 24.2	23-Apr	SO_4^{2-}	171.1	20	**3422**
Exp 25.1	23-Apr	SO_4^{2-}	178.2	20	**3564**
Exp 25.2	23-Apr	SO_4^{2-}	172.7	20	**3454**
Exp 26.1	23-Apr	SO_4^{2-}	178.5	20	**3570**
Exp 26.2	23-Apr	SO_4^{2-}	169.5	20	**3390**
Exp 27.1	23-Apr	SO_4^{2-}	185.4	20	**3708**
Exp 27.2	23-Apr	SO_4^{2-}	169.2	20	**3384**
Exp 28.1	23-Apr	SO_4^{2-}	181.2	20	**3624**
Exp 28.2	23-Apr	SO_4^{2-}	170.4	20	**3408**
Exp 29.1	3-May	Cl	37.3	20	**746**
Exp 29.2	3-May	Cl	37.4	20	**748**
Exp 30.1	3-May	Cl	37.4	20	**748**
Exp 30.2	3-May	Cl	37.3	20	**746**
Exp 31.1	3-May	Cl	37.6	20	**752**

Table B1.1 (Cont)					
Sample	**Date**	**Component**	**Concentration**	**Dilution**	**Actual Concentration**
			ppm		**ppm**
Exp 31.2	3-May	Cl	38.3	20	**766**
Exp 32.1	3-May	Cl	49.4	20	**988**
Exp 32.2	3-May	Cl	50.0	20	**1000**
Exp 33.1	3-May	Cl	49.9	20	**998**
Exp 33.2	3-May	Cl	52.8	20	**1056**
Exp 34.1	3-May	Cl	49.5	20	**990**
Exp 34.2	3-May	Cl	49.8	20	**996**
Exp 35.1	3-May	Cl	50.0	20	**1000**
Exp 35.2	3-May	Cl	40.0	20	**800**
Exp 36.1	3-May	Cl	49.8	20	**996**
Exp 36.2	3-May	Cl	49.7	20	**994**
Exp 37.1	3-May	Cl	50.4	20	**1008**
Exp 37.2	3-May	Cl	56.1	20	**1122**
Exp 38.1	3-May	Cl	56.2	20	**1124**
Exp 38.2	3-May	Cl	55.7	20	**1114**
Exp 39.1	3-May	Cl	57.7	20	**1154**
Exp 39.2	3-May	Cl	58.1	20	**1162**
Exp 40.1	3-May	Cl	56.1	20	**1122**
Exp 40.2	3-May	Cl	56.4	20	**1128**
Exp 29.1	3-May	SO_4^{2-}	113.3	20	**2266**
Exp 29.2	3-May	SO_4^{2-}	113.2	20	**2264**
Exp 30.1	3-May	SO_4^{2-}	113.1	20	**2262**
Exp 30.2	3-May	SO_4^{2-}	110.8	20	**2216**
Exp 31.1	3-May	SO_4^{2-}	114.5	20	**2290**
Exp 31.2	3-May	SO_4^{2-}	113.8	20	**2276**
Exp 32.1	3-May	SO_4^{2-}	147.9	20	**2958**
Exp 32.2	3-May	SO_4^{2-}	152.6	20	**3052**
Exp 33.1	3-May	SO_4^{2-}	145.8	20	**2916**
Exp 33.2	3-May	SO_4^{2-}	145.8	20	**2916**
Exp 34.1	3-May	SO_4^{2-}	144.0	20	**2880**
Exp 34.2	3-May	SO_4^{2-}	148.8	20	**2976**
Exp 35.1	3-May	SO_4^{2-}	152.1	100	**15210**
Exp 35.2	3-May	SO_4^{2-}	147.4	100	**14740**
Exp 36.1	3-May	SO_4^{2-}	153.2	100	**15320**
Exp 36.2	3-May	SO_4^{2-}	153.0	100	**15300**
Exp 37.1	3-May	SO_4^{2-}	153.3	100	**15330**
Exp 37.2	3-May	SO_4^{2-}	171.9	100	**17190**
Exp 38.1	3-May	SO_4^{2-}	93.0	100	**9300**
Exp 38.2	3-May	SO_4^{2-}	90.8	100	**9080**
Exp 39.1	3-May	SO_4^{2-}	93.4	100	**9340**
Exp 39.2	3-May	SO_4^{2-}	94.0	100	**9400**
Exp 40.1	3-May	SO_4^{2-}	92.8	100	**9280**
Exp 40.2	3-May	SO_4^{2-}	92.2	100	**9220**

Table B1.2: Phase 3 Cl and SO_4 analysis

Sample	Date	Component	Concentration	Dilution	Actual Concentration
			ppm		ppm
Exp 1.1	25-Sep	Cl	62.4	20	**1247**
Exp 1.2	25-Sep	Cl	66.7	20	**1334**
Exp 1.3	25-Sep	Cl	68.3	20	**1365**
Exp 2.1	25-Sep	Cl	62.8	20	**1255**
Exp 2.2	25-Sep	Cl	74.7	20	**1493**
Exp 2.3	25-Sep	Cl	90.8	20	**1816**
Exp 1.1	25-Sep	SO_4^{2-}	186.2	20	**3723**
Exp 1.2	25-Sep	SO_4^{2-}	200.5	20	**4010**
Exp 1.3	25-Sep	SO_4^{2-}	211.3	20	**4225**
Exp 2.1	25-Sep	SO_4^{2-}	188.9	20	**3778**
Exp 2.2	25-Sep	SO_4^{2-}	232.3	20	**4646**
Exp 2.3	25-Sep	SO_4^{2-}	290.0	20	**5799**
Exp 3.1	7-Oct	Cl	58.8	20	**1176**
Exp 3.2	7-Oct	Cl	65.4	20	**1308**
Exp 3.3	7-Oct	Cl	81.8	20	**1635**
Exp 4.1	7-Oct	Cl	59.9	20	**1197**
Exp 4.2	7-Oct	Cl	60.6	20	**1211**
Exp 4.3	7-Oct	Cl	63.6	20	**1271**
Exp 3.1	7-Oct	SO_4^{2-}	183.3	20	**3666**
Exp 3.2	7-Oct	SO_4^{2-}	212.0	20	**4239**
Exp 3.3	7-Oct	SO_4^{2-}	266.4	20	**5328**
Exp 4.1	7-Oct	SO_4^{2-}	190.9	20	**3817**
Exp 4.2	7-Oct	SO_4^{2-}	196.6	20	**3932**
Exp 4.3	7-Oct	SO_4^{2-}	207.9	20	**4157**
Exp 5.1	20-Oct	Cl	59.9	20	**1197**
Exp 5.2	20-Oct	Cl	63.3	20	**1266**
Exp 5.3	20-Oct	Cl	68.2	20	**1364**
Exp 6.1	20-Oct	Cl	62.1	20	**1242**
Exp 6.2	20-Oct	Cl	73.1	20	**1462**
Exp 6.3	20-Oct	Cl	106.2	20	**2124**
Exp 7.1	20-Oct	Cl	60.6	20	**1211**
Exp 7.2	20-Oct	Cl	85.4	20	**1707**
Exp 7.3	20-Oct	Cl	104.7	20	**2094**
Exp 8.1	20-Oct	Cl	65.0	20	**1300**
Exp 8.2	20-Oct	Cl	71.7	20	**1434**
Exp 8.3	20-Oct	Cl	73.3	20	**1465**
Exp 5.1	20-Oct	SO_4^{2-}	190.2	20	**3804**
Exp 5.2	20-Oct	SO_4^{2-}	200.2	20	**4003**
Exp 5.3	20-Oct	SO_4^{2-}	211.8	20	**4235**
Exp 6.1	20-Oct	SO_4^{2-}	195.3	20	**3906**
Exp 6.2	20-Oct	SO_4^{2-}	233.9	20	**4678**
Exp 6.3	20-Oct	SO_4^{2-}	325.7	20	**6513**
Exp 7.1	20-Oct	SO_4^{2-}	190.6	20	**3811**
Exp 7.2	20-Oct	SO_4^{2-}	270.8	20	**5415**
Exp 7.3	20-Oct	SO_4^{2-}	330.8	20	**6616**

Table B1.2 (Cont)					
Sample	**Date**	**Component**	**Concentration**	**Dilution**	**Actual Concentration**
			ppm		**ppm**
Exp 8.1	20-Oct	SO_4^{2-}	205.8	20	**4115**
Exp 8.2	20-Oct	SO_4^{2-}	226.6	20	**4532**
Exp 8.3	20-Oct	SO_4^{2-}	230.1	20	**4601**

B1.2: pH, Conductivity and TDS results

Table B1.3: Phase 1 pH, Conductivity and TDS analysis

Sample	Date	pH	Conductivity	TDS
			mS/m	**mg**
Exp 1.1	29-Oct	**6.95**	**1710**	**12920**
Exp 1.2	29-Oct	**12.05**	**1760**	**13310**
Exp 2.1	29-Oct	**5.89**	**1400**	**10300**
Exp 2.2	29-Oct	**12.35**	**2060**	**15580**
Exp 3.1	3-Nov	**10.07**	**1370**	**10130**
Exp 3.2	3-Nov	**12.38**	**2120**	**16060**
Exp 4.1	3-Nov	**10.41**	**1220**	**9100**
Exp 4.2	3-Nov	**12.33**	**1980**	**15270**
Exp 5.1	2-Mar	**11.48**	**986**	**6960**
Exp 5.2	2-Mar	**12.54**	**1317**	**9130**
Exp 6.1	2-Mar	**7.41**	**1896**	**13390**
Exp 6.2	2-Mar	**12.58**	**2100**	**14900**
Exp 7.1	2-Mar	**10.7**	**1277**	**8090**
Exp 7.2	2-Mar	**12.6**	**2240**	**14130**
Exp 8.1	2-Mar	**11.71**	**1135**	**7240**
Exp 8.2	2-Mar	**12.6**	**2140**	**13730**
Exp 9.1	2-Mar	**7.22**	**1450**	**9350**
Exp 9.2	2-Mar	**12.61**	**2320**	**15010**
Exp 10.1	2-Mar	**10.39**	**1266**	**8160**
Exp 10.2	2-Mar	**12.65**	**2190**	**14130**
Exp 11.1	4-Mar	**7.25**	**1765**	**11410**
Exp 11.2	4-Mar	**12.83**	**2700**	**17490**
Exp 12.1	4-Mar	**11.78**	**1102**	**7200**
Exp 12.2	4-Mar	**12.78**	**2130**	**13610**
Exp 13.1	4-Mar	**10.53**	**1417**	**9200**
Exp 13.2	4-Mar	**12.86**	**2360**	**15300**
Exp 14.1	4-Mar	**6.77**	**1758**	**11470**
Exp 14.2	4-Mar	**12.89**	**2670**	**17570**
Exp 15.1	4-Mar	**11.79**	**1075**	**7220**
Exp 15.2	4-Mar	**12.83**	**2030**	**14060**
Exp 16.1	4-Mar	**10.61**	**1301**	**9220**
Exp 16.2	4-Mar	**12.87**	**2190**	**15580**
Exp 17.1	10-Mar	**11.85**	**1076**	**7520**

Table B1.3 (cont)				
Sample	**Date**	**pH**	**Conductivity**	**TDS**
			mS/m	**mg**
Exp 17.2	10-Mar	**12.29**	**1140**	**7970**
Exp 18.1	10-Mar	**11.92**	**1064**	**7440**
Exp 18.2	10-Mar	**12.41**	**1174**	**8200**
Exp 19.1	10-Mar	**11.96**	**1063**	**7430**
Exp 19.2	10-Mar	**12.46**	**1172**	**8160**
Exp 20.1	21-Apr	**12.6**	**1018**	**7130**
Exp 20.2	21-Apr	**12.53**	**1000**	**7000**
Exp 21.1	21-Apr	**12.61**	**1010**	**7070**
Exp 21.2	21-Apr	**12.53**	**1016**	**7110**
Exp 22.1	21-Apr	**12.53**	**1014**	**7080**
Exp 22.2	21-Apr	**12.4**	**1006**	**7040**
Exp 23.1	21-Apr	**12.64**	**1050**	**7350**
Exp 23.2	21-Apr	**12.95**	**1070**	**7500**
Exp 24.1	21-Apr	**12.62**	**1046**	**7320**
Exp 24.2	21-Apr	**12.98**	**1076**	**7530**
Exp 25.1	21-Apr	**12.56**	**1053**	**7370**
Exp 25.2	21-Apr	**12.54**	**1050**	**7350**
Exp 26.1	21-Apr	**12.6**	**1063**	**7450**
Exp 26.2	21-Apr	**13.3**	**1216**	**8500**
Exp 27.1	21-Apr	**12.55**	**1062**	**7450**
Exp 27.2	21-Apr	**13.31**	**1226**	**8560**
Exp 28.1	21-Apr	**12.39**	**1041**	**7290**
Exp 28.2	21-Apr	**13.12**	**1207**	**8440**
Exp 29.1	27-Apr	**6.55**	**633**	**4440**
Exp 29.2	27-Apr	**7.52**	**637**	**4460**
Exp 30.1	27-Apr	**6.98**	**633**	**4420**
Exp 30.2	27-Apr	**7.34**	**630**	**4400**
Exp 31.1	27-Apr	**6.71**	**631**	**4420**
Exp 31.2	27-Apr	**7.66**	**633**	**4430**
Exp 32.1	27-Apr	**11.29**	**813**	**5690**
Exp 32.2	27-Apr	**11.06**	**825**	**5770**
Exp 33.1	27-Apr	**11.27**	**811**	**5680**
Exp 33.2	27-Apr	**11**	**817**	**5710**
Exp 34.1	27-Apr	**11.35**	**802**	**5620**
Exp 34.2	27-Apr	**11.11**	**814**	**5690**
Exp 35.1	27-Apr	**7.4**	**2240**	**15660**
Exp 35.2	27-Apr	**8.13**	**2270**	**15870**
Exp 36.1	27-Apr	**7.67**	**2210**	**15470**
Exp 36.2	27-Apr	**8.04**	**2280**	**15930**
Exp 37.1	27-Apr	**7.43**	**2250**	**15730**
Exp 37.2	27-Apr	**8.09**	**2275**	**15900**
Exp 38.1	27-Apr	**11.28**	**1660**	**11610**
Exp 38.2	27-Apr	**11.23**	**1668**	**12030**
Exp 39.1	27-Apr	**11.45**	**1675**	**11720**
Exp 39.2	27-Apr	**11.45**	**1695**	**11860**

Table B1.3 (cont)				
Sample	**Date**	**pH**	**Conductivity**	**TDS**
			mS/m	**mg**
Exp 40.1	27-Apr	**11.48**	**1690**	**11820**
Exp 40.2	27-Apr	**11.35**	**1701**	**11920**

Table B1.4: Phase 3 pH, Conductivity and TDS analysis

Sample	Date	pH	Conductivity	TDS
			mS/m	mg
Exp 1.1	24-Sep	**11.41**	**941**	**7910**
Exp 1.2	24-Sep	**8.76**	**928**	**7750**
Exp 1.3	24-Sep	**7.83**	**970**	**8070**
Exp 2.1	24-Sep	**11.38**	**969**	**7900**
Exp 2.2	24-Sep	**7.89**	**1045**	**8750**
Exp 2.3	24-Sep	**7.81**	**1166**	**10290**
Exp 3.1	6-Oct	**11.48**	**1080**	**7650**
Exp 3.2	6-Oct	**8.21**	**1080**	**7660**
Exp 3.3	6-Oct	**7.84**	**1280**	**9190**
Exp 4.1	6-Oct	**11.48**	**1080**	**7790**
Exp 4.2	6-Oct	**9.11**	**931**	**7300**
Exp 4.3	6-Oct	**7.82**	**1060**	**7610**
Exp 5.1	17-Oct	**11.6**	**1080**	**7740**
Exp 5.2	17-Oct	**9.45**	**939**	**7180**
Exp 5.3	17-Oct	**8.39**	**1080**	**7700**
Exp 6.1	17-Oct	**11.43**	**1060**	**7710**
Exp 6.2	17-Oct	**8.57**	**1140**	**8320**
Exp 6.3	17-Oct	**7.94**	**1470**	**10770**
Exp 7.1	17-Oct	**11.56**	**1080**	**7980**
Exp 7.2	17-Oct	**8.38**	**1270**	**9400**
Exp 7.3	17-Oct	**7.89**	**1470**	**11250**
Exp 8.1	17-Oct	**11.4**	**1080**	**8000**
Exp 8.2	17-Oct	**8.73**	**1080**	**8030**
Exp 8.3	17-Oct	**8.08**	**1120**	**8460**

B1.2: Ca, Na, Cl and SO_4 results

Table B1.5: Phase 1 Ca, Na, Cl and SO_4 analysis

Sample	Date	Component	Fuel	Support	Spectral Band Pass	Wavelength	Result			Average	Standard			
							1	2	3		1	2	3	4
					nm	nm	ppm				ppm			
Exp 1.1	27-Oct	Ca	Acetylene	Nitrous Oxide	0.2	239.9				**603**	250	500	750	1000
Exp 1.2	27-Oct	Ca	Acetylene	Nitrous Oxide	0.2	239.9				**570**	250	500	750	1000
Exp 2.1	27-Oct	Ca	Acetylene	Nitrous Oxide	0.2	239.9				**762**	250	500	750	1000
Exp 2.2	27-Oct	Ca	Acetylene	Nitrous Oxide	0.2	239.9				**1071**	250	500	750	1000
Exp 3.1	3-Nov	Ca	Acetylene	Nitrous Oxide	0.2	239.9				**669**	250	500	750	1000
Exp 3.2	3-Nov	Ca	Acetylene	Nitrous Oxide	0.2	239.9				**1011**	250	500	750	1000
Exp 4.1	3-Nov	Ca	Acetylene	Nitrous Oxide	0.2	239.9				**791**	250	500	750	1000
Exp 4.2	3-Nov	Ca	Acetylene	Nitrous Oxide	0.2	239.9				**1750**	250	500	750	1000
Exp 1.1	27-Oct	Na	Acetylene	Air	0.5	330.3				**3400**	100	200	500	1000
Exp 1.2	27-Oct	Na	Acetylene	Air	0.5	330.3				**3750**	100	200	500	1000
Exp 2.1	27-Oct	Na	Acetylene	Air	0.5	330.3				**2550**	100	200	500	1000
Exp 2.2	27-Oct	Na	Acetylene	Air	0.5	330.3				**2500**	100	200	500	1000
Exp 3.1	31-Oct	Na	Acetylene	Air	0.5	330.3				**2900**	100	200	500	1000
Exp 3.2	31-Oct	Na	Acetylene	Air	0.5	330.3				**3100**	100	200	500	1000
Exp 4.1	31-Oct	Na	Acetylene	Air	0.5	330.3				**2350**	100	200	500	1000
Exp 4.2	31-Oct	Na	Acetylene	Air	0.5	330.3				**2450**	100	200	500	1000
Exp 5.1	1-Mar	Ca	Acetylene	Nitrous Oxide	0.2	239.9	**617**	**608**	**610**	**612**	250	500	750	1000
Exp 5.2	1-Mar	Ca	Acetylene	Nitrous Oxide	0.2	239.9	**2100**	**2160**	**2060**	**2107**	250	500	750	1000
Exp 6.1	1-Mar	Ca	Acetylene	Nitrous Oxide	0.2	239.9	**900**	**889**	**885**	**891**	250	500	750	1000
Exp 6.2	1-Mar	Ca	Acetylene	Nitrous Oxide	0.2	239.9	**1640**	**1780**	**1740**	**1720**	250	500	750	1000
Exp 7.1	1-Mar	Ca	Acetylene	Nitrous Oxide	0.2	239.9	**758**	**766**	**779**	**768**	250	500	750	1000
Exp 7.2	1-Mar	Ca	Acetylene	Nitrous Oxide	0.2	239.9	**1680**	**1980**	**1880**	**1847**	250	500	750	1000
Exp 8.1	1-Mar	Ca	Acetylene	Nitrous Oxide	0.2	239.9	**636**	**642**	**663**	**647**	250	500	750	1000
Exp 8.2	1-Mar	Ca	Acetylene	Nitrous Oxide	0.2	239.9	**2220**	**2200**	**2160**	**2193**	250	500	750	1000

Table B1.5 (Cont)														
Sample	**Date**	**Component**	**Fuel**	**Support**	**Spectral Band Pass**	**Wavelength**	**Result**			**Average**	**Standard**			
							1	**2**	**3**		**1**	**2**	**3**	**4**
					nm	**nm**	**ppm**	**ppm**						
Exp 9.1	1-Mar	Ca	Acetylene	Nitrous Oxide	0.2	239.9	**877**	**888**	**871**	**879**	250	500	750	1000
Exp 9.2	1-Mar	Ca	Acetylene	Nitrous Oxide	0.2	239.9	**1840**	**1740**	**1680**	**1753**	250	500	750	1000
Exp 10.1	1-Mar	Ca	Acetylene	Nitrous Oxide	0.2	239.9	**758**	**770**	**780**	**769**	250	500	750	1000
Exp 10.2	1-Mar	Ca	Acetylene	Nitrous Oxide	0.2	239.9	**1860**	**1920**	**2040**	**1940**	250	500	750	1000
Exp 5.1	1-Mar	Na	Acetylene	Air	0.5	330.3	**1980**	**2000**	**2000**	**1993**	100	200	500	1000
Exp 5.2	1-Mar	Na	Acetylene	Air	0.5	330.3	**2120**	**2120**	**2100**	**2113**	100	200	500	1000
Exp 6.1	1-Mar	Na	Acetylene	Air	0.5	330.3	**2780**	**2820**	**2800**	**2800**	100	200	500	1000
Exp 6.2	1-Mar	Na	Acetylene	Air	0.5	330.3	**2920**	**2940**	**2940**	**2933**	100	200	500	1000
Exp 7.1	1-Mar	Na	Acetylene	Air	0.5	330.3	**2380**	**2420**	**2420**	**2407**	100	200	500	1000
Exp 7.2	1-Mar	Na	Acetylene	Air	0.5	330.3	**2520**	**2520**	**2520**	**2520**	100	200	500	1000
Exp 8.1	1-Mar	Na	Acetylene	Air	0.5	330.3	**2040**	**2040**	**2040**	**2040**	100	200	500	1000
Exp 8.2	1-Mar	Na	Acetylene	Air	0.5	330.3	**2140**	**2140**	**2140**	**2140**	100	200	500	1000
Exp 9.1	1-Mar	Na	Acetylene	Air	0.5	330.3	**2880**	**2880**	**2880**	**2880**	100	200	500	1000
Exp 9.2	1-Mar	Na	Acetylene	Air	0.5	330.3	**2940**	**2940**	**2960**	**2947**	100	200	500	1000
Exp 10.1	1-Mar	Na	Acetylene	Air	0.5	330.3	**2460**	**2460**	**2480**	**2467**	100	200	500	1000
Exp 10.2	1-Mar	Na	Acetylene	Air	0.5	330.3	**2580**	**2600**	**2580**	**2587**	100	200	500	1000
Exp 11.1	4-Mar	Ca	Acetylene	Nitrous Oxide	0.2	239.9	**535**	**548**	**553**	**545**	250	500	750	1000
Exp 11.2	4-Mar	Ca	Acetylene	Nitrous Oxide	0.2	239.9	**1300**	**1340**	**1240**	**1293**	250	500	750	1000
Exp 12.1	4-Mar	Ca	Acetylene	Nitrous Oxide	0.2	239.9	**660**	**667**	**663**	**663**	250	500	750	1000
Exp 12.2	4-Mar	Ca	Acetylene	Nitrous Oxide	0.2	239.9	**2160**	**2180**	**2180**	**2173**	250	500	750	1000
Exp 13.1	4-Mar	Ca	Acetylene	Nitrous Oxide	0.2	239.9	**599**	**597**	**604**	**600**	250	500	750	1000
Exp 13.2	4-Mar	Ca	Acetylene	Nitrous Oxide	0.2	239.9	**1640**	**1860**	**1660**	**1720**	250	500	750	1000
Exp 14.1	4-Mar	Ca	Acetylene	Nitrous Oxide	0.2	239.9	**550**	**553**	**545**	**549**	250	500	750	1000
Exp 14.2	4-Mar	Ca	Acetylene	Nitrous Oxide	0.2	239.9	**1380**	**1700**	**1440**	**1507**	250	500	750	1000
Exp 15.1	4-Mar	Ca	Acetylene	Nitrous Oxide	0.2	239.9	**655**	**651**	**663**	**656**	250	500	750	1000
Exp 15.2	4-Mar	Ca	Acetylene	Nitrous Oxide	0.2	239.9	**2240**	**2460**	**2220**	**2307**	250	500	750	1000
Exp 16.1	4-Mar	Ca	Acetylene	Nitrous Oxide	0.2	239.9	**586**	**579**	**610**	**592**	250	500	750	1000
Exp 16.2	4-Mar	Ca	Acetylene	Nitrous Oxide	0.2	239.9	**1540**	**1780**	**1740**	**1687**	250	500	750	1000

Table B1.5 (Cont)

Sample	Date	Component	Fuel	Support	Spectral Band Pass	Wavelength	Result			Average	Standard			
							1	2	3		1	2	3	4
					nm	nm	ppm	ppm						
Exp 11.1	4-Mar	Na	Acetylene	Air	0.5	330.3	**3660**	**3660**	**3680**	**3667**	100	200	500	1000
Exp 11.2	4-Mar	Na	Acetylene	Air	0.5	330.3	**3780**	**3800**	**3780**	**3787**	100	200	500	1000
Exp 12.1	4-Mar	Na	Acetylene	Air	0.5	330.3	**1900**	**1900**	**1900**	**1900**	100	200	500	1000
Exp 12.2	4-Mar	Na	Acetylene	Air	0.5	330.3	**1940**	**1940**	**1940**	**1940**	100	200	500	1000
Exp 13.1	4-Mar	Na	Acetylene	Air	0.5	330.3	**2800**	**2800**	**2800**	**2800**	100	200	500	1000
Exp 13.2	4-Mar	Na	Acetylene	Air	0.5	330.3	**2880**	**2880**	**2880**	**2880**	100	200	500	1000
Exp 14.1	4-Mar	Na	Acetylene	Air	0.5	330.3	**3680**	**3680**	**3680**	**3680**	100	200	500	1000
Exp 14.2	4-Mar	Na	Acetylene	Air	0.5	330.3	**3920**	**3940**	**3920**	**3927**	100	200	500	1000
Exp 15.1	4-Mar	Na	Acetylene	Air	0.5	330.3	**1920**	**1900**	**1920**	**1913**	100	200	500	1000
Exp 15.2	4-Mar	Na	Acetylene	Air	0.5	330.3	**1920**	**1940**	**1920**	**1927**	100	200	500	1000
Exp 16.1	4-Mar	Na	Acetylene	Air	0.5	330.3	**2780**	**2780**	**2780**	**2780**	100	200	500	1000
Exp 16.2	4-Mar	Na	Acetylene	Air	0.5	330.3	**2840**	**2860**	**2880**	**2860**	100	200	500	1000
Exp 17.1	8-Mar	Ca	Acetylene	Nitrous Oxide	0.2	239.9	**632**	**620**	**635**	**629**	250	500	750	1000
Exp 17.2	8-Mar	Ca	Acetylene	Nitrous Oxide	0.2	239.9	**654**	**660**	**656**	**657**	250	500	750	1000
Exp 18.1	9-Mar	Ca	Acetylene	Nitrous Oxide	0.2	239.9	**624**	**633**	**642**	**633**	250	500	750	1000
Exp 18.2	9-Mar	Ca	Acetylene	Nitrous Oxide	0.2	239.9	**699**	**701**	**700**	**700**	250	500	750	1000
Exp 19.1	9-Mar	Ca	Acetylene	Nitrous Oxide	0.2	239.9	**630**	**622**	**623**	**625**	250	500	750	1000
Exp 19.2	9-Mar	Ca	Acetylene	Nitrous Oxide	0.2	239.9	**683**	**687**	**672**	**681**	250	500	750	1000
Exp 17.1	8-Mar	Na	Acetylene	Air	0.5	330.3	**1920**	**1880**	**1900**	**1900**	100	200	500	1000
Exp 17.2	8-Mar	Na	Acetylene	Air	0.5	330.3	**1900**	**1880**	**1900**	**1893**	100	200	500	1000
Exp 18.1	9-Mar	Na	Acetylene	Air	0.5	330.3	**1880**	**1880**	**1880**	**1880**	100	200	500	1000
Exp 18.2	9-Mar	Na	Acetylene	Air	0.5	330.3	**1920**	**1920**	**1900**	**1913**	100	200	500	1000
Exp 19.1	9-Mar	Na	Acetylene	Air	0.5	330.3	**1880**	**1880**	**1880**	**1880**	100	200	500	1000
Exp 19.2	9-Mar	Na	Acetylene	Air	0.5	330.3	**1900**	**1920**	**1920**	**1913**	100	200	500	1000
Exp 20.1	19-Apr	Ca	Acetylene	Nitrous Oxide	0.2	239.9	**637**	**626**	**628**	**630**	250	500	750	1000
Exp 20.2	19-Apr	Ca	Acetylene	Nitrous Oxide	0.2	239.9	**607**	**600**	**582**	**596**	250	500	750	1000
Exp 21.1	19-Apr	Ca	Acetylene	Nitrous Oxide	0.2	239.9	**604**	**624**	**625**	**618**	250	500	750	1000
Exp 21.2	19-Apr	Ca	Acetylene	Nitrous Oxide	0.2	239.9	**608**	**594**	**617**	**606**	250	500	750	1000

Table B1.5 (Cont)

Sample	Date	Component	Fuel	Support	Spectral Band Pass	Wavelength	Result			Average	Standard			
							1	2	3		1	2	3	4
					nm	nm	ppm	ppm						
Exp 22.1	19-Apr	Ca	Acetylene	Nitrous Oxide	0.2	239.9	**605**	**620**	**617**	**614**	250	500	750	1000
Exp 22.2	19-Apr	Ca	Acetylene	Nitrous Oxide	0.2	239.9	**593**	**604**	**592**	**596**	250	500	750	1000
Exp 23.1	19-Apr	Ca	Acetylene	Nitrous Oxide	0.2	239.9	**617**	**624**	**621**	**621**	250	500	750	1000
Exp 23.2	19-Apr	Ca	Acetylene	Nitrous Oxide	0.2	239.9	**644**	**637**	**638**	**640**	250	500	750	1000
Exp 24.1	19-Apr	Ca	Acetylene	Nitrous Oxide	0.2	239.9	**631**	**618**	**627**	**625**	250	500	750	1000
Exp 24.2	19-Apr	Ca	Acetylene	Nitrous Oxide	0.2	239.9	**609**	**631**	**644**	**628**	250	500	750	1000
Exp 25.1	19-Apr	Ca	Acetylene	Nitrous Oxide	0.2	239.9	**529**	**627**	**612**	**589**	250	500	750	1000
Exp 25.2	19-Apr	Ca	Acetylene	Nitrous Oxide	0.2	239.9	**589**	**584**	**594**	**589**	250	500	750	1000
Exp 26.1	19-Apr	Ca	Acetylene	Nitrous Oxide	0.2	239.9	**617**	**630**	**618**	**622**	250	500	750	1000
Exp 26.2	19-Apr	Ca	Acetylene	Nitrous Oxide	0.2	239.9	**714**	**741**	**736**	**730**	250	500	750	1000
Exp 27.1	19-Apr	Ca	Acetylene	Nitrous Oxide	0.2	239.9	**617**	**608**	**617**	**614**	250	500	750	1000
Exp 27.2	19-Apr	Ca	Acetylene	Nitrous Oxide	0.2	239.9	**724**	**715**	**712**	**717**	250	500	750	1000
Exp 28.1	19-Apr	Ca	Acetylene	Nitrous Oxide	0.2	239.9	**607**	**611**	**617**	**612**	250	500	750	1000
Exp 28.2	19-Apr	Ca	Acetylene	Nitrous Oxide	0.2	239.9	**715**	**731**	**728**	**725**	250	500	750	1000
Exp 20.1	20-Apr	Na	Acetylene	Air	0.5	330.3	**1900**	**1880**	**1880**	**1887**	100	200	500	1000
Exp 20.2	20-Apr	Na	Acetylene	Air	0.5	330.3	**1880**	**1860**	**1880**	**1873**	100	200	500	1000
Exp 21.1	20-Apr	Na	Acetylene	Air	0.5	330.3	**1860**	**1880**	**1860**	**1867**	100	200	500	1000
Exp 21.2	20-Apr	Na	Acetylene	Air	0.5	330.3	**1860**	**1860**	**1860**	**1860**	100	200	500	1000
Exp 22.1	20-Apr	Na	Acetylene	Air	0.5	330.3	**1880**	**1900**	**1900**	**1893**	100	200	500	1000
Exp 22.2	20-Apr	Na	Acetylene	Air	0.5	330.3	**1900**	**1900**	**1880**	**1893**	100	200	500	1000
Exp 23.1	20-Apr	Na	Acetylene	Air	0.5	330.3	**1900**	**1900**	**1920**	**1907**	100	200	500	1000
Exp 23.2	20-Apr	Na	Acetylene	Air	0.5	330.3	**1940**	**1920**	**1920**	**1927**	100	200	500	1000
Exp 24.1	20-Apr	Na	Acetylene	Air	0.5	330.3	**1900**	**1900**	**1900**	**1900**	100	200	500	1000
Exp 24.2	20-Apr	Na	Acetylene	Air	0.5	330.3	**1900**	**1900**	**1920**	**1907**	100	200	500	1000
Exp 25.1	20-Apr	Na	Acetylene	Air	0.5	330.3	**1900**	**1900**	**1900**	**1900**	100	200	500	1000
Exp 25.2	20-Apr	Na	Acetylene	Air	0.5	330.3	**1920**	**1900**	**1920**	**1913**	100	200	500	1000
Exp 26.1	20-Apr	Na	Acetylene	Air	0.5	330.3	**1920**	**1900**	**1920**	**1913**	100	200	500	1000
Exp 26.2	20-Apr	Na	Acetylene	Air	0.5	330.3	**1960**	**1960**	**1960**	**1960**	100	200	500	1000

Table B1.5 (Cont)

Sample	Date	Component	Fuel	Support	Spectral Band Pass	Wavelength	Result			Average	Standard			
							1	2	3		1	2	3	4
					nm	nm	ppm	ppm						
Exp 27.1	20-Apr	Na	Acetylene	Air	0.5	330.3	**1920**	**1920**	**1940**	**1927**	100	200	500	1000
Exp 27.2	20-Apr	Na	Acetylene	Air	0.5	330.3	**1940**	**1960**	**1960**	**1953**	100	200	500	1000
Exp 28.1	20-Apr	Na	Acetylene	Air	0.5	330.3	**1940**	**1940**	**1940**	**1940**	100	200	500	1000
Exp 28.2	20-Apr	Na	Acetylene	Air	0.5	330.3	**1960**	**1960**	**1960**	**1960**	100	200	500	1000
Exp 29.1	26-Apr	Ca	Acetylene	Nitrous Oxide	0.2	239.9	**374**	**365**	**375**	**371**	250	500	750	1000
Exp 29.2	26-Apr	Ca	Acetylene	Nitrous Oxide	0.2	239.9	**374**	**394**	**378**	**382**	250	500	750	1000
Exp 30.1	26-Apr	Ca	Acetylene	Nitrous Oxide	0.2	239.9	**367**	**374**	**372**	**371**	250	500	750	1000
Exp 30.2	26-Apr	Ca	Acetylene	Nitrous Oxide	0.2	239.9	**366**	**375**	**382**	**374**	250	500	750	1000
Exp 31.1	26-Apr	Ca	Acetylene	Nitrous Oxide	0.2	239.9	**367**	**364**	**354**	**362**	250	500	750	1000
Exp 31.2	26-Apr	Ca	Acetylene	Nitrous Oxide	0.2	239.9	**366**	**368**	**371**	**368**	250	500	750	1000
Exp 32.1	26-Apr	Ca	Acetylene	Nitrous Oxide	0.2	239.9	**489**	**488**	**498**	**492**	250	500	750	1000
Exp 32.2	26-Apr	Ca	Acetylene	Nitrous Oxide	0.2	239.9	**495**	**495**	**493**	**494**	250	500	750	1000
Exp 33.1	26-Apr	Ca	Acetylene	Nitrous Oxide	0.2	239.9	**497**	**495**	**495**	**496**	250	500	750	1000
Exp 33.2	26-Apr	Ca	Acetylene	Nitrous Oxide	0.2	239.9	**504**	**504**	**498**	**502**	250	500	750	1000
Exp 34.1	26-Apr	Ca	Acetylene	Nitrous Oxide	0.2	239.9	**486**	**480**	**490**	**485**	250	500	750	1000
Exp 34.2	26-Apr	Ca	Acetylene	Nitrous Oxide	0.2	239.9	**495**	**494**	**489**	**493**	250	500	750	1000
Exp 35.1	26-Apr	Ca	Acetylene	Nitrous Oxide	0.2	239.9	**1148**	**1160**	**1157**	**1155**	250	500	750	1000
Exp 35.2	26-Apr	Ca	Acetylene	Nitrous Oxide	0.2	239.9	**1076**	**1109**	**1105**	**1097**	250	500	750	1000
Exp 36.1	26-Apr	Ca	Acetylene	Nitrous Oxide	0.2	239.9	**1084**	**1058**	**1064**	**1069**	250	500	750	1000
Exp 36.2	26-Apr	Ca	Acetylene	Nitrous Oxide	0.2	239.9	**1069**	**1073**	**1042**	**1061**	250	500	750	1000
Exp 37.1	26-Apr	Ca	Acetylene	Nitrous Oxide	0.2	239.9	**1116**	**1109**	**1111**	**1112**	250	500	750	1000
Exp 37.2	26-Apr	Ca	Acetylene	Nitrous Oxide	0.2	239.9	**1072**	**1091**	**1074**	**1079**	250	500	750	1000
Exp 38.1	26-Apr	Ca	Acetylene	Nitrous Oxide	0.2	239.9	**850**	**850**	**868**	**856**	250	500	750	1000
Exp 38.2	26-Apr	Ca	Acetylene	Nitrous Oxide	0.2	239.9	**859**	**877**	**862**	**866**	250	500	750	1000
Exp 39.1	26-Apr	Ca	Acetylene	Nitrous Oxide	0.2	239.9	**874**	**864**	**858**	**865**	250	500	750	1000
Exp 39.2	26-Apr	Ca	Acetylene	Nitrous Oxide	0.2	239.9	**881**	**862**	**808**	**850**	250	500	750	1000
Exp 40.1	26-Apr	Ca	Acetylene	Nitrous Oxide	0.2	239.9	**815**	**822**	**843**	**827**	250	500	750	1000
Exp 40.2	26-Apr	Ca	Acetylene	Nitrous Oxide	0.2	239.9	**829**	**825**	**839**	**831**	250	500	750	1000

Table B1.5 (Cont)

Sample	Date	Component	Fuel	Support	Spectral Band Pass	Wavelength	Result			Average	Standard			
							1	2	3		1	2	3	4
					nm	nm	ppm	ppm						
Exp 29.1	27-Apr	Na	Acetylene	Air	0.5	330.3	**1100**	**1120**	**1120**	**1113**	100	200	500	1000
Exp 29.2	27-Apr	Na	Acetylene	Air	0.5	330.3	**1100**	**1100**	**1100**	**1100**	100	200	500	1000
Exp 30.1	27-Apr	Na	Acetylene	Air	0.5	330.3	**1100**	**1100**	**1100**	**1100**	100	200	500	1000
Exp 30.2	27-Apr	Na	Acetylene	Air	0.5	330.3	**1100**	**1100**	**1100**	**1100**	100	200	500	1000
Exp 31.1	27-Apr	Na	Acetylene	Air	0.5	330.3	**1100**	**1120**	**1100**	**1107**	100	200	500	1000
Exp 31.2	27-Apr	Na	Acetylene	Air	0.5	330.3	**1100**	**1100**	**1100**	**1100**	100	200	500	1000
Exp 32.1	27-Apr	Na	Acetylene	Air	0.5	330.3	**1500**	**1500**	**1500**	**1500**	100	200	500	1000
Exp 32.2	27-Apr	Na	Acetylene	Air	0.5	330.3	**1520**	**1520**	**1500**	**1513**	100	200	500	1000
Exp 33.1	27-Apr	Na	Acetylene	Air	0.5	330.3	**1500**	**1480**	**1480**	**1487**	100	200	500	1000
Exp 33.2	27-Apr	Na	Acetylene	Air	0.5	330.3	**1520**	**1520**	**1520**	**1520**	100	200	500	1000
Exp 34.1	27-Apr	Na	Acetylene	Air	0.5	330.3	**1500**	**1500**	**1480**	**1493**	100	200	500	1000
Exp 34.2	27-Apr	Na	Acetylene	Air	0.5	330.3	**1520**	**1520**	**1520**	**1520**	100	200	500	1000
Exp 35.1	27-Apr	Na	Acetylene	Air	0.5	330.3	**5260**	**5260**	**5260**	**5260**	100	200	500	1000
Exp 35.2	27-Apr	Na	Acetylene	Air	0.5	330.3	**5240**	**5260**	**5240**	**5247**	100	200	500	1000
Exp 36.1	27-Apr	Na	Acetylene	Air	0.5	330.3	**5260**	**5260**	**5240**	**5253**	100	200	500	1000
Exp 36.2	27-Apr	Na	Acetylene	Air	0.5	330.3	**5260**	**5240**	**5220**	**5240**	100	200	500	1000
Exp 37.1	27-Apr	Na	Acetylene	Air	0.5	330.3	**5220**	**5200**	**5200**	**5207**	100	200	500	1000
Exp 37.2	27-Apr	Na	Acetylene	Air	0.5	330.3	**5260**	**5240**	**5260**	**5253**	100	200	500	1000
Exp 38.1	27-Apr	Na	Acetylene	Air	0.5	330.3	**3660**	**3640**	**3600**	**3633**	100	200	500	1000
Exp 38.2	27-Apr	Na	Acetylene	Air	0.5	330.3	**3620**	**3620**	**3600**	**3613**	100	200	500	1000
Exp 39.1	27-Apr	Na	Acetylene	Air	0.5	330.3	**3580**	**3560**	**3600**	**3580**	100	200	500	1000
Exp 39.2	27-Apr	Na	Acetylene	Air	0.5	330.3	**3620**	**3640**	**3640**	**3633**	100	200	500	1000
Exp 40.1	27-Apr	Na	Acetylene	Air	0.5	330.3	**3600**	**3580**	**3580**	**3587**	100	200	500	1000
Exp 40.2	27-Apr	Na	Acetylene	Air	0.5	330.3	**3720**	**3740**	**3720**	**3727**	100	200	500	1000

Table B1.6: Phase 3 Ca, Na, Cl and SO_4 analysis

Sample	Date	Component	Fuel	Support	Spectral Band Pass	Wavelength	Average	Standard			
								1	2	3	4
					nm	nm	ppm	ppm			
Exp 1.1	22-Sep	Ca	Acetylene	Nitrous Oxide	0.2	239.9	699	250	500	750	1000
Exp 1.2	22-Sep	Ca	Acetylene	Nitrous Oxide	0.2	239.9	627	250	500	750	1000
Exp 1.3	22-Sep	Ca	Acetylene	Nitrous Oxide	0.2	239.9	622	250	500	750	1000
Exp 2.1	22-Sep	Ca	Acetylene	Nitrous Oxide	0.2	239.9	691	250	500	750	1000
Exp 2.2	22-Sep	Ca	Acetylene	Nitrous Oxide	0.2	239.9	693	250	500	750	1000
Exp 2.3	22-Sep	Ca	Acetylene	Nitrous Oxide	0.2	239.9	780	250	500	750	1000
Exp 1.1	23-Sep	Na	Acetylene	Air	0.5	330.3	1820	100	200	500	1000
Exp 1.2	23-Sep	Na	Acetylene	Air	0.5	330.3	1920	100	200	500	1000
Exp 1.3	23-Sep	Na	Acetylene	Air	0.5	330.3	2000	100	200	500	1000
Exp 2.1	23-Sep	Na	Acetylene	Air	0.5	330.3	1860	100	200	500	1000
Exp 2.2	23-Sep	Na	Acetylene	Air	0.5	330.3	2200	100	200	500	1000
Exp 2.3	23-Sep	Na	Acetylene	Air	0.5	330.3	2700	100	200	500	1000
Exp 3.1	6-Oct	Ca	Acetylene	Nitrous Oxide	0.2	239.9	691	250	500	750	1000
Exp 3.2	6-Oct	Ca	Acetylene	Nitrous Oxide	0.2	239.9	595	250	500	750	1000
Exp 3.3	6-Oct	Ca	Acetylene	Nitrous Oxide	0.2	239.9	708	250	500	750	1000
Exp 4.1	6-Oct	Ca	Acetylene	Nitrous Oxide	0.2	239.9	680	250	500	750	1000
Exp 4.2	6-Oct	Ca	Acetylene	Nitrous Oxide	0.2	239.9	563	250	500	750	1000
Exp 4.3	6-Oct	Ca	Acetylene	Nitrous Oxide	0.2	239.9	600	250	500	750	1000
Exp 3.1	6-Oct	Na	Acetylene	Air	0.5	330.3	1860	100	200	500	1000
Exp 3.2	6-Oct	Na	Acetylene	Air	0.5	330.3	2060	100	200	500	1000
Exp 3.3	6-Oct	Na	Acetylene	Air	0.5	330.3	2540	100	200	500	1000
Exp 4.1	6-Oct	Na	Acetylene	Air	0.5	330.3	1820	100	200	500	1000
Exp 4.2	6-Oct	Na	Acetylene	Air	0.5	330.3	1920	100	200	500	1000
Exp 4.3	6-Oct	Na	Acetylene	Air	0.5	330.3	2000	100	200	500	1000
Exp 5.1	8-Oct	Ca	Acetylene	Nitrous Oxide	0.2	239.9	682	250	500	750	1000
Exp 5.2	8-Oct	Ca	Acetylene	Nitrous Oxide	0.2	239.9	539	250	500	750	1000
Exp 5.3	8-Oct	Ca	Acetylene	Nitrous Oxide	0.2	239.9	579	250	500	750	1000
Exp 6.1	8-Oct	Ca	Acetylene	Nitrous Oxide	0.2	239.9	648	250	500	750	1000

Table B1.6 (Cont)

Sample	Date	Component	Fuel	Support	Spectral Band Pass	Wavelength	Average	Standard			
								1	2	3	4
					nm	nm	ppm	ppm			
Exp 6.2	8-Oct	Ca	Acetylene	Nitrous Oxide	0.2	239.9	619	250	500	750	1000
Exp 6.3	8-Oct	Ca	Acetylene	Nitrous Oxide	0.2	239.9	815	250	500	750	1000
Exp 5.1	9-Oct	Na	Acetylene	Air	0.5	330.3	1740	100	200	500	1000
Exp 5.2	9-Oct	Na	Acetylene	Air	0.5	330.3	1880	100	200	500	1000
Exp 5.3	9-Oct	Na	Acetylene	Air	0.5	330.3	2020	100	200	500	1000
Exp 6.1	9-Oct	Na	Acetylene	Air	0.5	330.3	1840	100	200	500	1000
Exp 6.2	9-Oct	Na	Acetylene	Air	0.5	330.3	2180	100	200	500	1000
Exp 6.3	9-Oct	Na	Acetylene	Air	0.5	330.3	2900	100	200	500	1000
Exp 7.1	15-Oct	Ca	Acetylene	Nitrous Oxide	0.2	239.9	705	250	500	750	1000
Exp 7.2	15-Oct	Ca	Acetylene	Nitrous Oxide	0.2	239.9	729	250	500	750	1000
Exp 7.3	15-Oct	Ca	Acetylene	Nitrous Oxide	0.2	239.9	819	250	500	750	1000
Exp 8.1	15-Oct	Ca	Acetylene	Nitrous Oxide	0.2	239.9	683	250	500	750	1000
Exp 8.2	15-Oct	Ca	Acetylene	Nitrous Oxide	0.2	239.9	627	250	500	750	1000
Exp 8.3	15-Oct	Ca	Acetylene	Nitrous Oxide	0.2	239.9	619	250	500	750	1000
Exp 7.1	16-Oct	Na	Acetylene	Air	0.5	330.3	1640	100	200	500	1000
Exp 7.2	16-Oct	Na	Acetylene	Air	0.5	330.3	2220	100	200	500	1000
Exp 7.3	16-Oct	Na	Acetylene	Air	0.5	330.3	2920	100	200	500	1000
Exp 8.1	16-Oct	Na	Acetylene	Air	0.5	330.3	1700	100	200	500	1000
Exp 8.2	16-Oct	Na	Acetylene	Air	0.5	330.3	1860	100	200	500	1000
Exp 8.3	16-Oct	Na	Acetylene	Air	0.5	330.3	1840	100	200	500	1000

Appendix C

Statistical analysis

C1: TRO Brine

C1.1: Calcium

Response: Calcium Leaching

ANOVA for Mixture Quadratic Model

Analysis of variance table [Partial sum of squares]

Source	Sum of Squares	DF	Mean Square	F Value	Prob > F	
Model	171462883	5	34292577	435.35	< 0.0001	significant
Linear Mixture	170042878	2	85021439	1079.35	< 0.0001	
AB	706422	1	706422	8.97	0.0122	
AC	705560	1	705560	8.96	0.0122	
BC	8022	1	8022	0.10	0.7556	
Pure Error	866479	11	78771			
Cor Total	172329362	16				

The Model F-value of 435.35 implies the model is significant. There is only a 0.01% chance that a "Model F-Value" this large could occur due to noise.

Values of "Prob > F" less than 0.0500 indicate model terms are significant.
In this case Linear Mixture Components, AB, AC are significant model terms.
Values greater than 0.1000 indicate the model terms are not significant.
If there are many insignificant model terms (not counting those required to support hierarchy), model reduction may improve your model.

Std. Dev.	280.7	R-Squared	0.99
Mean	2820.9	Adj R-Squared	0.99
C.V.	9.9	Pred R-Squared	0.99
PRESS	1993875.0	Adeq Precision	47.69

The "Pred R-Squared" of 0.9884 is in reasonable agreement with the "Adj R-Squared" of 0.9927.

"Adeq Precision" measures the signal to noise ratio. A ratio greater than 4 is desirable. Your ratio of 47.690 indicates an adequate signal. This model can be used to navigate the design space.

Component	Coefficient Estimate	DF	Standard Error	95% CI Low	95% CI High
A-Ash	37212526	1	12418424	9879760	64545292
B-TRO	33	1	162	-323	390

C-CAE	-107	1	162	-463	250
AB	-44626368	1	14901914	-77425259	-11827477
AC	-44599702	1	14902104	-77399012	-11800393
BC	253	1	794	-1494	2001

Final Equation in Terms of Pseudo Components:

Calcium Leaching	=
37212526	* A
33	* B
-107	* C
-44626368	* A * B
-44599702	* A * C
253	* B * C

Final Equation in Terms of Real Components:

Calcium Leaching	=
37212526	* Ash
33	* TRO
-107	* CAE
-44626368	* Ash * TRO
-44599702	* Ash * CAE
253	* TRO * CAE

Final Equation in Terms of Actual Components:

Calcium Leaching	=
372125	* Ash
0	* TRO
-1	* CAE
-4463	* Ash * TRO
-4460	* Ash * CAE
0	* TRO * CAE

Diagnostics Case Statistics

Standard Order	Actual Value	Predicted Value	Residual	Leverage	Student Residual	Cook's Distance	Outlier t
1	7730.00	7845.00	-115.00	0.33	-0.50	0.02	-0.48
3	10.00	26.67	-16.67	0.33	-0.07	0.00	-0.07
4	40.00	26.67	13.33	0.33	0.06	0.00	0.06
5	5395.00	5348.33	46.67	0.33	0.20	0.00	0.19
6	4795.00	5348.33	-553.33	0.33	-2.41	0.49	-3.36
7	4370.00	4257.50	112.50	0.50	0.57	0.05	0.55
8	30.00	26.67	3.33	0.33	0.01	0.00	0.01
9	30.00	33.33	-3.33	0.33	-0.01	0.00	-0.01
10	8255.00	7845.00	410.00	0.33	1.79	0.27	2.03
11	7550.00	7845.00	-295.00	0.33	-1.29	0.14	-1.33
12	55.00	33.33	21.67	0.33	0.09	0.00	0.09
13	-90.00	-106.67	16.67	0.33	0.07	0.00	0.07

14	-60.00	-106.67	46.67	0.33	0.20	0.00	0.19
15	4145.00	4257.50	-112.50	0.50	-0.57	0.05	-0.55
16	-170.00	-106.67	-63.33	0.33	-0.28	0.01	-0.26
17	5855.00	5348.33	506.67	0.33	2.21	0.41	2.83
18	15.00	33.33	-18.33	0.33	-0.08	0.00	-0.08

C1.2: Sulphate

Response: Sulphate Removal

ANOVA for Mixture Quadratic Model

Analysis of variance table [Partial sum of squares]

Source	Sum of Squares	DF	Mean Square	F Value	Prob > F	
Model	324883807	5	64976761	140	< 0.0001	significant
Linear Mixture	323641332	2	161820666	347	< 0.0001	
AB	409055	1	409055	1	0.3672	
AC	407147	1	407147	1	0.3683	
BC	426272	1	426272	1	0.3576	
Pure Error	5589383	12	465782			
Cor Total	330473190	17				

The Model F-value of 139.50 implies the model is significant. There is only a 0.01% chance that a "Model F-Value" this large could occur due to noise.

Values of "Prob > F" less than 0.0500 indicate model terms are significant.
In this case Linear Mixture Components are significant model terms.
Values greater than 0.1000 indicate the model terms are not significant.
If there are many insignificant model terms (not counting those required to support hierarchy), model reduction may improve your model.

Std. Dev.	682	R-Squared	1
Mean	-2919	Adj R-Squared	1
C.V.	-23	Pred R-Squared	1
PRESS	12576112	Adeq Precision	29

The "Pred R-Squared" of 0.9619 is in reasonable agreement with the "Adj R-Squared" of 0.9760.

"Adeq Precision" measures the signal to noise ratio. A ratio greater than 4 is desirable. Your ratio of 28.961 indicates an adequate signal. This model can be used to navigate the design space.

Component	Coefficient Estimate	DF	Standard Error	95% CI Low	95% CI High
A-Ash	27469074	1	29383649	-36552398	91490546
B-TRO	-103	1	394	-962	755
C-CAE	-187	1	394	-1045	672
AB	-33043458	1	35260289	-109869028	43782111
AC	-32966303	1	35260289	-109791872	43859267
BC	1847	1	1930	-2359	6053

Final Equation in Terms of Pseudo Components:

Sulphate Removal	=
27469074	* A
-103	* B
-187	* C
-33043458	* A * B
-32966303	* A * C
1847	* B * C

Final Equation in Terms of Real Components:

Sulphate Removal	=
27469074	* Ash
-103	* TRO
-187	* CAE
-33043458	* Ash * TRO
-32966303	* Ash * CAE
1847	* TRO * CAE

Final Equation in Terms of Actual Components:

Sulphate Removal	=
274691	* Ash
-1	* TRO
-2	* CAE
-3304	* Ash * TRO
-3297	* Ash * CAE
0	* TRO * CAE

Diagnostics Case Statistics

Standard Order	Actual Value	Predicted Value	Residual	Leverage	Student Residual	Cook's Distance	Outlier t
1	-230.00	-103.33	-126.67	0.33	-0.23	0.00	-0.22
2	-10.00	-103.33	93.33	0.33	0.17	0.00	0.16
3	-70.00	-103.33	33.33	0.33	0.06	0.00	0.06
4	-130.00	-186.67	56.67	0.33	0.10	0.00	0.10
5	-280.00	-186.67	-93.33	0.33	-0.17	0.00	-0.16
6	-150.00	-186.67	36.67	0.33	0.07	0.00	0.06
7	470.00	316.67	153.33	0.33	0.28	0.01	0.26
8	0.00	316.67	-316.67	0.33	-0.57	0.03	-0.55
9	480.00	316.67	163.33	0.33	0.29	0.01	0.28
10	-9715.00	-11095.00	1380.00	0.33	2.48	0.51	3.39
11	-11980.00	-11095.00	-885.00	0.33	-1.59	0.21	-1.71
12	-11590.00	-11095.00	-495.00	0.33	-0.89	0.07	-0.88
13	-560.00	-446.67	-113.33	0.33	-0.20	0.00	-0.20
14	-260.00	-446.67	186.67	0.33	0.33	0.01	0.32
15	-520.00	-446.67	-73.33	0.33	-0.13	0.00	-0.13
16	-4850.00	-5996.67	1146.67	0.33	2.06	0.35	2.45
17	-7040.00	-5996.67	-1043.33	0.33	-1.87	0.29	-2.13
18	-6100.00	-5996.67	-103.33	0.33	-0.19	0.00	-0.18

C1.3: TDS

Response: TDS Leaching

ANOVA for Mixture Quadratic Model

Analysis of variance table [Partial sum of squares]

Source	Sum of Squares	DF	Mean Square	F Value	Prob > F	
Model	3672973266	5	734594653	6120	< 0.0001	significant
Linear Mixture	3671738085	2	1835869042	15295	< 0.0001	
AB	446712	1	446712	4	0.0826	
AC	445953	1	445953	4	0.0828	
BC	342516	1	342516	3	0.1221	
Pure Error	1200343	10	120034			
Cor Total	3674173608	15				

The Model F-value of 6119.87 implies the model is significant. There is only a 0.01% chance that a "Model F-Value" this large could occur due to noise.

Values of "Prob > F" less than 0.0500 indicate model terms are significant.
In this case Linear Mixture Components are significant model terms.
Values greater than 0.1000 indicate the model terms are not significant.
If there are many insignificant model terms (not counting those required to support hierarchy), model reduction may improve your model.

Std. Dev.	346	R-Squared	1
Mean	13354	Adj R-Squared	1
C.V.	3	Pred R-Squared	1
PRESS	3184208	Adeq Precision	155

The "Pred R-Squared" of 0.9991 is in reasonable agreement with the "Adj R-Squared" of 0.9995.

"Adeq Precision" measures the signal to noise ratio. A ratio greater than 4 is desirable. Your ratio of 155.149 indicates an adequate signal. This model can be used to navigate the design space.

Component	Coefficient Estimate	DF	Standard Error	95% CI Low	95% CI High
A-Ash	30519435	1	15732235	-4534168	65573038
B-TRO	-11	1	200	-457	435
C-CAE	-217	1	200	-662	229
AB	-36419014	1	18878486	-78482901	5644873
AC	-36388085	1	18878486	-78451972	5675802
BC	1655	1	980	-528	3839

Final Equation in Terms of Pseudo Components:

TDS Leaching =
30519435 * A
-11 * B
-217 * C
-36419014 * A * B
-36388085 * A * C

1655 * B * C

Final Equation in Terms of Real Components:

TDS Leaching	=
30519435	* Ash
-11	* TRO
-217	* CAE
-36419014	* Ash * TRO
-36388085	* Ash * CAE
1655	* TRO * CAE

Final Equation in Terms of Actual Components:

TDS Leaching	=
305194	* Ash
0	* TRO
-2	* CAE
-3642	* Ash * TRO
-3639	* Ash * CAE
0	* TRO * CAE

Diagnostics Case Statistics

Standard Order	Actual Value	Predicted Value	Residual	Leverage	Student Residual	Cook's Distance	Outlier t
1	17.00	-11.00	28.00	0.33	0.10	0.00	0.09
2	50.00	-11.00	61.00	0.33	0.22	0.00	0.21
3	-650.00	-216.67	-433.33	0.33	-1.53	0.20	-1.66
4	-100.00	-11.00	-89.00	0.33	-0.31	0.01	-0.30
5	200.00	-216.67	416.67	0.33	1.47	0.18	1.58
6	-200.00	-216.67	16.67	0.33	0.06	0.00	0.06
7	400.00	300.00	100.00	0.33	0.35	0.01	0.34
8	150.00	300.00	-150.00	0.33	-0.53	0.02	-0.51
9	350.00	300.00	50.00	0.33	0.18	0.00	0.17
11	28850.00	28575.00	275.00	0.50	1.12	0.21	1.14
12	28300.00	28575.00	-275.00	0.50	-1.12	0.21	-1.14
13	32450.00	32700.00	-250.00	0.50	-1.02	0.17	-1.02
14	32950.00	32700.00	250.00	0.50	1.02	0.17	1.02
16	30850.00	30300.00	550.00	0.33	1.94	0.32	2.34
17	30200.00	30300.00	-100.00	0.33	-0.35	0.01	-0.34
18	29850.00	30300.00	-450.00	0.33	-1.59	0.21	-1.75

C2: EDR Brine

C2.1: Calcium

Response: Calcium Leaching

ANOVA for Mixture Quadratic Model

Analysis of variance table [Partial sum of squares]

Source	Sum of Squares	DF	Mean Square	F Value	Prob > F	
Model	170519754	5	34103951	390	< 0.0001	significant
Linear Mixture	169707445	2	84853723	971	< 0.0001	
AB	388429	1	388429	4	0.0612	
AC	387879	1	387879	4	0.0613	
BC	36001	1	36001	0	0.5354	
Pure Error	873646	10	87365			
Cor Total	171393400	15				

The Model F-value of 390.36 implies the model is significant. There is only a 0.01% chance that a "Model F-Value" this large could occur due to noise.

Values of "Prob > F" less than 0.0500 indicate model terms are significant.
In this case Linear Mixture Components are significant model terms.
Values greater than 0.1000 indicate the model terms are not significant.
If there are many insignificant model terms (not counting those required to support hierarchy), model reduction may improve your model.

Std. Dev.	296	R-Squared	1
Mean	2645	Adj R-Squared	1
C.V.	11	Pred R-Squared	1
PRESS	2944062	Adeq Precision	44

The "Pred R-Squared" of 0.9828 is in reasonable agreement with the "Adj R-Squared" of 0.9924.

"Adeq Precision" measures the signal to noise ratio. A ratio greater than 4 is desirable. Your ratio of 44.254 indicates an adequate signal. This model can be used to navigate the design space.

Component	Coefficient Estimate	DF	Standard Error	95% CI Low	95% CI High
A-Ash	30396554	1	14403826	-1697169	62490277
B-TRO	-165	1	171	-545	215
C-CAE	-107	1	171	-487	274
AB	-36445631	1	17284526	-74957955	2066693
AC	-36420209	1	17284708	-74932938	2092520
BC	537	1	836	-1326	2399

Final Equation in Terms of Pseudo Components:

Calcium Leaching	=
30396554	* A
-165	* B
-107	* C
-36445631	* A * B
-36420209	* A * C
537	* B * C

Final Equation in Terms of Real Components:

Calcium Leaching	=
30396554	* Ash
-165	* TRO
-107	* CAE
-36445631	* Ash * TRO
-36420209	* Ash * CAE
537	* TRO * CAE

Final Equation in Terms of Actual Components:

Calcium Leaching	=
303966	* Ash
-2	* TRO
-1	* CAE
-3645	* Ash * TRO
-3642	* Ash * CAE
0	* TRO * CAE

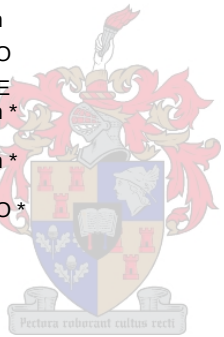

Diagnostics Case Statistics

Standard Order	Actual Value	Predicted Value	Residual	Leverage	Student Residual	Cook's Distance	Outlier t
1	7730.00	7845.00	-115.00	0.33	-0.48	0.02	-0.46
3	50.00	-1.67	51.67	0.33	0.21	0.00	0.20
4	20.00	-1.67	21.67	0.33	0.09	0.00	0.09
5	5600.00	5537.50	62.50	0.50	0.30	0.01	0.28
7	4790.00	4265.00	525.00	0.50	2.51	1.05	3.923 *
8	-75.00	-1.67	-73.33	0.33	-0.30	0.01	-0.29
9	-165.00	-165.00	0.00	0.33	0.00	0.00	0.00
10	8255.00	7845.00	410.00	0.33	1.70	0.24	1.91
11	7550.00	7845.00	-295.00	0.33	-1.22	0.12	-1.26
12	-290.00	-165.00	-125.00	0.33	-0.52	0.02	-0.50
13	-90.00	-106.67	16.67	0.33	0.07	0.00	0.07
14	-60.00	-106.67	46.67	0.33	0.19	0.00	0.18
15	3740.00	4265.00	-525.00	0.50	-2.51	1.05	-3.923 *
16	-170.00	-106.67	-63.33	0.33	-0.26	0.01	-0.25
17	5475.00	5537.50	-62.50	0.50	-0.30	0.01	-0.28
18	-40.00	-165.00	125.00	0.33	0.52	0.02	0.50

* Case(s) with |Outlier T| > 3.50

C2.2: Sulphate

Response: Sulphate Removal

ANOVA for Mixture Quadratic Model

Analysis of variance table [Partial sum of squares]

Source	Sum of Squares	DF	Mean Square	F Value	Prob > F	
Model	1544966311	5	308993262	789	< 0.0001	significant
Linear Mixture	1542340069	2	771170035	1969	< 0.0001	
AB	1162289	1	1162289	3	0.1129	
AC	1154530	1	1154530	3	0.1140	
BC	309422	1	309422	1	0.3932	
Pure Error	4309183	11	391744			
Cor Total	1549275494	16				

The Model F-value of 788.76 implies the model is significant. There is only a 0.01% chance that a "Model F-Value" this large could occur due to noise.

Values of "Prob > F" less than 0.0500 indicate model terms are significant.
In this case Linear Mixture Components are significant model terms.
Values greater than 0.1000 indicate the model terms are not significant.
If there are many insignificant model terms (not counting those required to support hierarchy), model reduction may improve your model.

Std. Dev.	626	R-Squared	1
Mean	-6311	Adj R-Squared	1
C.V.	-10	Pred R-Squared	1
PRESS	9790950	Adeq Precision	74

The "Pred R-Squared" of 0.9937 is in reasonable agreement with the "Adj R-Squared" of 0.9960.

"Adeq Precision" measures the signal to noise ratio. A ratio greater than 4 is desirable. Your ratio of 74.491 indicates an adequate signal. This model can be used to navigate the design space.

Component	Coefficient Estimate	DF	Standard Error	95% CI Low	95% CI High
A-Ash	47539319	1	27693949	-13414652	108493290
B-TRO	-1333	1	361	-2129	-538
C-CAE	-187	1	361	-982	609
AB	-57242206	1	33232305	-130386016	15901604
AC	-57051561	1	33232729	-130196304	16093183
BC	1573	1	1770	-2323	5470

Final Equation in Terms of Pseudo Components:

Sulphate Removal	=
47539319	* A
-1333	* B
-187	* C
-57242206	* A * B

-57051561	* A * C
1573	* B * C

Final Equation in Terms of Real Components:

Sulphate Removal	=
47539319	* Ash
-1333	* TRO
-187	* CAE
-57242206	* Ash * TRO
-57051561	* Ash * CAE
1573	* TRO * CAE

Final Equation in Terms of Actual Components:

Sulphate Removal	=
475393	* Ash
-13	* TRO
-2	* CAE
-5724	* Ash * TRO
-5705	* Ash * CAE
0	* TRO * CAE

Diagnostics Case Statistics

Standard Order	Actual Value	Predicted Value	Residual	Leverage	Student Residual	Cook's Distance	Outlier t
1	-100.00	-1333.33	1233.33	0.33	2.41	0.49	3.35
2	-2350.00	-1333.33	-1016.67	0.33	-1.99	0.33	-2.37
3	-1550.00	-1333.33	-216.67	0.33	-0.42	0.01	-0.41
4	-130.00	-186.67	56.67	0.33	0.11	0.00	0.11
5	-280.00	-186.67	-93.33	0.33	-0.18	0.00	-0.17
6	-150.00	-186.67	36.67	0.33	0.07	0.00	0.07
7	-1100.00	-366.67	-733.33	0.33	-1.43	0.17	-1.52
8	300.00	-366.67	666.67	0.33	1.30	0.14	1.35
9	-300.00	-366.67	66.67	0.33	0.13	0.00	0.12
11	-27720.00	-27885.00	165.00	0.50	0.37	0.02	0.36
12	-28050.00	-27885.00	-165.00	0.50	-0.37	0.02	-0.36
13	-560.00	-446.67	-113.33	0.33	-0.22	0.00	-0.21
14	-260.00	-446.67	186.67	0.33	0.37	0.01	0.35
15	-520.00	-446.67	-73.33	0.33	-0.14	0.00	-0.14
16	-14900.00	-14836.67	-63.33	0.33	-0.12	0.00	-0.12
17	-14260.00	-14836.67	576.67	0.33	1.13	0.11	1.14
18	-15350.00	-14836.67	-513.33	0.33	-1.00	0.08	-1.00

C2.3: TDS

Response: TDS Leaching

ANOVA for Mixture Quadratic Model

Analysis of variance table [Partial sum of squares]

Source	Sum of Squares	DF	Mean Square	F Value	Prob > F	
Model	4033955686	5	806791137	1251	< 0.0001	significant
Linear Mixture	4027616187	2	2013808094	3124	< 0.0001	
AB	2912332	1	2912332	5	0.0570	
AC	2910362	1	2910362	5	0.0571	
BC	516806	1	516806	1	0.3898	
Pure Error	7091667	11	644697			
Cor Total	4041047353	16				

The Model F-value of 1251.43 implies the model is significant. There is only a 0.01% chance that a "Model F-Value" this large could occur due to noise.

Values of "Prob > F" less than 0.0500 indicate model terms are significant.
In this case Linear Mixture Components are significant model terms.
Values greater than 0.1000 indicate the model terms are not significant.
If there are many insignificant model terms (not counting those required to support hierarchy), model reduction may improve your model.

Std. Dev.	803	R-Squared	1
Mean	15253	Adj R-Squared	1
C.V.	5	Pred R-Squared	1
PRESS	15965000	Adeq Precision	70

The "Pred R-Squared" of 0.9960 is in reasonable agreement with the "Adj R-Squared" of 0.9974.

"Adeq Precision" measures the signal to noise ratio. A ratio greater than 4 is desirable. Your ratio of 70.054 indicates an adequate signal. This model can be used to navigate the design space.

Component	Coefficient Estimate	DF	Standard Error	95% CI Low	95% CI High
A-Ash	75681608	1	35527248	-2513337	153876552
B-EDR	1400	1	464	380	2420
C-CAE	-217	1	464	-1237	804
AB	-90610755	1	42632140	-184443463	3221953
AC	-90581260	1	42632684	-184415166	3252645
BC	2033	1	2271	-2965	7032

Final Equation in Terms of Pseudo Components:

TDS Leaching =
75681608 * A
1400 * B
-217 * C
-90610755 * A * B
-90581260 * A * C
2033 * B * C

Final Equation in Terms of Real Components:

TDS Leaching =
75681608 * Ash

1400	* EDR
-217	* CAE
-90610755	* Ash * EDR
-90581260	* Ash * CAE
2033	* EDR * CAE

Final Equation in Terms of Actual Components:

TDS Leaching	=
756816	* Ash
14	* EDR
-2	* CAE
-9061	* Ash * EDR
-9058	* Ash * CAE
0	* EDR * CAE

Diagnostics Case Statistics

Standard Order	Actual Value	Predicted Value	Residual	Leverage	Student Residual	Cook's Distance	Outlier t
1	850.00	1400.00	-550.00	0.33	-0.84	0.06	-0.83
2	2300.00	1400.00	900.00	0.33	1.37	0.16	1.44
3	-650.00	-216.67	-433.33	0.33	-0.66	0.04	-0.64
4	1050.00	1400.00	-350.00	0.33	-0.53	0.02	-0.52
5	200.00	-216.67	416.67	0.33	0.64	0.03	0.62
6	-200.00	-216.67	16.67	0.33	0.03	0.00	0.02
7	2100.00	1100.00	1000.00	0.33	1.53	0.19	1.64
8	700.00	1100.00	-400.00	0.33	-0.61	0.03	-0.59
9	500.00	1100.00	-600.00	0.33	-0.92	0.07	-0.91
11	30400.00	30450.00	-50.00	0.50	-0.09	0.00	-0.08
12	30500.00	30450.00	50.00	0.50	0.09	0.00	0.08
13	32450.00	33200.00	-750.00	0.33	-1.14	0.11	-1.16
14	32950.00	33200.00	-250.00	0.33	-0.38	0.01	-0.37
15	34200.00	33200.00	1000.00	0.33	1.53	0.19	1.64
16	29650.00	30650.00	-1000.00	0.33	-1.53	0.19	-1.64
17	30500.00	30650.00	-150.00	0.33	-0.23	0.00	-0.22
18	31800.00	30650.00	1150.00	0.33	1.75	0.26	1.97

Appendix D

Salt balances

D1: Salt balances

Table D1: Calcium

Calcium			
Inlet streams	**Flowrate (m^3/h)**	**Concentration (mg/l)**	**Mass In (t/h)**
FAD 5	537.35	404	0.2171
FAD 4 (Emmet)	425	327	0.1390
FAD 3	458.67	604	0.2770
U69 Brine	539.4	719	0.3878
Other	127	445	0.0565
Outlet streams	**Flowrate (m^3/h)**	**Concentration (mg/l)**	**Mass Out (t/h)**
Sasol 2	2070.3	388	0.8033
Sasol 3			
U69			
U67			
Total Increase/Decrease			**0.2742**

Table D2: Sodium

Sodium			
Inlet streams	**Flowrate (m^3/h)**	**Concentration (mg/l)**	**Mass In (t/h)**
FAD 5	537.35	1568	0.8426
FAD 4 (Emmet)	425	1331	0.5657
FAD 3	458.67	1468	0.6733
U69 Brine	539.4	2116	1.1414
Other	127	1456	0.1849
Outlet streams	**Flowrate (m^3/h)**	**Concentration (mg/l)**	**Mass Out (t/h)**
Sasol 2	2070.3	1519	3.1448
Sasol 3			
U69			
U67			
Total Increase/Decrease			**0.2630**

Table D3: Chloride

Chloride			
Inlet streams	**Flowrate (m^3/h)**	**Concentration (mg/l)**	**Mass In (t/h)**
FAD 5	537.35	873	0.4691
FAD 4 (Emmet)	425	813	0.3455
FAD 3	458.67	813	0.3729
U69 Brine	539.4	1316	0.7099
Other	127	833	0.1058
Outlet streams	**Flowrate (m^3/h)**	**Concentration (mg/l)**	**Mass Out (t/h)**
Sasol 2	2070.3	896	1.8550
Sasol 3			
U69			
U67			
Total Increase/Decrease			**0.1482**

Table D4: Sulphate

Sulphate			
Inlet streams	**Flowrate (m^3/h)**	**Concentration (mg/l)**	**Mass In (t/h)**
FAD 5	537.35	3042	1.6346
FAD 4 (Emmet)	425	2820	1.1985
FAD 3	458.67	3640	1.6696
U69 Brine	539.4	4300	2.3194
Other	127	3167	0.4023
Outlet streams	**Flowrate (m^3/h)**	**Concentration (mg/l)**	**Mass Out (t/h)**
Sasol 2	2070.3	4020	8.3226
Sasol 3			
U69			
U67			
Total Increase/Decrease			**-1.0983**

Table D5: TDS

TDS			
Inlet streams	**Flowrate (m^3/h)**	**Concentration (mg/l)**	**Mass In (t/h)**
FAD 5	537.35	6730	3.6164
FAD 4 (Emmet)	425	5668	2.4089
FAD 3	458.67	7263	3.3313
U69 Brine	539.4	10260	5.5342
Other	127	6554	0.8323
Outlet streams	**Flowrate (m^3/h)**	**Concentration (mg/l)**	**Mass Out (t/h)**
Sasol 2	2070.3	6454	13.3617
Sasol 3			
U69			
U67			
Total Increase/Decrease			**2.3614**